Statistical Properties of Algorithms for Analysis of Cell Images

Ilya Ravkin

Consultant

ilya@ravkin.net

www.ravkin.net

Plan of Presentation

- Motivation
- Measures of quality for cell imaging assays
- Simulation of image-derived measures
- Factors affecting assay quality:

Algorithms:

Cytoplasm to Nucleus Translocation

Mitotic Index

Transfluor™

Image Sets

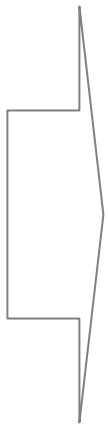

  - Image analysis algorithm
  - Number of cells/image size
  - Image resolution
  - Illumination uniformity
  - Shift between fluorescent channels
  - Accuracy of focusing
  - Depth of field (widefield and confocal)
  - Surface coating

Other factors affecting assay quality (not analyzed in this presentation):

- Flatness of plate
- Optical flatness of field
- Image acquisition parameters
- Operator dependency

- Assay quality after statistical processing
- Cell-by-cell vs. global analysis
- Conclusions and recommendations

Motivation: Specifications Paradox

Plate readers

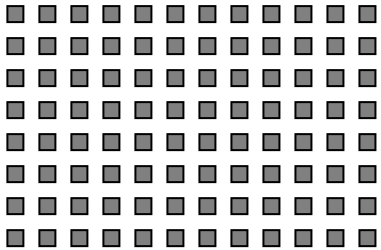

Measurements are the data

Cell imagers

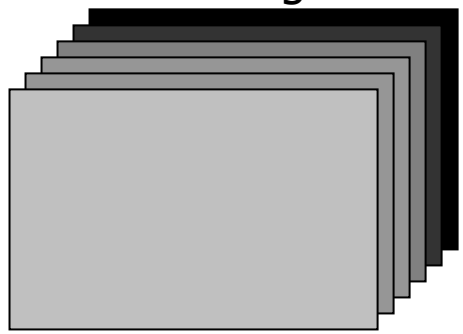

Sophisticated data extraction. Megabytes of pixel data are converted to a small number of data points

Specifications

From manufacturers' web sites and product literature

Numerical values:

Dynamic range
Detection limit
Accuracy
Precision
Linearity
Crosstalk
Z-factor
Reading times

Verbal description:

Rapid and accurate imaging and analysis
Unmatched combination of speed, accuracy, and precision
Proprietary and patented technology
Superior image processing software
Broadest set of spatial and intensity measurements
Highest fidelity measurements
True cell-by-cell measurements
Validated algorithms with optimized protocols

Contradiction exists between quantitative data derived from images and qualitative and emotional characterization of performance of cell imagers

We are attempting to start quantitative characterization of cell imaging systems

Quality Assessment in Cellular Imaging at Present

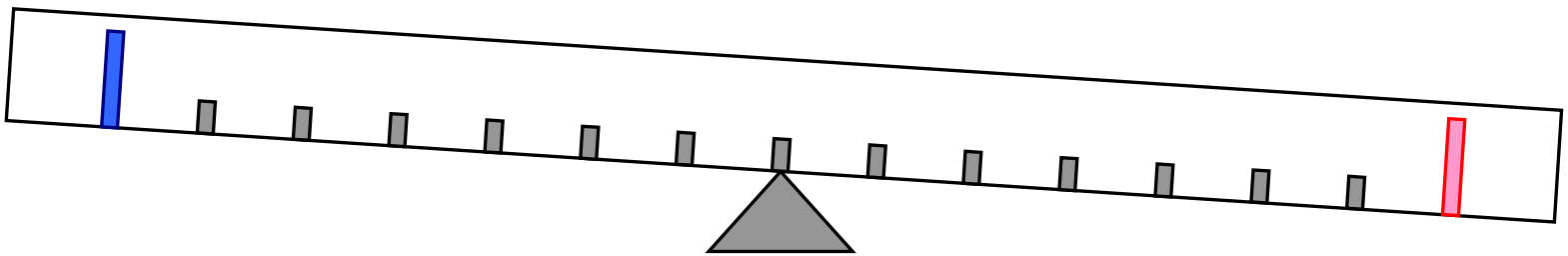

Compare to visual assessment by a human

Use existing HTS quality measures

- *Very laborious*
- *Hard to quantify*
- *Subjective*

May not capture specific effects introduced by image acquisition and analysis

Manipulation of Z-factor

(1) $$Z = 1 - 3\left(\frac{SD_{pos} + SD_{neg}}{\left|M_{pos} - M_{neg}\right|}\right)$$

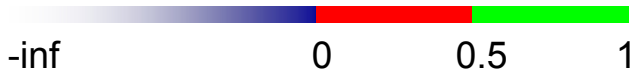

SD is standard deviation, *M* is mean, *pos* and *neg* are the two extreme states of the assay, which define its dynamic range

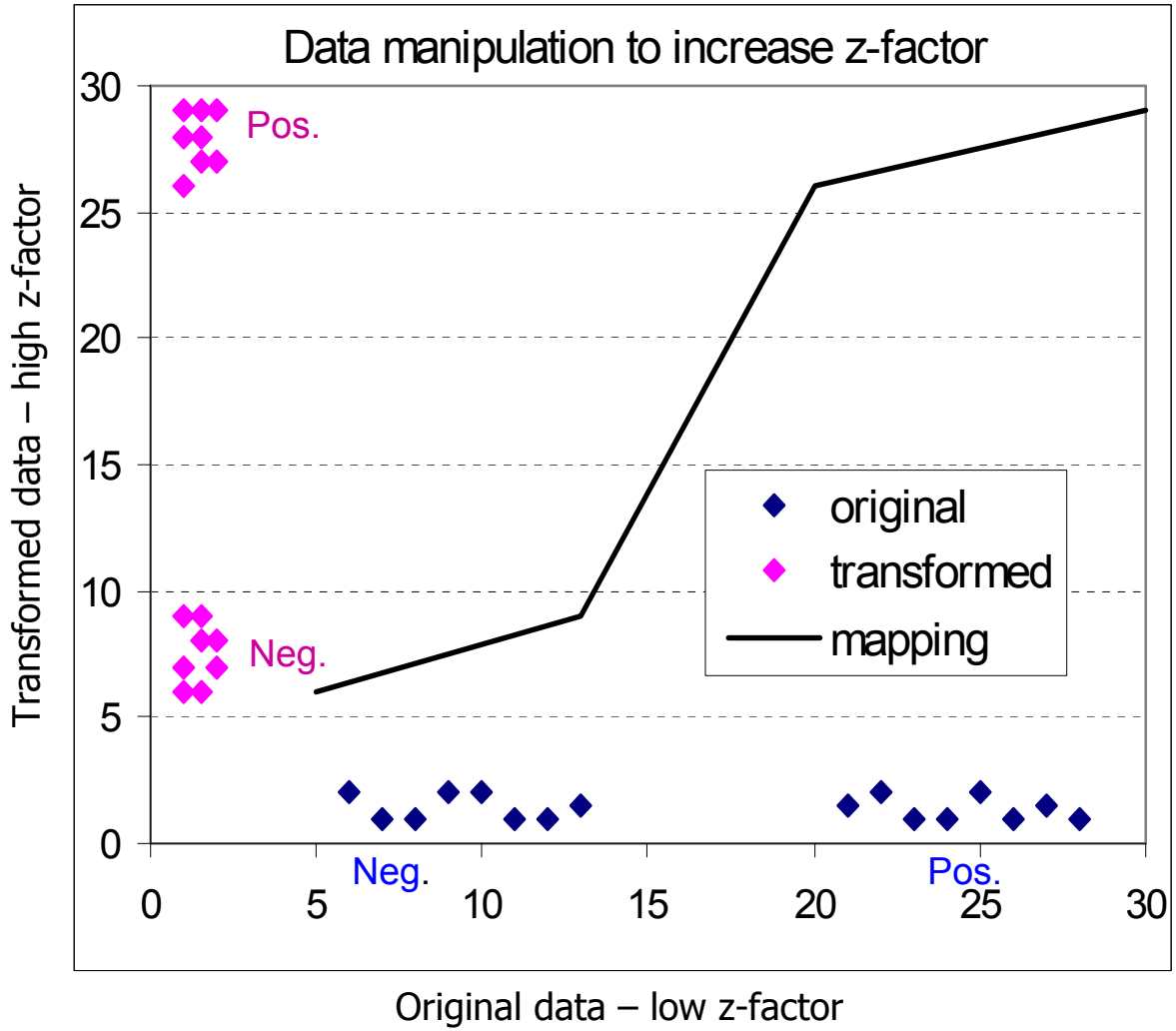

Saturation of values from the positive and negative states of the assay is possible due to image processing or intentional manipulation. A mathematical transformation that maps all positive values into a single value and all negative values into another single value results in Z-factor of 1.

Solution – use many dose points.

V-factor, a Generalization of Z-factor

(2) $$V = 1 - 6\left(\frac{SD_{of\_fit}}{\left|M_{pos} - M_{neg}\right|}\right)$$

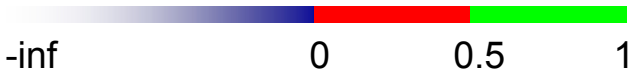

(3) $$SD_{of\_fit} = \sqrt{\frac{1}{n}\sum_{1}^{n}\left(f_{\text{model}} - f_{\text{experiment}}\right)^2}$$

e.g. logistic model

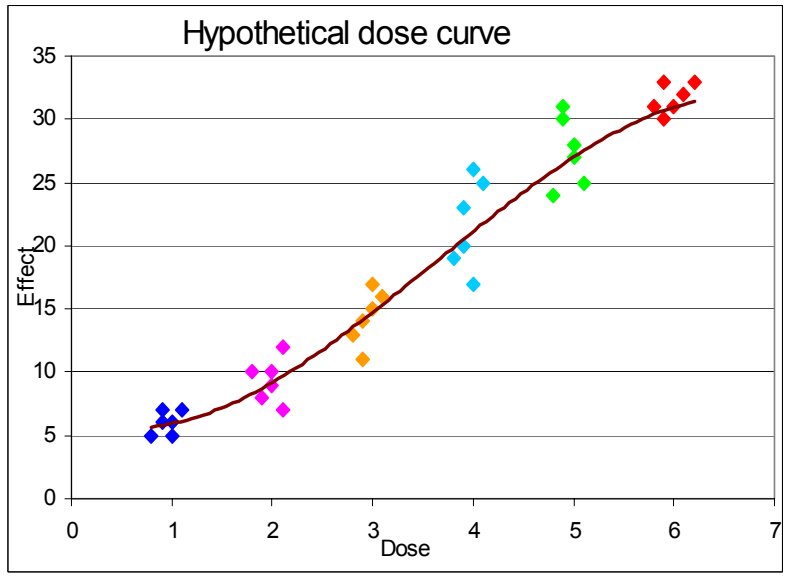

Weights of different concentrations in calculation of Z and V-factors

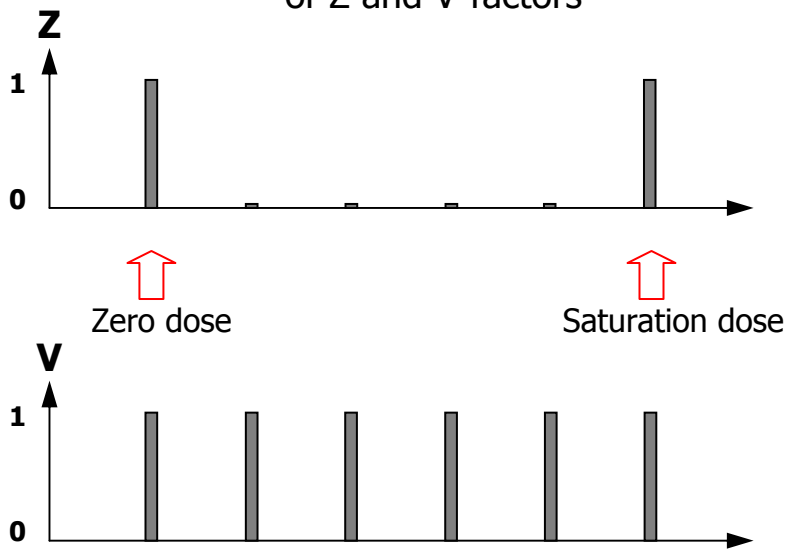

(4) $$V = 1 - 6\left(\frac{Average\_SD}{\left|M_{pos} - M_{neg}\right|}\right)$$

(Alternative definition without a model)

Simulation – Different Patterns and Levels of Noise Over Logistic Curve

Each curve was generated 16 times

Pattern 1. Uniform distribution of noise

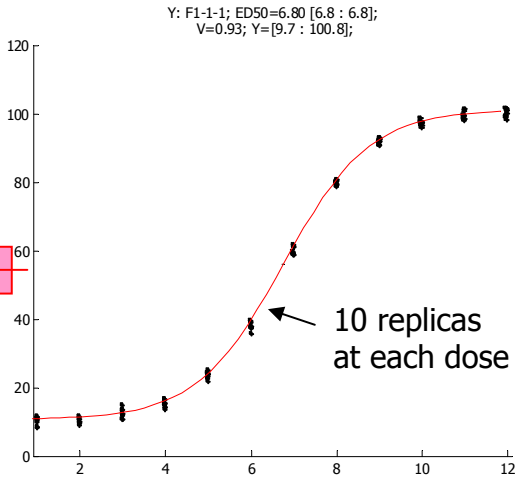

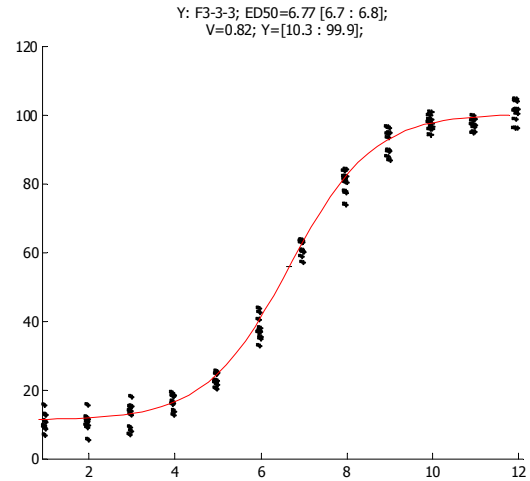

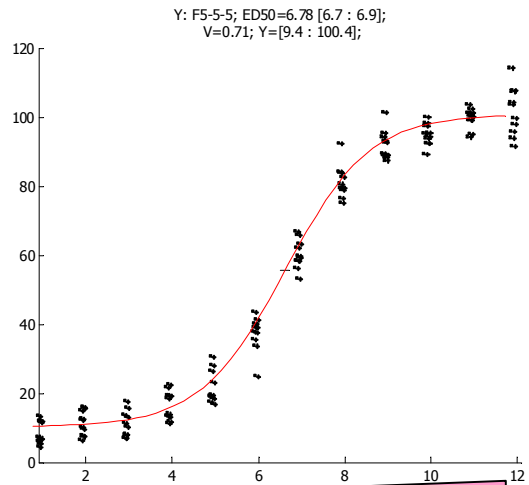

Noise increase

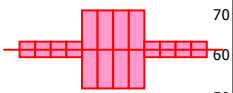

Pattern 2. Noise in the center of the curve

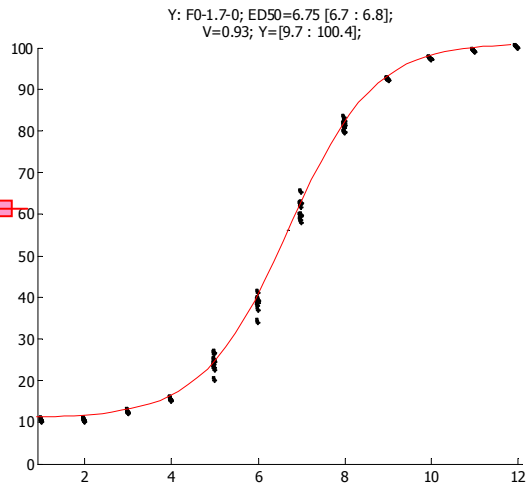

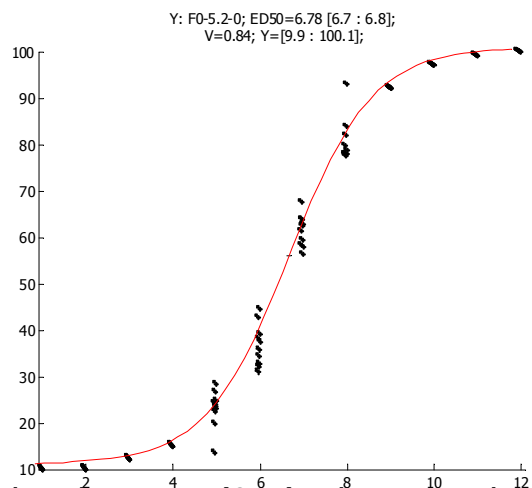

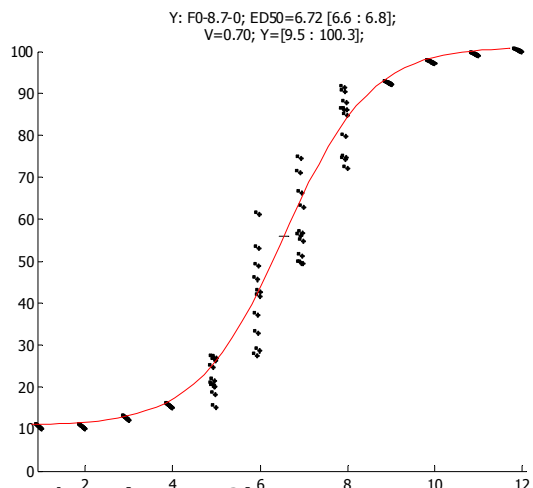

Noise at each dose has normal distribution $N(0,s_i)$ where i is dose number (1,…,12)

Average noise $S_{Av} = \frac{\sqrt{\sum_i S_i^2}}{n}$ is the same for patterns 1 and 2 at the same noise level.

Distribution of ED_{50} in Simulation

Noise level 1

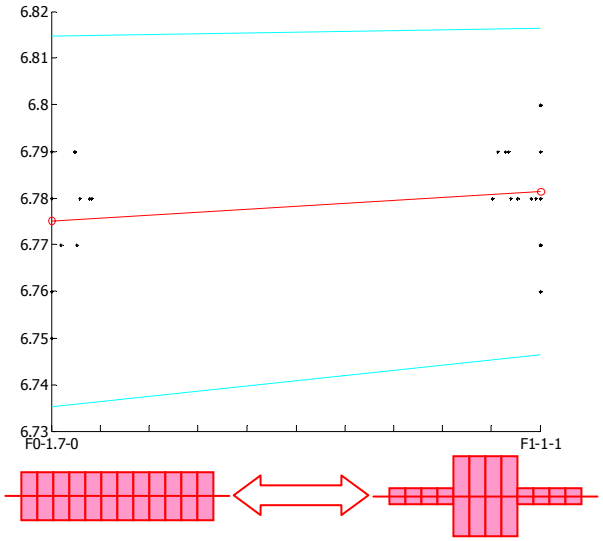

Comparison of averages:

Student's t: p>0.18

Z test: p>0.17

Comparison of variances:

Fisher's test: p>0.63

Bartlett's test: p>0.63

Noise level 2

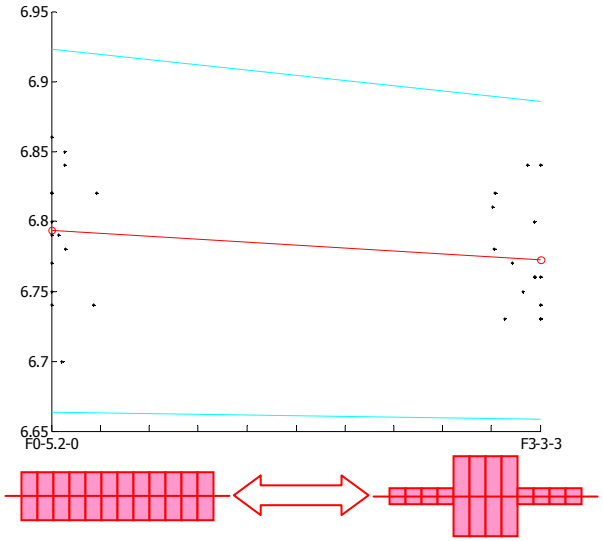

Comparison of averages:

Student's t: p>0.16

Z test: p>0.15

Comparison of variances:

Fisher's test: p>0.61

Bartlett's test: p>0.61

Noise level 3

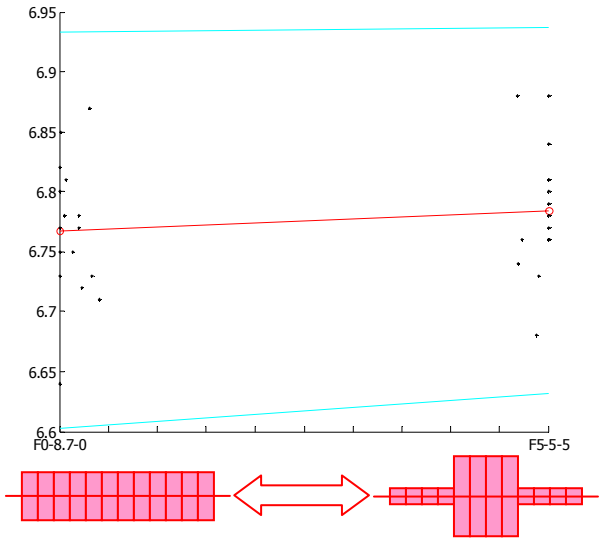

Comparison of averages:

Student's t: p>0.39

Z test: p>0.38

Comparison of variances:

Fisher's test: p>0.76

Bartlett's test: p>0.76

Conclusion: There is no significant difference between distributions of simulated ED_{50} between different patterns of noise: uniform across doses or concentrated in the middle of the curve. This suggests that equal weights in the V-factor formula are justified.

Dose-response for Measures Derived from Simulated Image Series

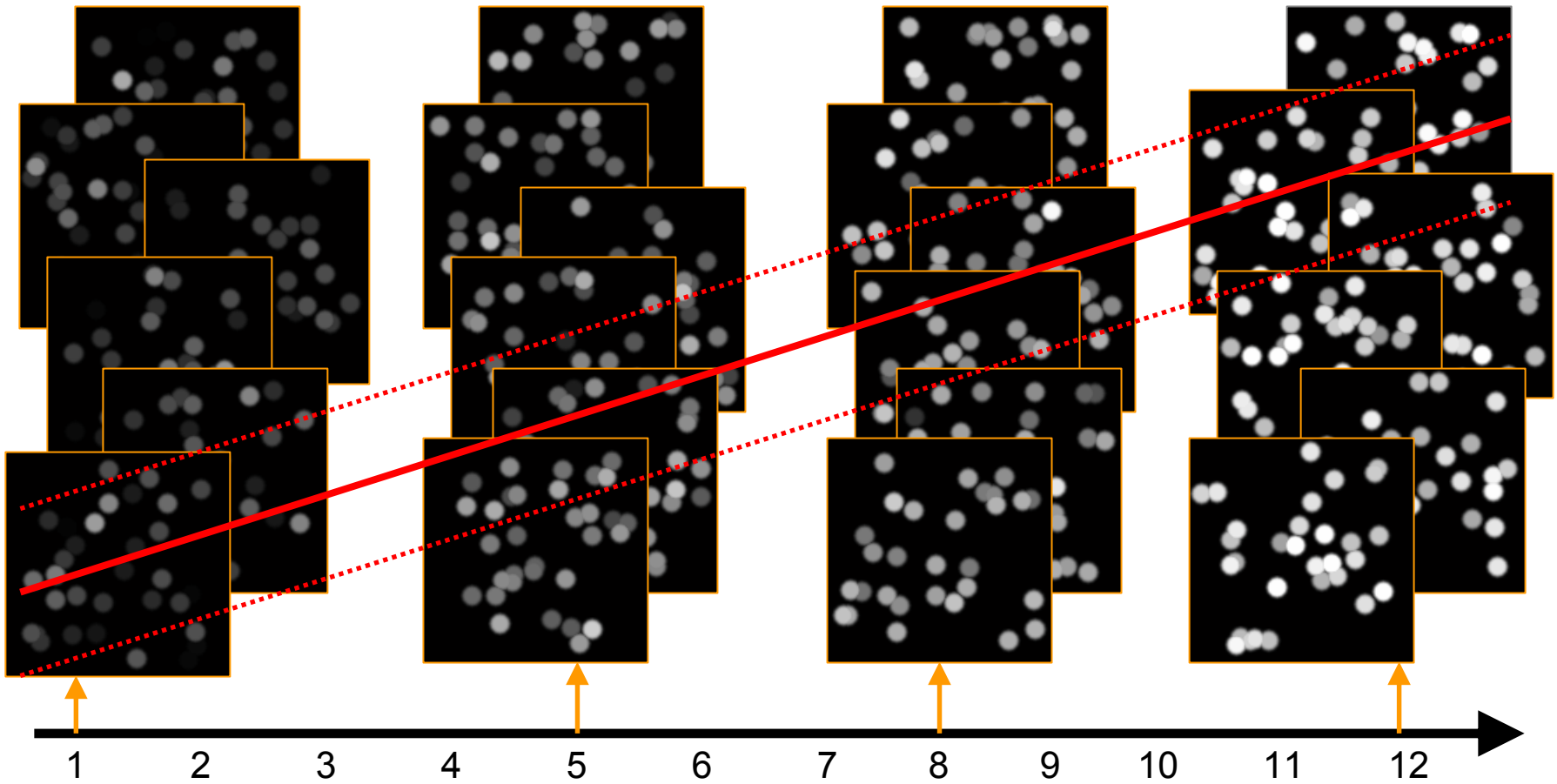

Circles ("cells") uniformly distributed in an image

Intensities of circles normally distributed

Average intensities increasing linearly with "dose"

A number of replica images at each "dose"

40 "cells"

$N(m_i, s)$, s = 17; intensity range 0-255

$m_i = a + d*i$, i=1,…12; a=20, d=7

15 replicas (images)

Calculations for Monte Carlo Simulation

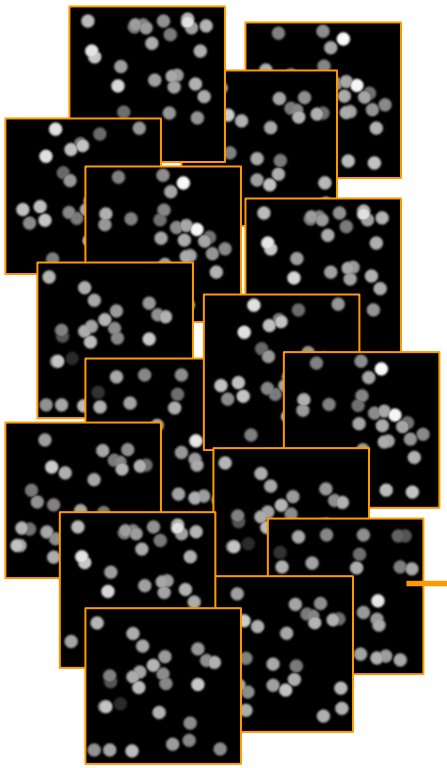

At every "dose" point for each replica image two measures are calculated:

1. Population Average of "Average Cell Intensity" (ACI)
2. "% of Cells with intensity > Threshold" (PCT)

These values are plotted and Z and V factors are calculated using formulas (1) and (4).

(ACI_j, PCT_j)

Simulation of "Average Intensity" Measure

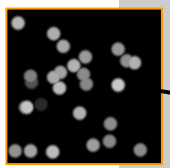

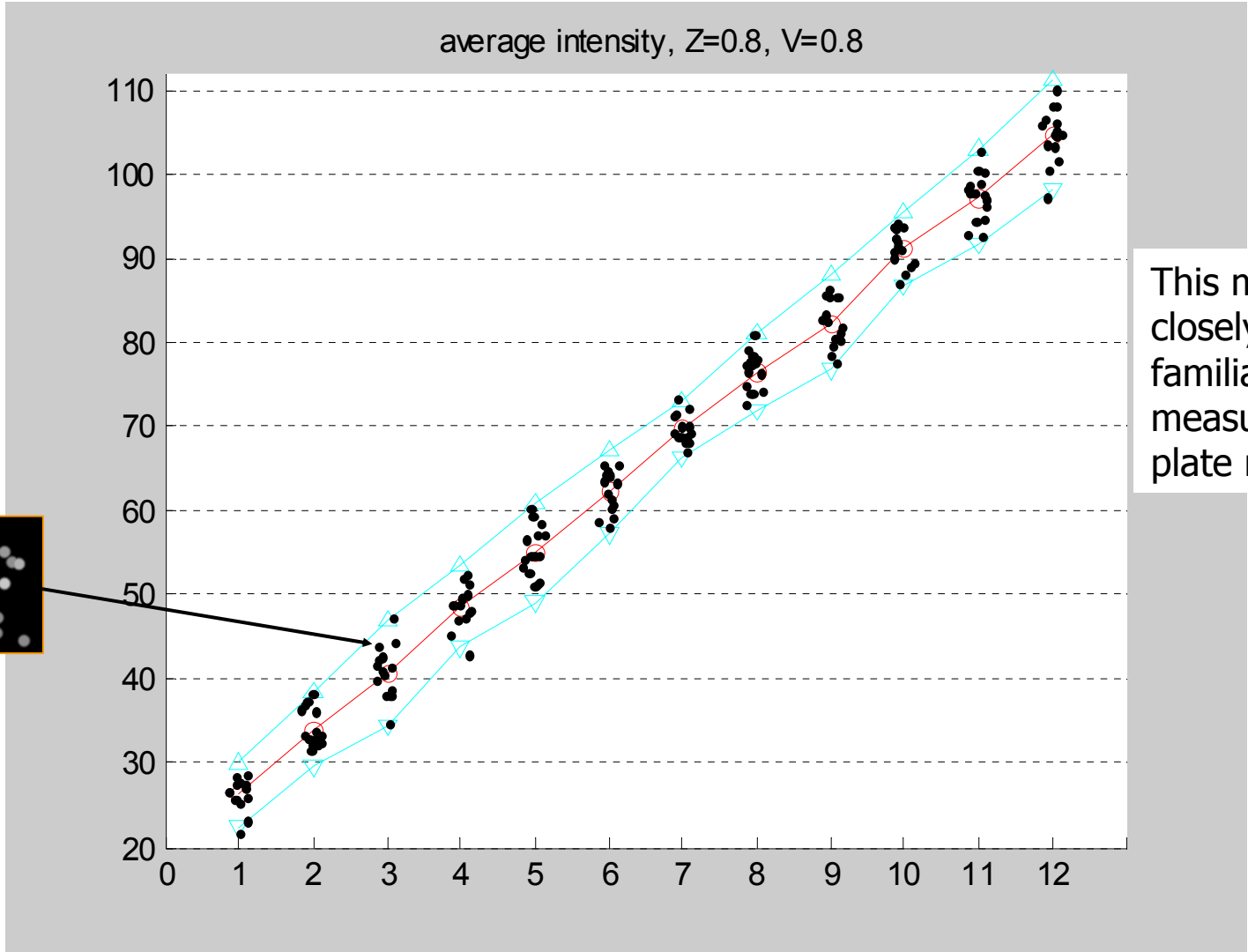

This measure most closely resembles familiar whole-well measurements of plate readers

Each black dot represents the cell population average of "average cell intensity" in one image; 15 replica images were generated per "dose" point. The red line represents averages of replicas. The cyan lines represent average +-2*SD of replicas within each "dose".

Simulation of "%Cells>Threshold" Measure

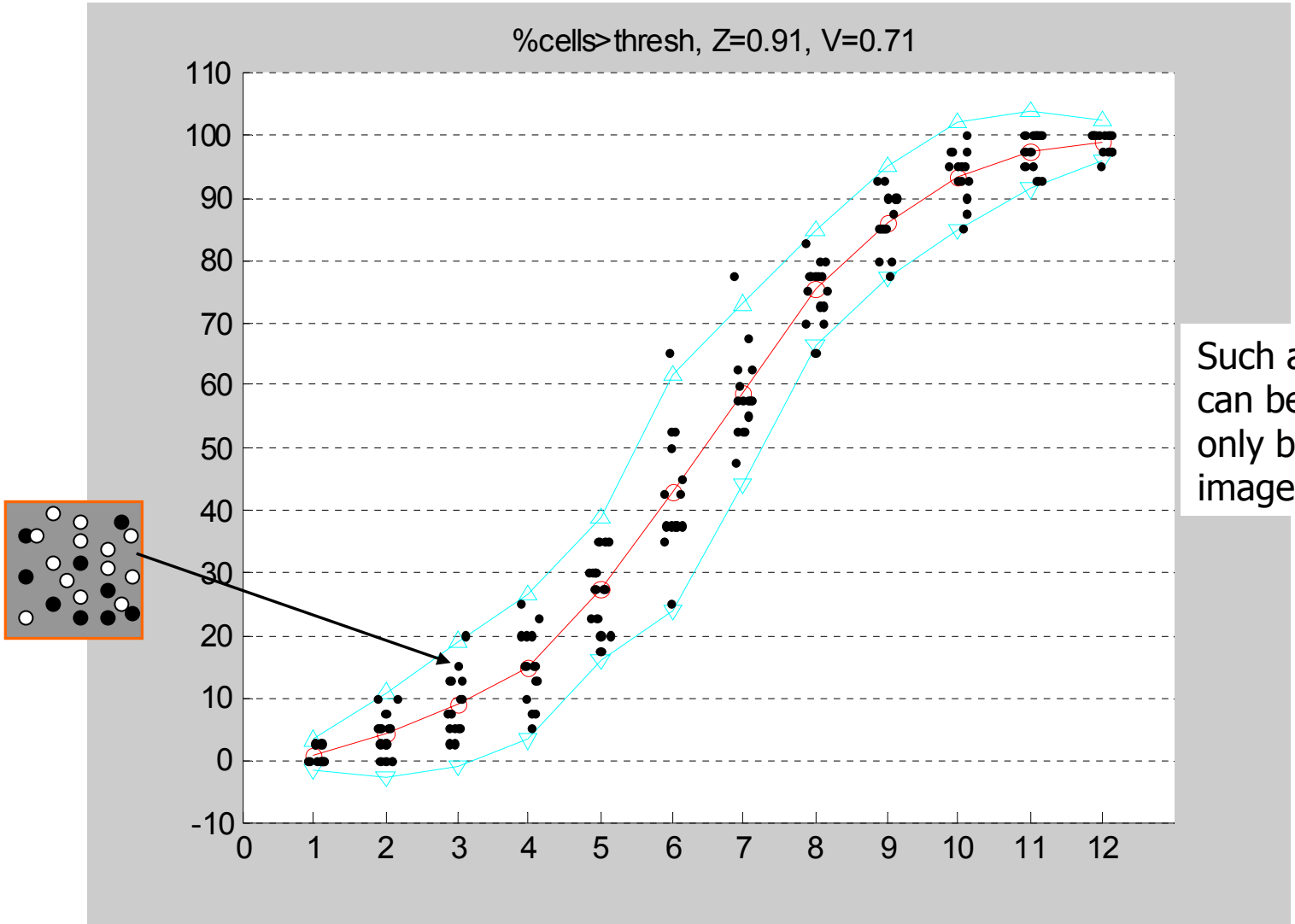

Such a measure can be calculated only by means of image analysis

Each black dot represents the "% of cells with intensity greater than threshold" measure in one image; 15 replica images were generated per "dose" point. Threshold = 65. The red line represents averages of replicas. The cyan lines represent average +-2*SD of replicas within each "dose".

Simulation of "%Cells>Threshold" at Different Thresholds

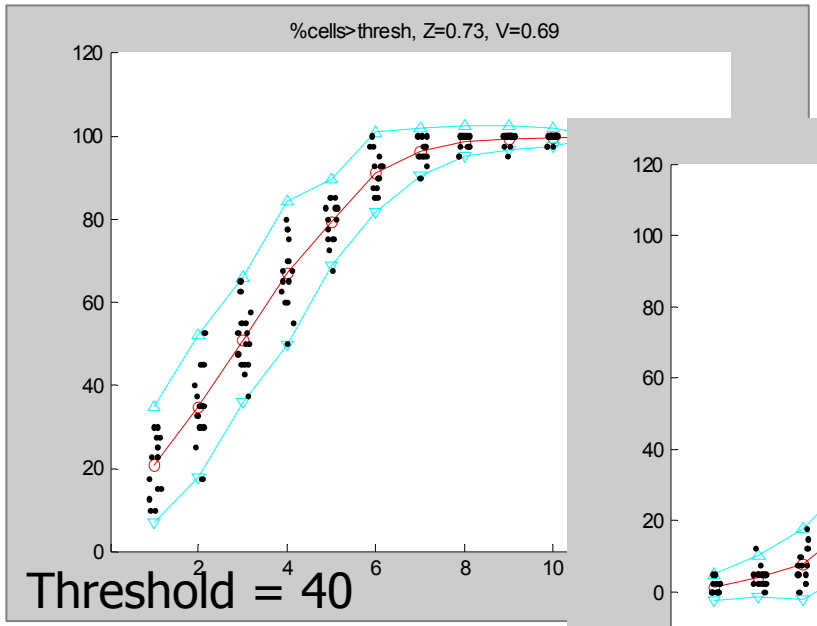

Threshold = 40

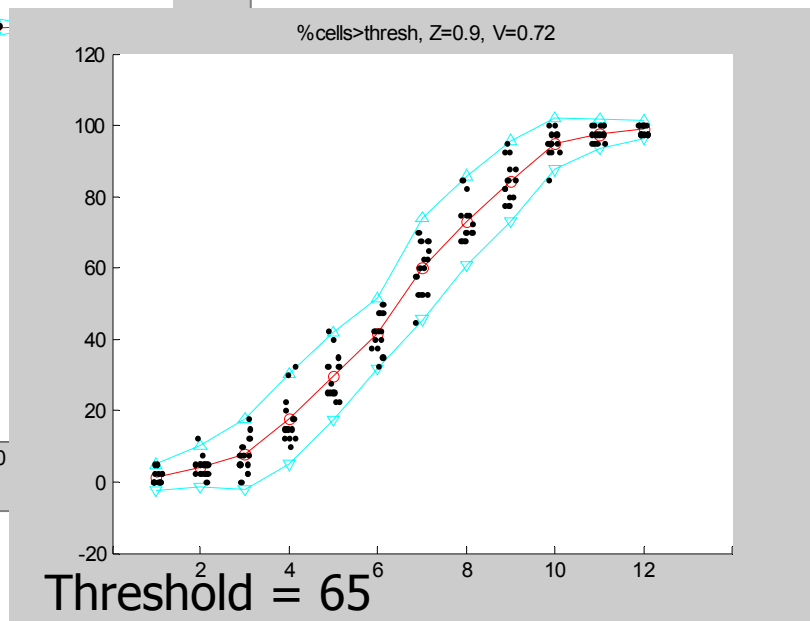

Threshold = 65

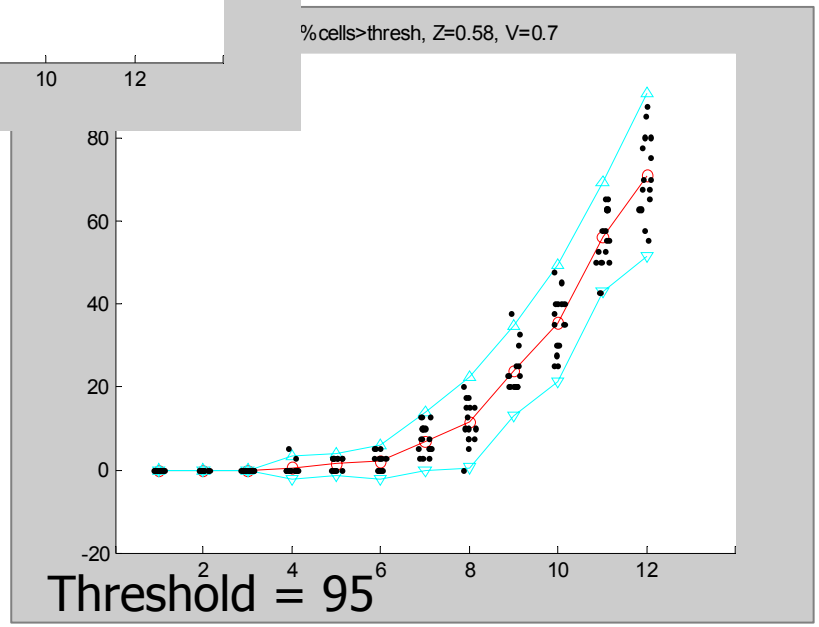

Threshold = 95

Conclusion from simulations:

- Even simple image-derived measures may behave differently from whole-well measures.
- Sample distribution at the extremes of the dose curve may be quite different from sample distribution in the middle of the curve. Saturation effects may be present at one or both ends of the dose curve.
- V-factor gives a more stable and a more realistic picture of the overall behavior.

Conclusions for Quality Measures and Simulations

- Imaging-based cellular assays have new computational properties compared to whole-well assays and their assessment calls for new quality measures.
- V-factor is less susceptible to computational artifacts than Z-factor.
- V-factor is more sensitive to dispensing errors, which are larger in the middle of the dose curve and gives a more realistic measure of assay performance.

Factors Affecting Assay Quality: Image Analysis Algorithm

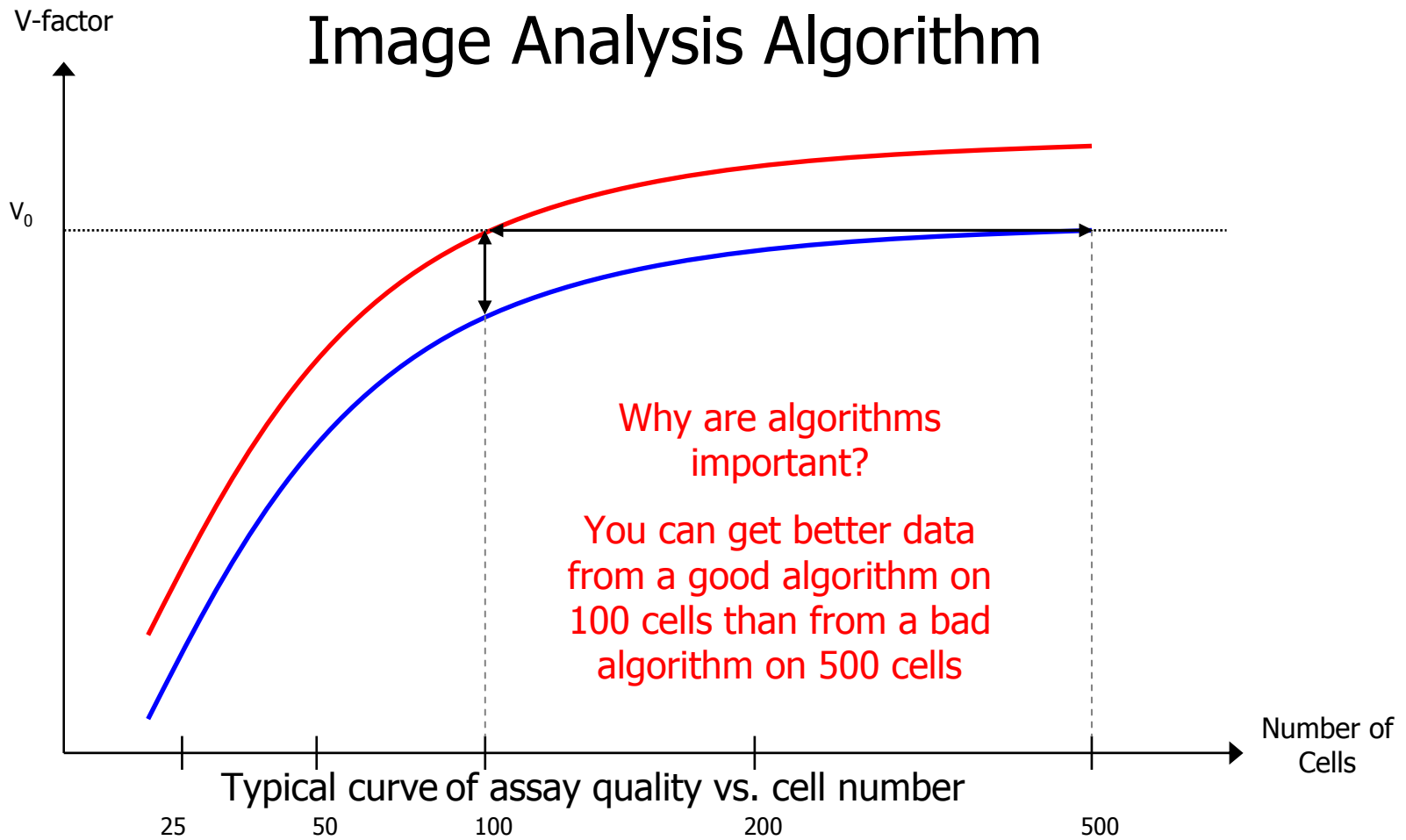

Typical curve of assay quality vs. cell number

Study of algorithm and parameter dependency of assay quality is easier to implement than studies of other dependencies because it does not require biological sample or imaging equipment and can be done on fixed sets of images asynchronously by different people. We have collected several sets of images which are now publicly available through the Society for Biomolecular Screening (*www.ravkin.net/SBS/D&IA_SIG.htm*). These images will be for the most part used in this presentation.

Available Image Sets: Cytoplasm to Nucleus Translocation

1. Vitra plate

This 96-well plate has images of cytoplasm to nucleus translocation of the transcription factor NFκB in MCF7 and A549 cells in response to TNFα concentration. It has 12 concentration points in columns and 4 replica rows for each cell type. The plate was acquired at Vitra Bioscience on the CellCard reader - a microscope-based system at 10X, 4X, 2X objective magnification. For each well there is one field with two images - a nuclear counterstain (DAPI) image and a signal stain (FITC) image. Image size is 1360*1024 pixels. Images are in 8-bit BMP format. File name structure is <channel>-<well-number>-<row>-<column>-<field>.BMP

negative

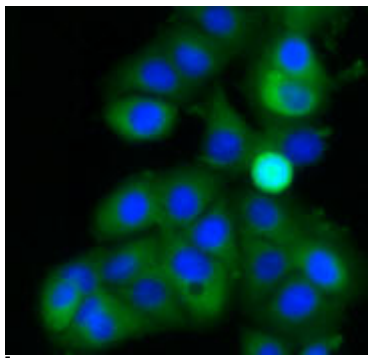

positive

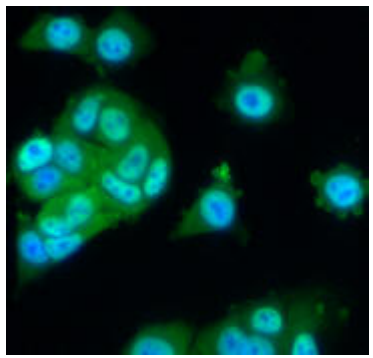

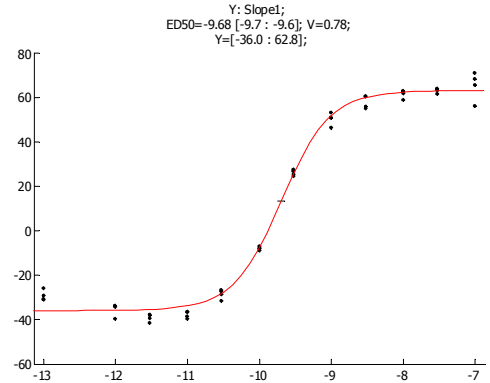

2. BioImage plate

This 96-well plate has images of cytoplasm to nucleus translocation of the Forkhead (FKHR-EGFP) fusion protein in stably transfected human osteosarcoma cells, U2OS. In proliferating cells FKHR is localized in the cytoplasm. Even without stimulation, Forkhead is constantly moving into the nucleus, but is transported out again by export proteins. Upon inhibition of nuclear export, FKHR accumulates in the nucleus. In this assay, export is inhibited by blocking PI3 kinase / PKB signaling by incubating cells for 1 hr with Wortmannin and with compound LY294002. There are 4 replicas of the 9-point dose curve for each drug. Nuclear counterstain is DRAQ. The images were acquired at BioImage on the IN Cell Analyzer 3000 and are available in native FRM format and converted to 8-bit BMP format with one image per channel. Image size is 640*640 pixels. File name structure in FRM format is <prefix>_<row><column>_<suffix>.frm; file name structure in BMP format is <channel>-<well-number>-<row>-<column>.BMP

negative

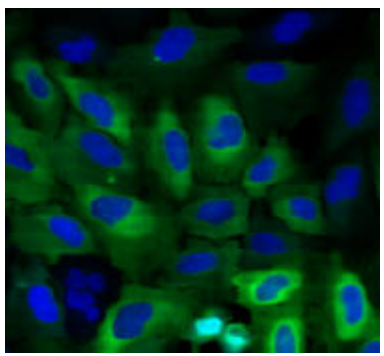

positive

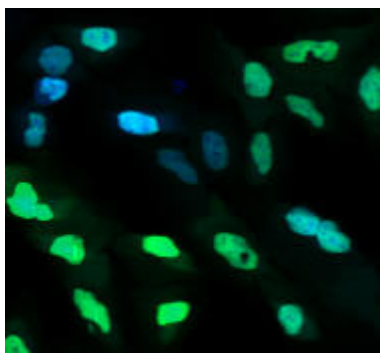

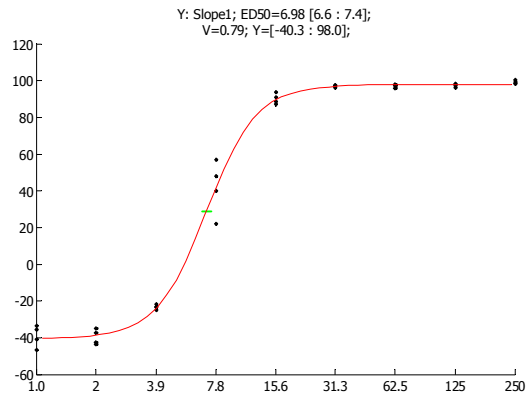

Available Image Sets: Transfluor™

1. CompuCyte image set

This image set has a portion of a 96-well plate containing 3 replica rows and 12 concentration points of isoproterenol. In each well four fields were acquired. The images are of U2OS cell line co-expressing beta2 adrenergic receptor (b2AR) and arrestin-GFP protein molecules. The receptor was modified-type that generates "vesicle-type" spots upon ligand stimulation. The plate was acquired on iCyte imaging cytometer with iCyte software version 2.5.1. Image file format is JPEG with one image for green channel and one image for crimson channel. Image size is 1000*768 pixels. File name structure: <well-number>_<field>_<channel>.JPG

negative 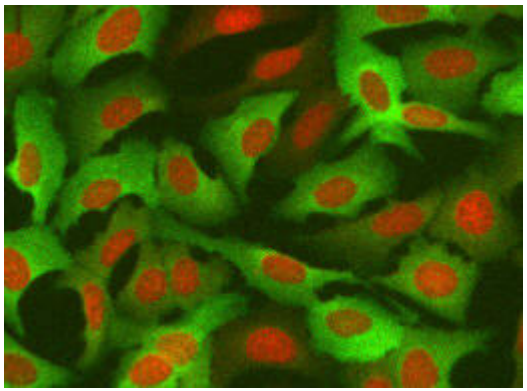

positive 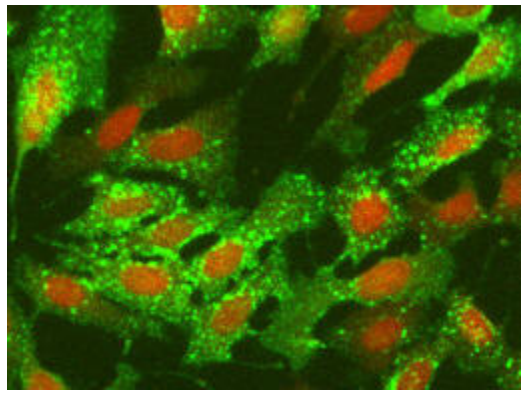

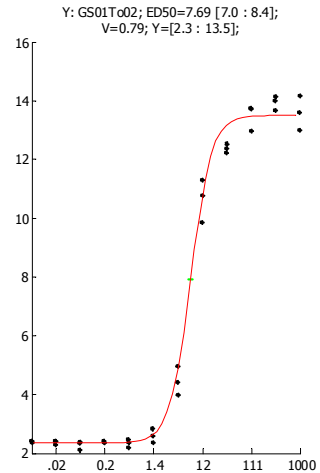

2. Roche image set

This image set is of Transfluor assay where an orphan GPCR is stably integrated into the b-arrestin GFP expressing U2OS cell line. After one hour incubation with a compound the cells were quenched with fixative (formaldehyde) and the plate was read on Cellomics ArrayScan HCS Reader using the GPCR Bioapplication. The images constitute one row of a 348 well plate. The dose curve consists of 11 dose points and one control. Each concentration is duplicated in adjacent wells. Each well has three fields. File format is 8-bit TIFF with one image for green channel and one image for blue channel. Image size is 512*512 pixels. File name structure: <prefix>_<row><column><field><channel>.TIF

negative 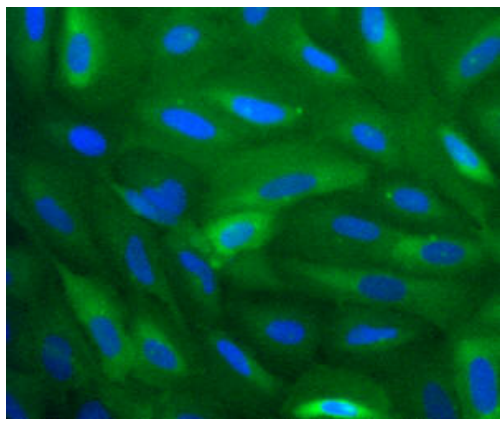

positive 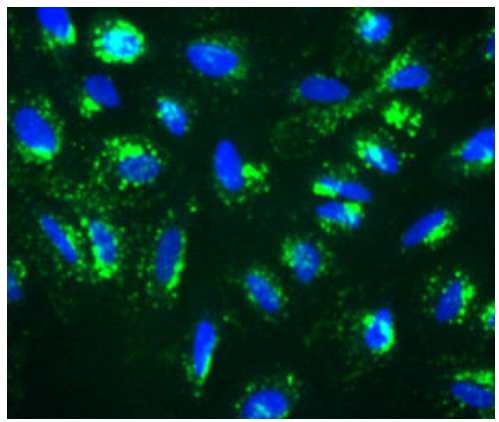

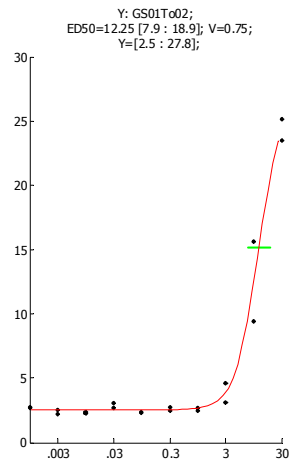

Comparison of Algorithms for Cytoplasm to Nucleus Translocation

Algorithms for Image Analysis of Cytoplasm to Nucleus Translocation

Algorithms based on 2D distributions of signal stain and counter stain in the whole cell, e.g. "Slope" algorithms

2 measures

Algorithms based on measuring signal stain in cellular compartments: nucleus, cytoplasm, or part of cytoplasm (ring)

Algorithms based on measuring by segmenting the image into cellular compartments

6 measures

Algorithms based on measuring without image segmentation into cellular compartments

6 measures

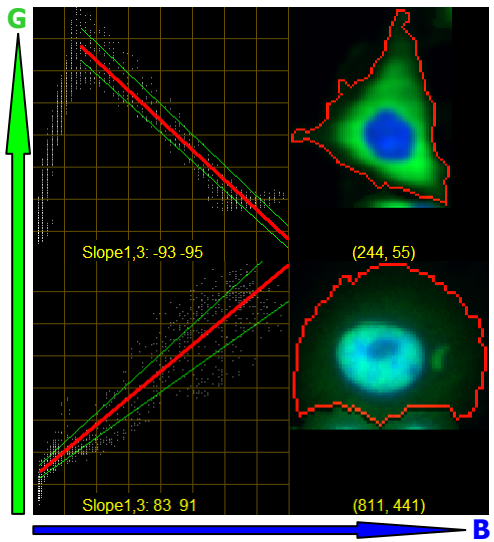

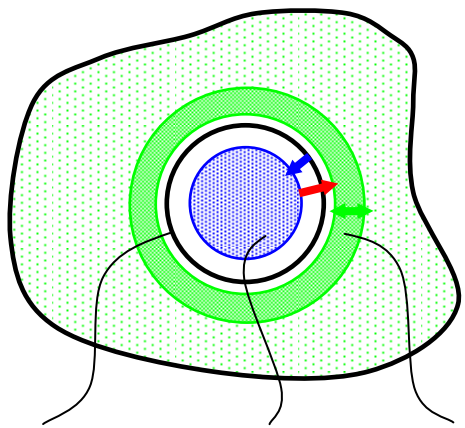

Nuclear mask

Eroded nuclear mask used for measurement

Ring mask

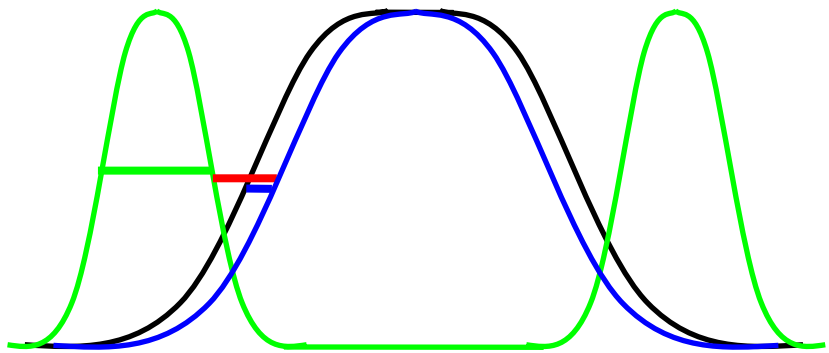

nuclear indicator function

eroded nuclear indicator function

ring indicator function

Family of Measures for Algorithms Based on Measuring Signal Stain in Cellular Compartments

A family of assay measures can be constructed as ratios of the average (A) or total (T) amounts of stained protein in the three compartments: nucleus (N), cytoplasm (C), and ring (R). For more convenient scaling we use $100*\log_2()$ of all ratio measures. In addition, a non-ratio measure of the amount of signal stain in the nucleus may be also useful. The measures may be produced by segmentation into masks of nucleus and cytoplasm (M) or without segmentation by the use of indicator functions (W). Each measure may be calculated for each cell and then the well measure is some statistic of the cell population, e.g. mean or median; alternatively these measures may be calculated globally on the whole image (G).

The family of measures is given by the formulas: **N2{R|C}_{A|T}{W|M}{ |G}** and **N_{A|T}{W|M}{ |G}**.

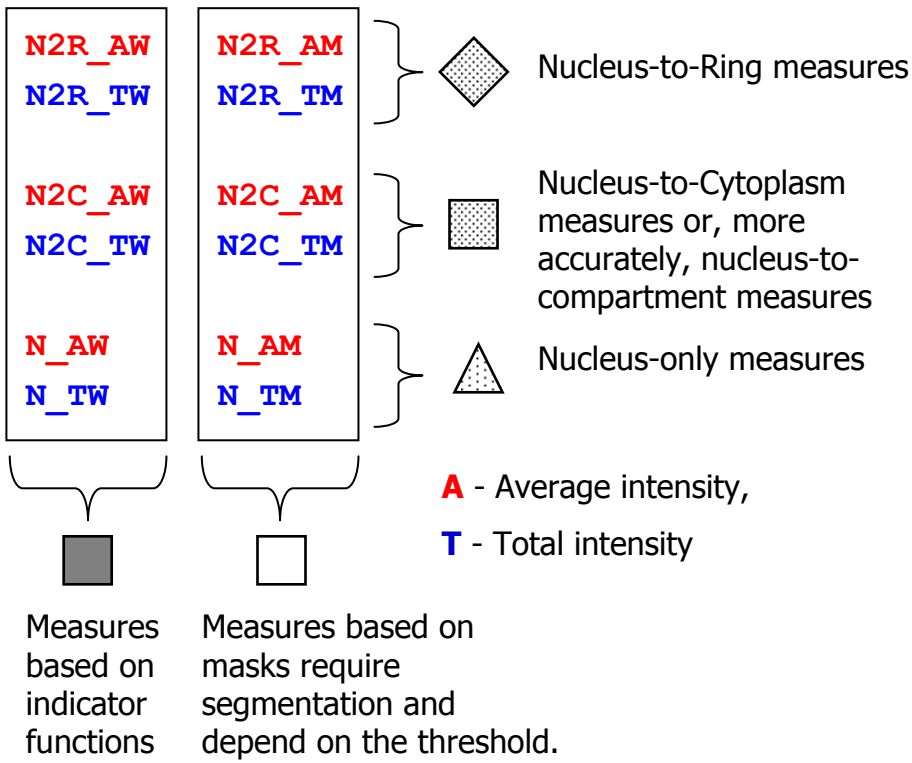

Factors Affecting Assay Quality: Algorithms and Parameters

Vitra Plate, MCF7 cells

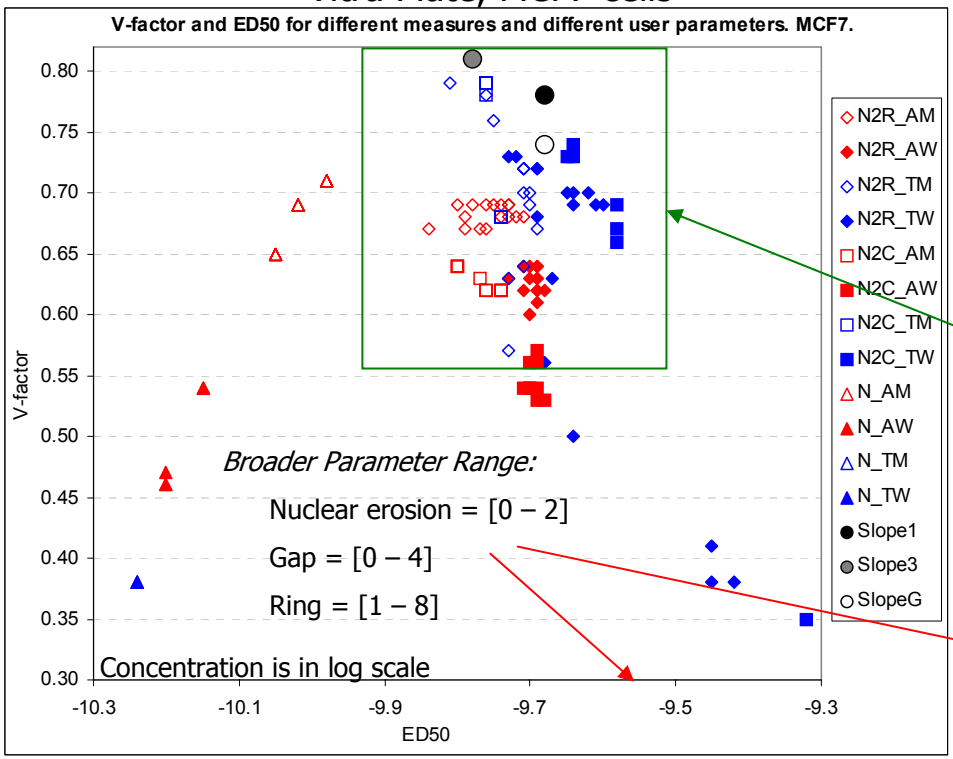

BioImage Plate, Wortmannin

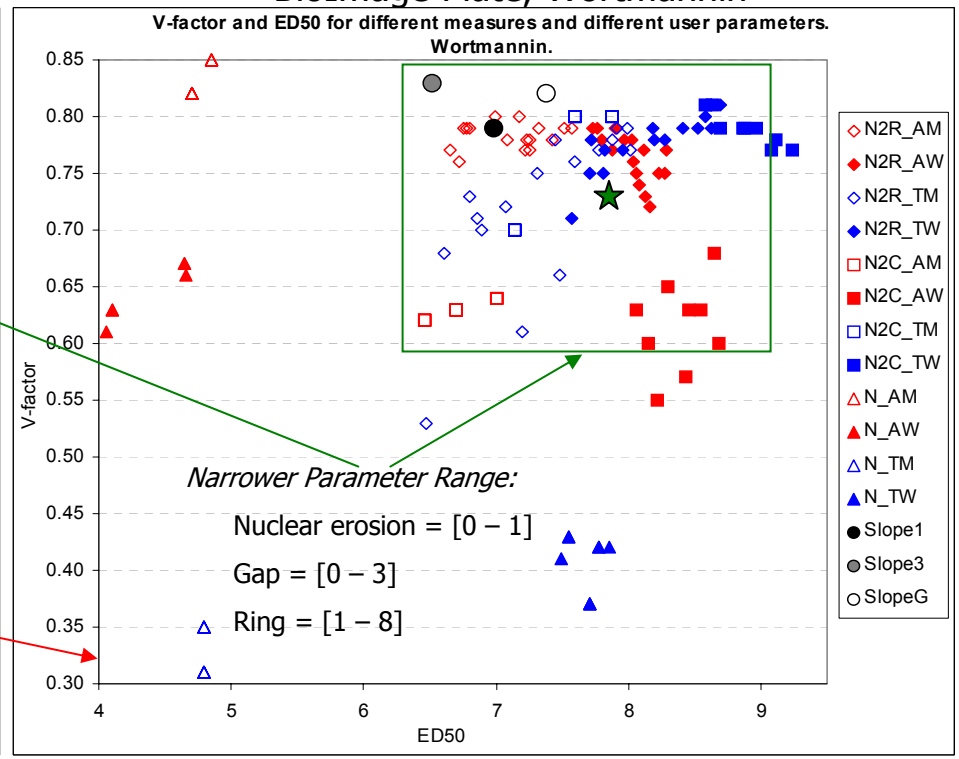

- There is a systematic shift between ED_{50} of different measures. If the goal is comparing drugs or cell types, then the same measure should be used for the whole experiment.
- Some measures have very strong parameter-dependency; other measures have mild parameter dependency and group in compact clusters.
- Different measures have maximum quality at different parameter values, which depend on drug and cell type. This means that in a real experiment algorithms operate not at optimal parameter settings for all conditions. For a fair comparison, the quality of different measures must be averaged over a reasonable parameter range. Therefore, measures which do not depend on parameters, have a big advantage.
- Conceptually similar measures implemented by different vendors can show noticeable difference in quality.

Factors Affecting Assay Quality: Cell Number

Vitra Plate, MCF7 cells

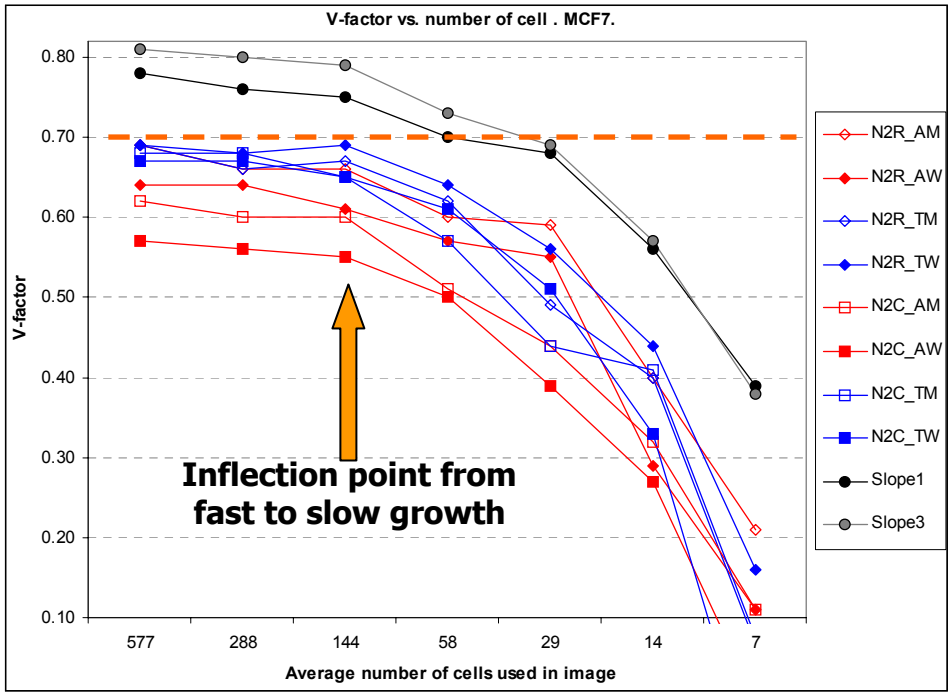

BioImage Plate, Wortmannin

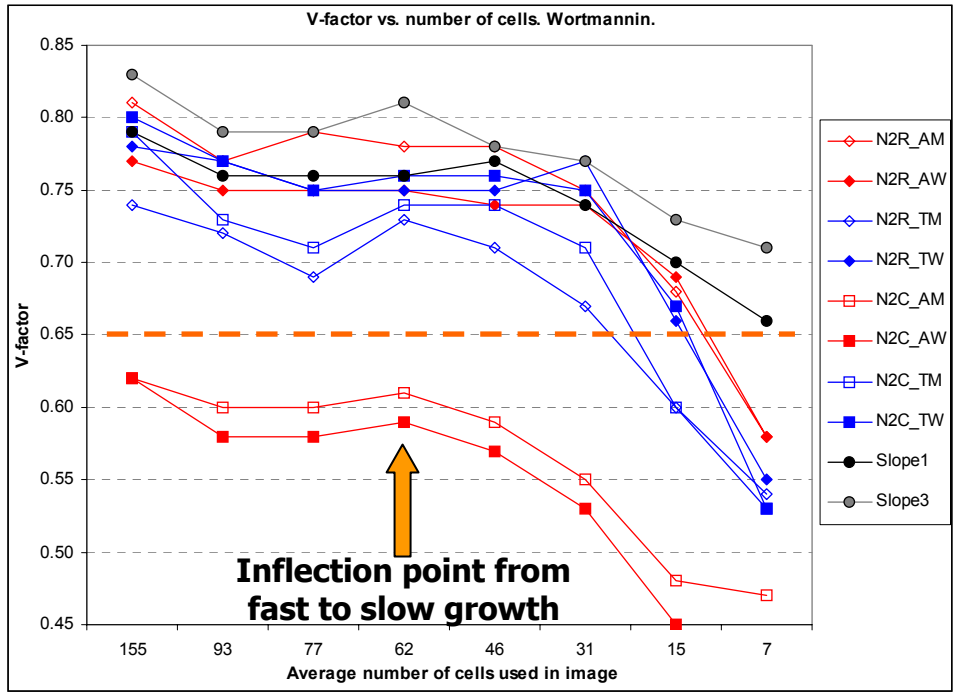

Parameters:

Nuclear erosion = 1

Gap = 2

Ring = 4

The factor that most directly affects assay quality is the number of analyzed cells. To eliminate possible positional dependency we selected random subsets of cells from the whole image, and not contiguous image fragments.

- At a certain number of cells the quality curve changes from fast to slow growth; the curves in each plot are shifted only in Y, but not in X, which means that this number depends on images, but not on algorithm.
- Some algorithms never reach quality of other algorithms.
- The quality curve does not really plateau, but keeps rising very slowly.

Factors Affecting Assay Quality: Magnification and Image Size

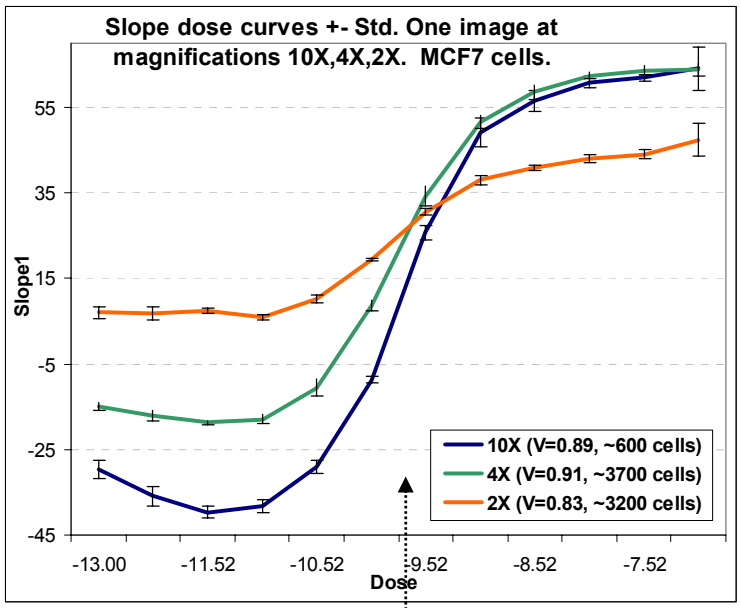

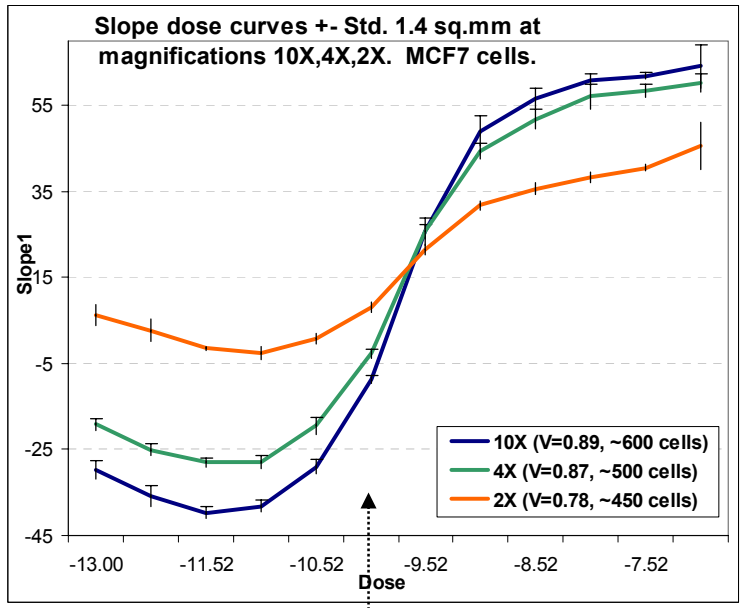

Vitra plate.
MCF7 cells.

At lower magnifications the dynamic range is reduced, but the variability is also reduced, so the quality (V-factor) remains stable.

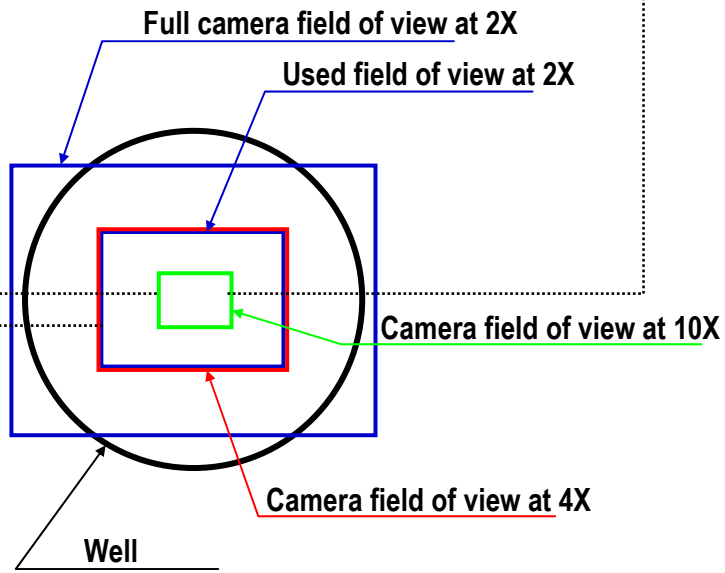

For the same imaged area (right plot) higher magnification improves quality. However, the increased number of cells in one camera image at lower magnification (left plot) works in the opposite direction. The maximum is at 4X.

Cell Proliferation Assay

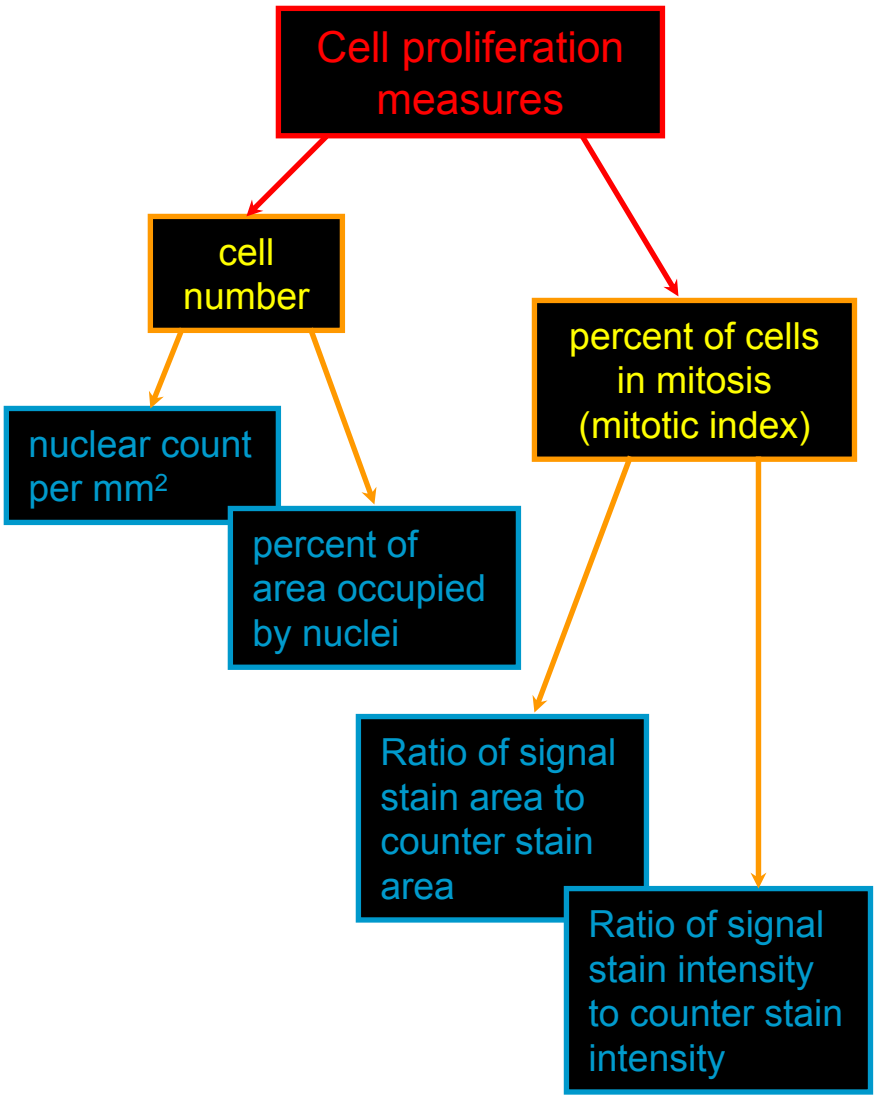

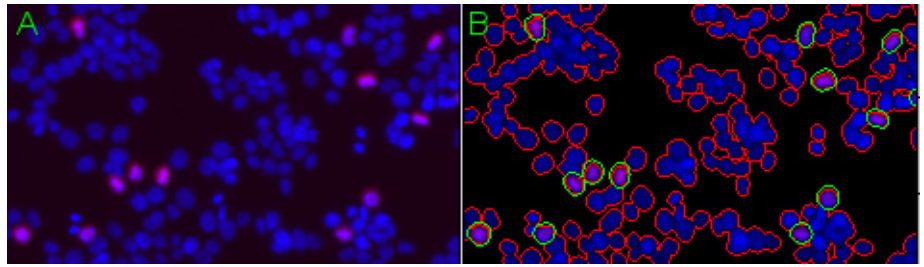

A – image of Mitotic Index assay.
Counter stain - blue,
Mitotic phase stain - red

B – adaptive threshold contours.
For the counter stain - red,
for the signal stain - green

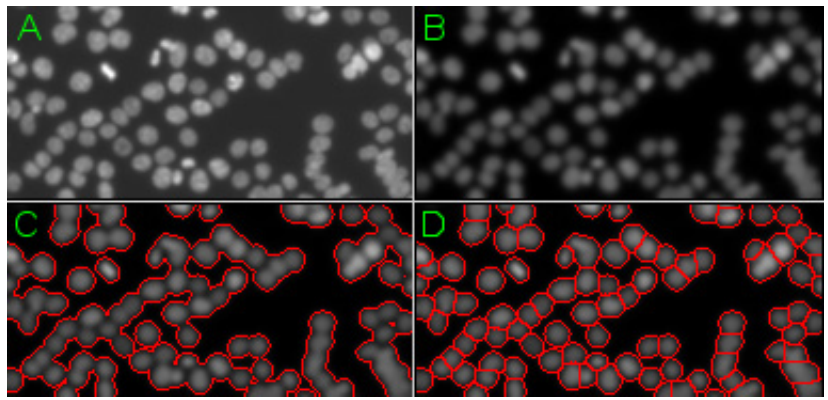

Counting of nuclei:
A - image of counter stain,
B - smoothed image,
C - smoothed image with adaptive threshold contours,
D – contours with watershed separation lines inside.

Dose Curves for Cell Proliferation Measures

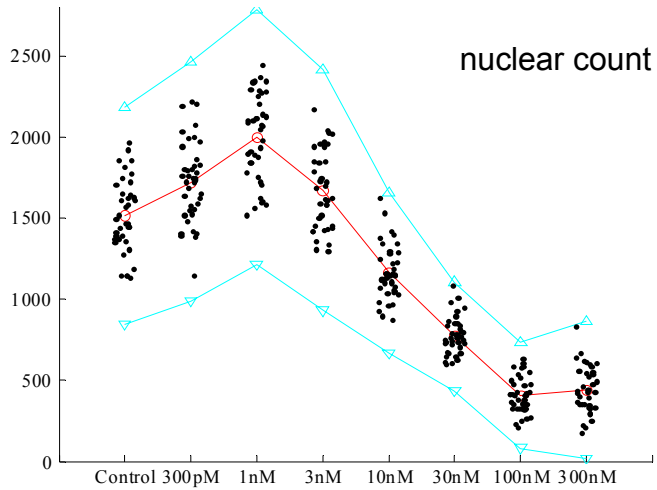

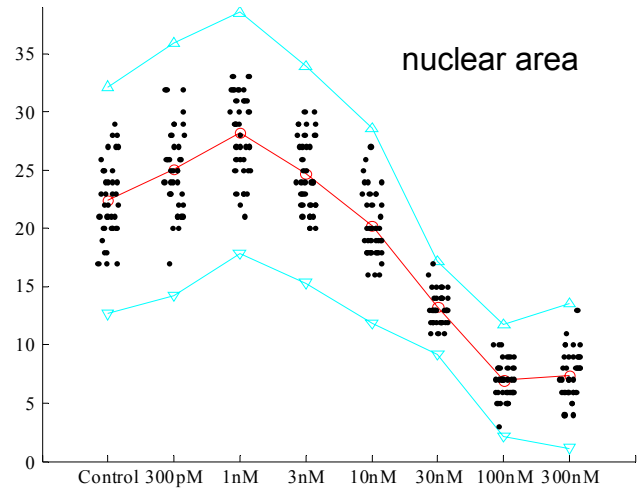

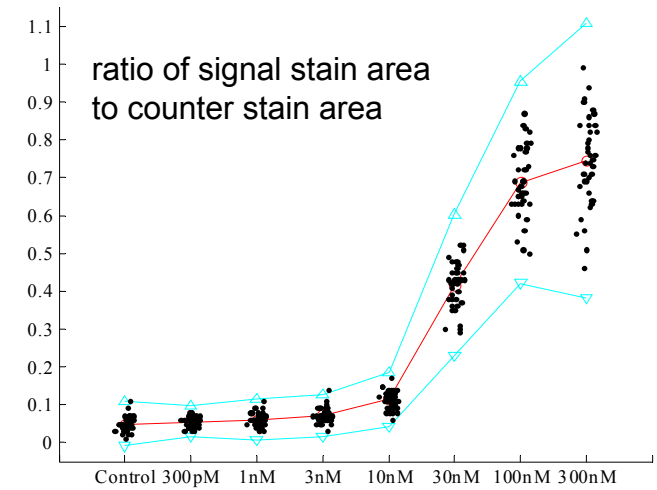

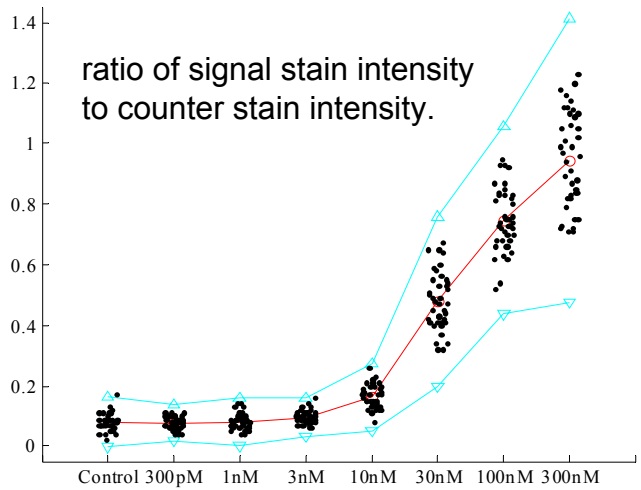

Response of HCT116 cells to Paclitaxel at different concentrations.
Dots are values from fragment images of 0.4mm^2 at 2X magnification.
Middle line - average, top and bottom lines - average +/- 3*SD.

Factors Affecting Assay Quality: Image Resolution and Image Size

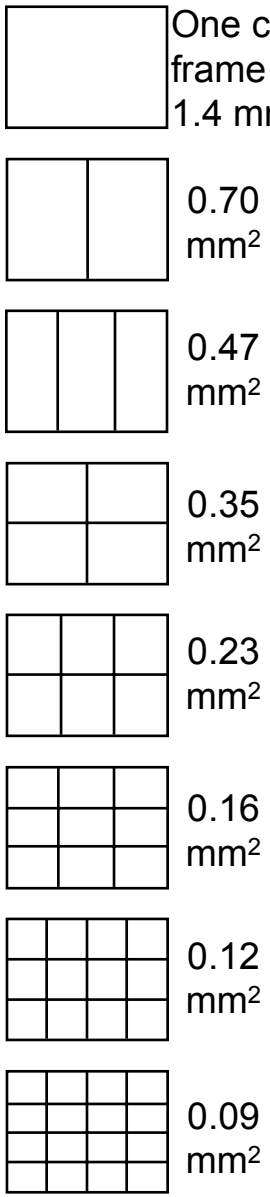

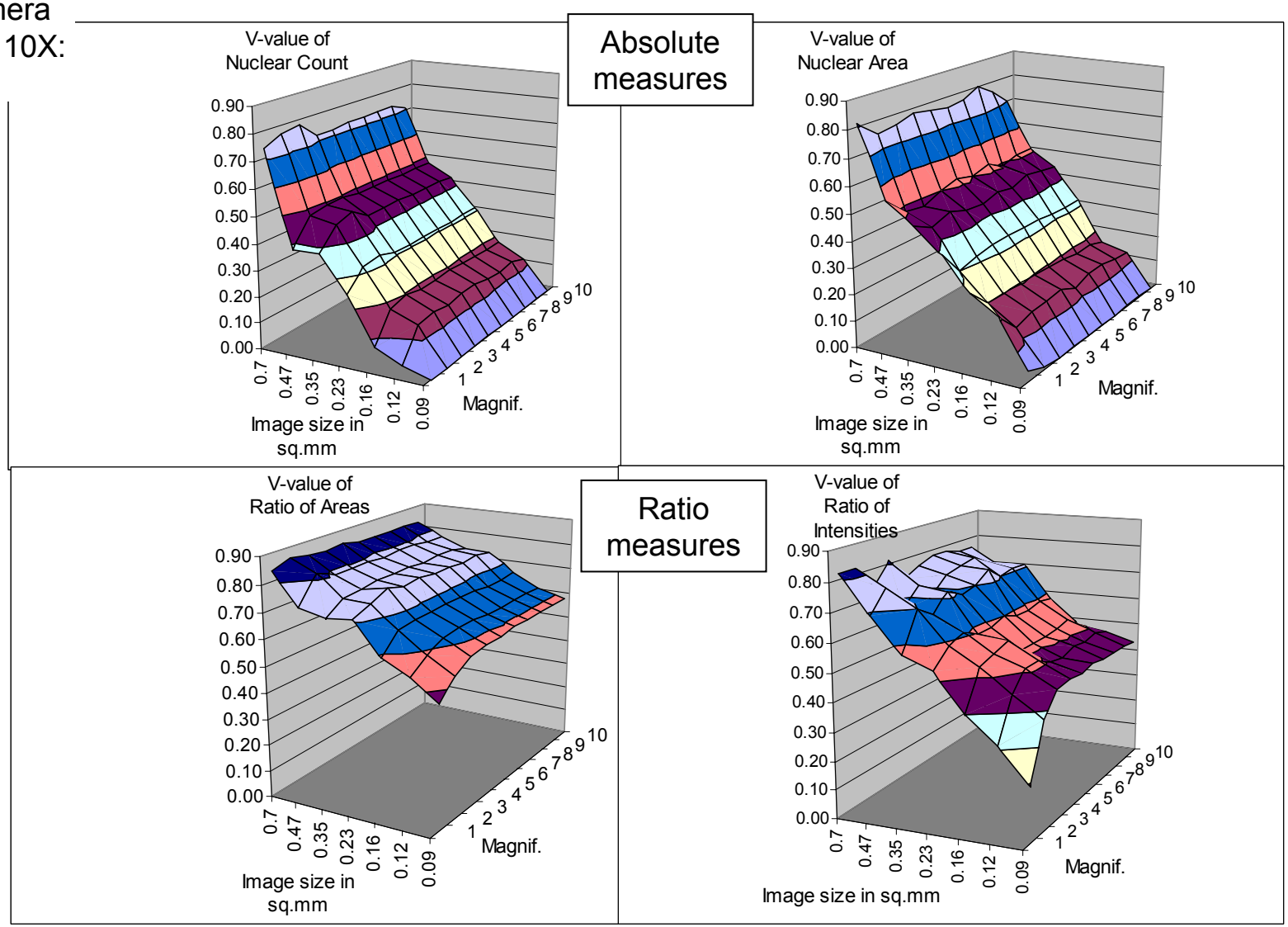

Magnification is interpolated from 10X.

Factors Affecting Assay Quality: Image Size

V-factors of four measures of cell proliferation at objective magnification 2X as a function of image size.

Whole image size = 16mm^2.

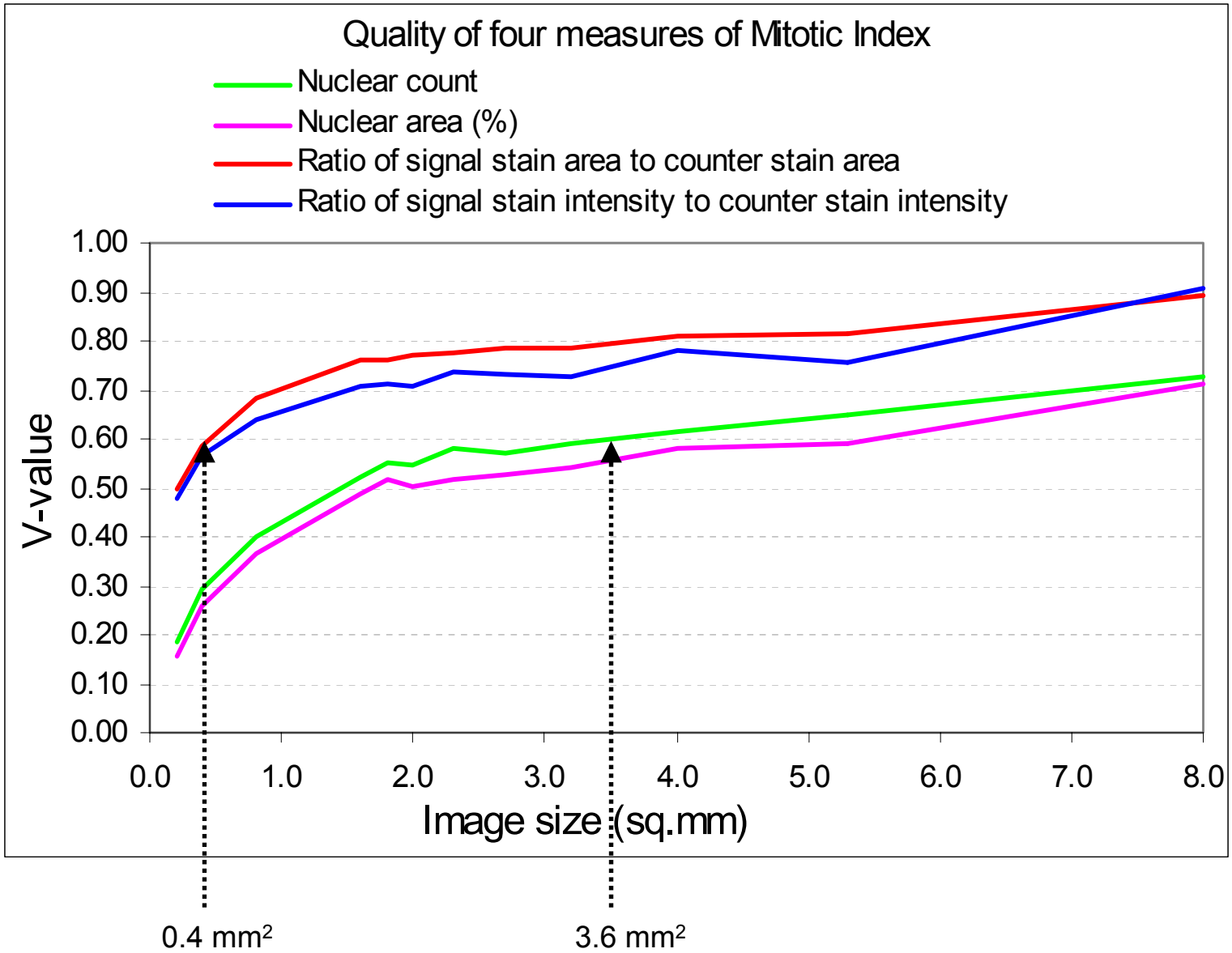

Transfluor™ Assay - Analysis of Granularity

The basis of the method is the concept known in mathematical morphology as size distribution[1], granulometry[3,4], pattern spectrum[2] or granular spectrum[5]. This distribution is produced by a series of openings of the original image with structuring elements of increasing size. At each step the volume of the open image is calculated as the sum of all pixels. The difference in volume between the successive steps of opening is the granular spectrum. The distribution is normalized to the total volume (integrated intensity) of the image. This diagram shows how openings of increasing size affect images with different granularity.

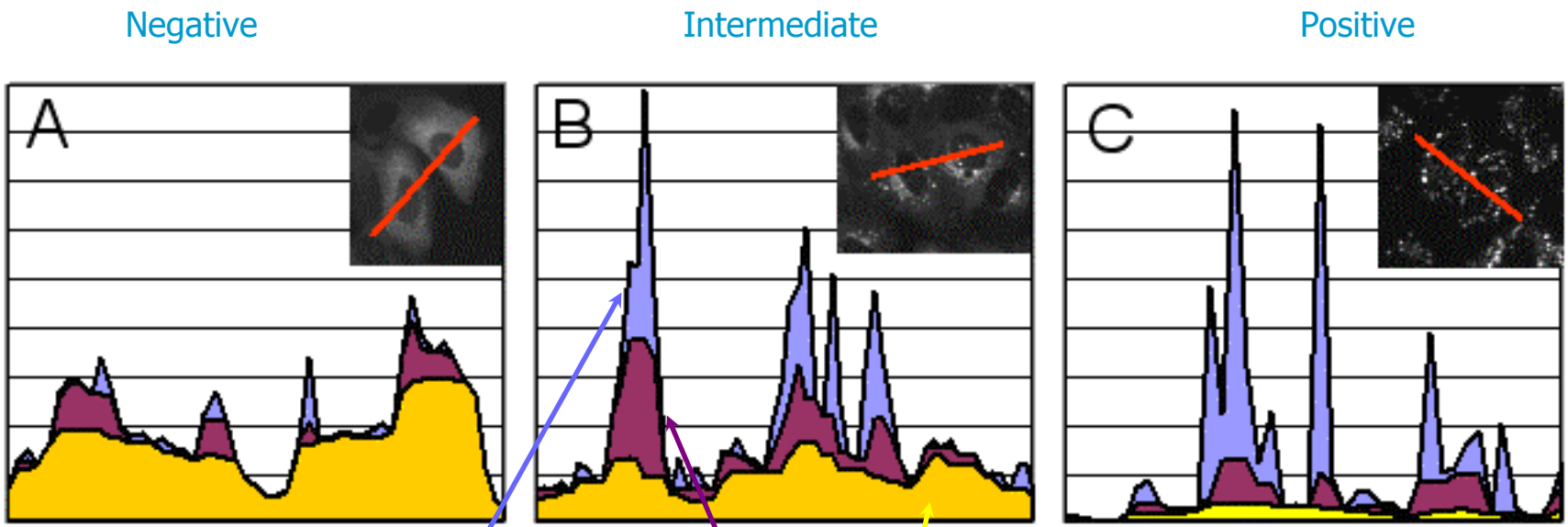

Brightness profiles through cells:

in the original image (blue),

in the image opened by structuring element of size 1 (red)

in the image opened by structuring element of size 4 (yellow)

Note: the method uses only one color and does not require segmentation into individual cells

Transfluor™ Assay - CompuCyte Image Set

	1	2	3	4	5	6	7	8	9	10	11	12
A												
B												
C												
D												
E	1 uM	333 nM	111 nM	37 nM	12 nM	4.1 nM	1.4 nM	457 pM	152 pM	51 pM	17 pM	5.6 pM
F	1 uM	333 nM	111 nM	37 nM	12 nM	4.1 nM	1.4 nM	457 pM	152 pM	51 pM	17 pM	5.6 pM
G	1 uM	333 nM	111 nM	37 nM	12 nM	4.1 nM	1.4 nM	457 pM	152 pM	51 pM	17 pM	5.6 pM
H												

Effector: isoproterenol

This image set has a portion of a 96-well plate containing 3 replica rows and 12 concentration points of isoproterenol. In each well four fields were acquired. The images are of U2OS cell line co-expressing beta2 adrenergic receptor (b2AR) and arrestin-GFP protein molecules. The receptor was modified-type that generates "vesicle-type" spots upon ligand stimulation. The plate was acquired on iCyte imaging cytometer with iCyte software version 2.5.1. Image file format is JPEG with one image for green channel and one image for crimson channel. Image size is 1000*768 pixels.

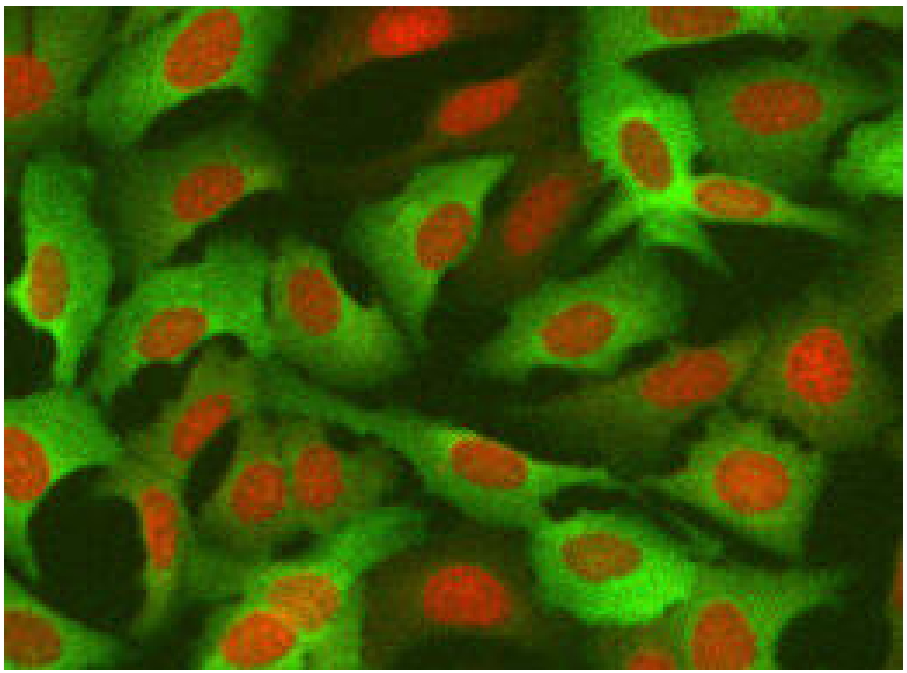

Negative

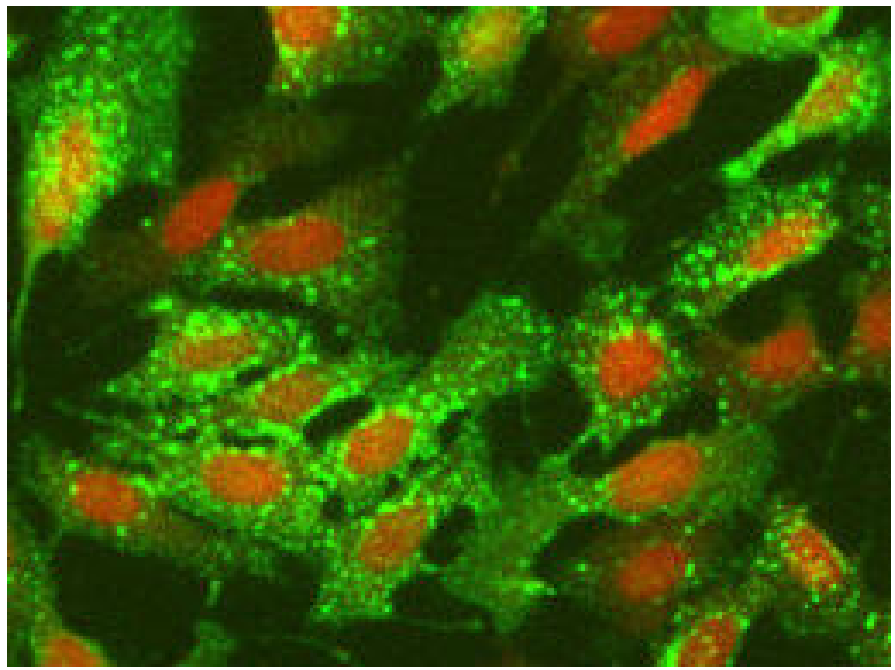

Positive

Factors Affecting Assay Quality: Image Resolution

Dose-independent granular component GS01 suggests "empty" magnification (oversampling)

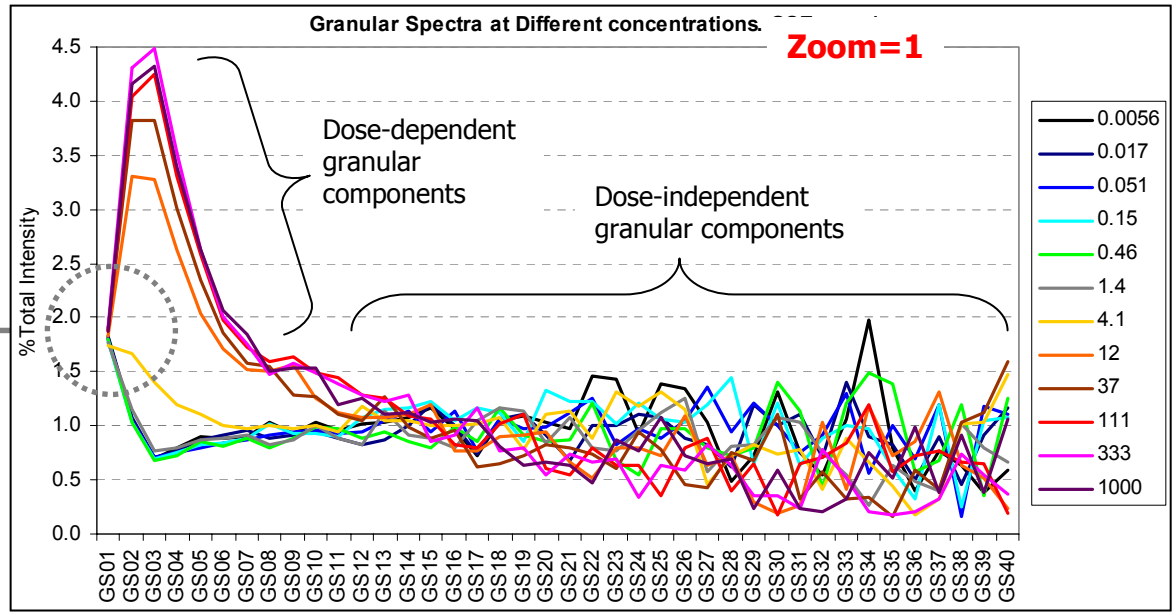

CompuCyte image set

Subsampling of 0.25 is chosen for further analysis.

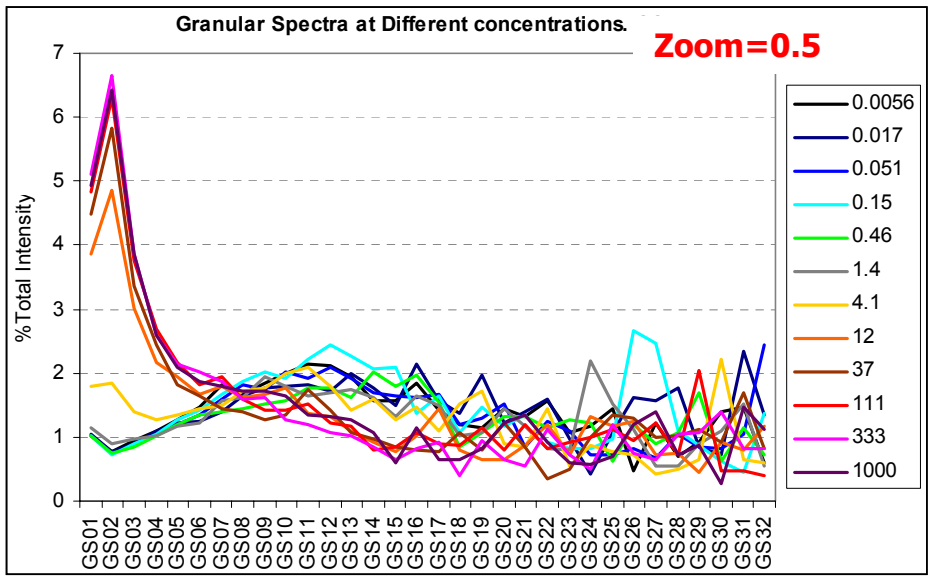

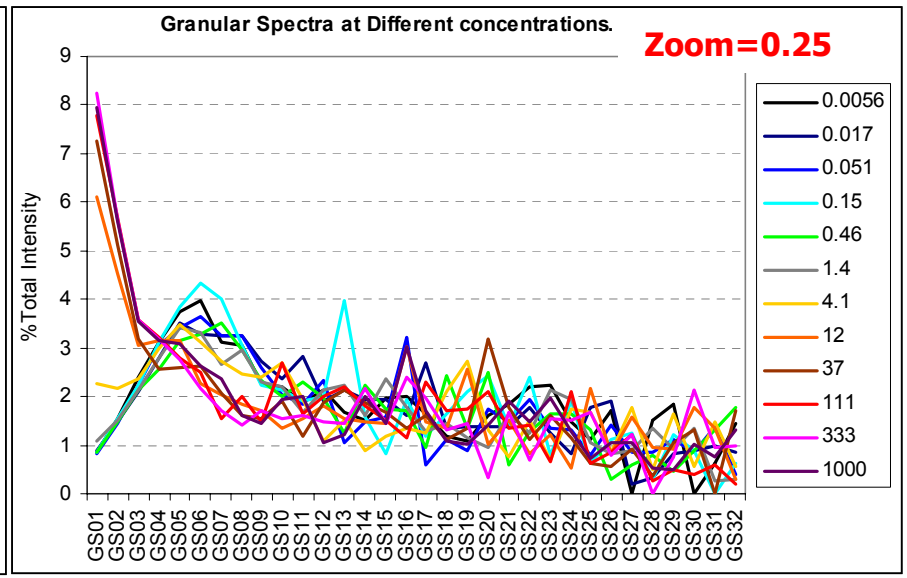

Transfluor™ Assay - Roche/Cellomics Image Set

	1	2	3	4	5	6	7	8	9	10	11	12	13	14	15	16	17	18	19	20	21	22	23	24
A	GRK	Untreated	Untreated	Untreated	30 uM	30 uM	10 uM	10 uM	3 uM	3 uM	1 uM	1 uM	300 nM	300 nM	100 nM	100 nM	30 nM	30 nM	10 nM	10 nM	3 nM	3 nM	1 nM	1 nM
B	GRK	Untreated	Untreated	Untreated	30 uM	30 uM	10 uM	10 uM	3 uM	3 uM	1 uM	1 uM	300 nM	300 nM	100 nM	100 nM	30 nM	30 nM	10 nM	10 nM	3 nM	3 nM	1 nM	1 nM
C	GRK	Untreated	Untreated	Untreated	30 uM	30 uM	10 uM	10 uM	3 uM	3 uM	1 uM	1 uM	300 nM	300 nM	100 nM	100 nM	30 nM	30 nM	10 nM	10 nM	3 nM	3 nM	1 nM	1 nM
D	GRK	Untreated	Untreated	Untreated	30 uM	30 uM	10 uM	10 uM	3 uM	3 uM	1 uM	1 uM	300 nM	300 nM	100 nM	100 nM	30 nM	30 nM	10 nM	10 nM	3 nM	3 nM	1 nM	1 nM
E	GRK	Untreated	Untreated	Untreated	30 uM	30 uM	10 uM	10 uM	3 uM	3 uM	1 uM	1 uM	300 nM	300 nM	100 nM	100 nM	30 nM	30 nM	10 nM	10 nM	3 nM	3 nM	1 nM	1 nM
F	GRK	Untreated	Untreated	Untreated	30 uM	30 uM	10 uM	10 uM	3 uM	3 uM	1 uM	1 uM	300 nM	300 nM	100 nM	100 nM	30 nM	30 nM	10 nM	10 nM	3 nM	3 nM	1 nM	1 nM
G	GRK	Untreated	Untreated	Untreated	30 uM	30 uM	10 uM	10 uM	3 uM	3 uM	1 uM	1 uM	300 nM	300 nM	100 nM	100 nM	30 nM	30 nM	10 nM	10 nM	3 nM	3 nM	1 nM	1 nM
H	GRK	Untreated	Untreated	Untreated	30 uM	30 uM	10 uM	10 uM	3 uM	3 uM	1 uM	1 uM	300 nM	300 nM	100 nM	100 nM	30 nM	30 nM	10 nM	10 nM	3 nM	3 nM	1 nM	1 nM
I	GRK	Untreated	Untreated	Untreated	30 uM	30 uM	10 uM	10 uM	3 uM	3 uM	1 uM	1 uM	300 nM	300 nM	100 nM	100 nM	30 nM	30 nM	10 nM	10 nM	3 nM	3 nM	1 nM	1 nM
J	GRK	Untreated	Untreated	Untreated	30 uM	30 uM	10 uM	10 uM	3 uM	3 uM	1 uM	1 uM	300 nM	300 nM	100 nM	100 nM	30 nM	30 nM	10 nM	10 nM	3 nM	3 nM	1 nM	1 nM
K	GRK	Untreated	Untreated	Untreated	30 uM	30 uM	10 uM	10 uM	3 uM	3 uM	1 uM	1 uM	300 nM	300 nM	100 nM	100 nM	30 nM	30 nM	10 nM	10 nM	3 nM	3 nM	1 nM	1 nM
L	GRK	Untreated	Untreated	Untreated	30 uM	30 uM	10 uM	10 uM	3 uM	3 uM	1 uM	1 uM	300 nM	300 nM	100 nM	100 nM	30 nM	30 nM	10 nM	10 nM	3 nM	3 nM	1 nM	1 nM
M	GRK	Untreated	Untreated	Untreated	30 uM	30 uM	10 uM	10 uM	3 uM	3 uM	1 uM	1 uM	300 nM	300 nM	100 nM	100 nM	30 nM	30 nM	10 nM	10 nM	3 nM	3 nM	1 nM	1 nM
N	GRK	Untreated	Untreated	Untreated	30 uM	30 uM	10 uM	10 uM	3 uM	3 uM	1 uM	1 uM	300 nM	300 nM	100 nM	100 nM	30 nM	30 nM	10 nM	10 nM	3 nM	3 nM	1 nM	1 nM
O	GRK	Untreated	Untreated	Untreated	30 uM	30 uM	10 uM	10 uM	3 uM	3 uM	1 uM	1 uM	300 nM	300 nM	100 nM	100 nM	30 nM	30 nM	10 nM	10 nM	3 nM	3 nM	1 nM	1 nM
P	GRK	Untreated	Untreated	Untreated	30 uM	30 uM	10 uM	10 uM	3 uM	3 uM	1 uM	1 uM	300 nM	300 nM	100 nM	100 nM	30 nM	30 nM	10 nM	10 nM	3 nM	3 nM	1 nM	1 nM

In this Transfluor assay an orphan GPCR is stably integrated into the b-arrestin GFP expressing U2OS cell line. After one hour incubation with a compound the cells were quenched with fixative (formaldehyde) and the plate was read on Cellomics ArrayScan HCS Reader using the GPCR Bioapplication. The images constitute one row of a 348 well plate. The dose curve consists of 11 dose points. Each concentration is duplicated in adjacent wells. Each well has three fields. File format is 8-bit TIFF with one image for green channel and one image for blue channel. Image size is 512*512 pixels.

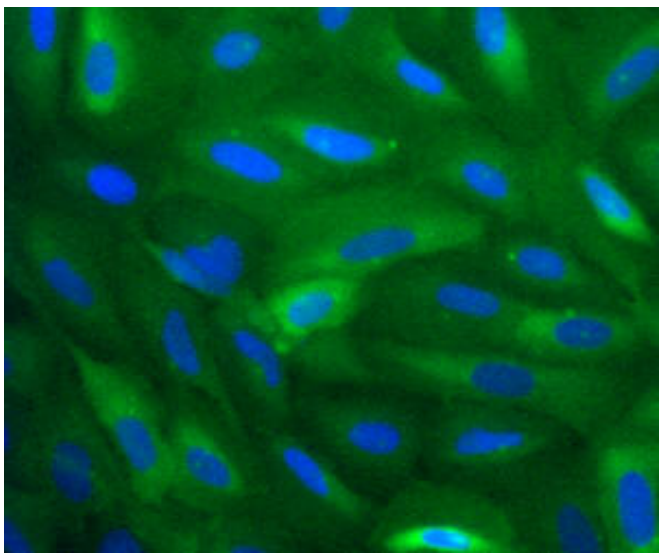

Negative

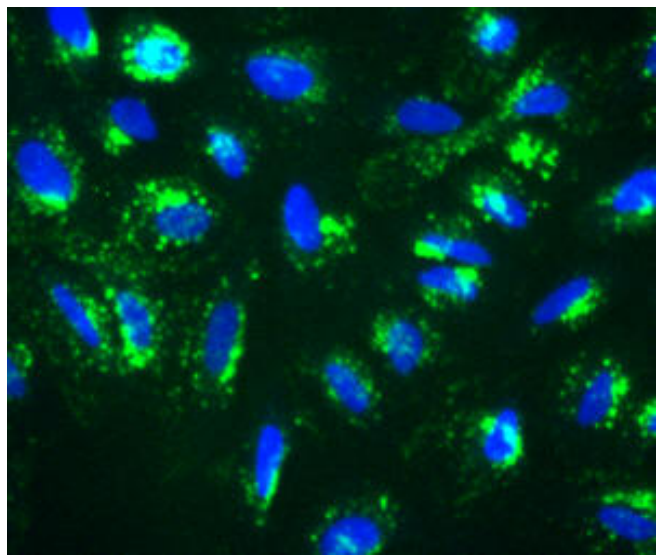

Positive

Factors Affecting Assay Quality: Image Resolution

Roche/Cellomics Image Set

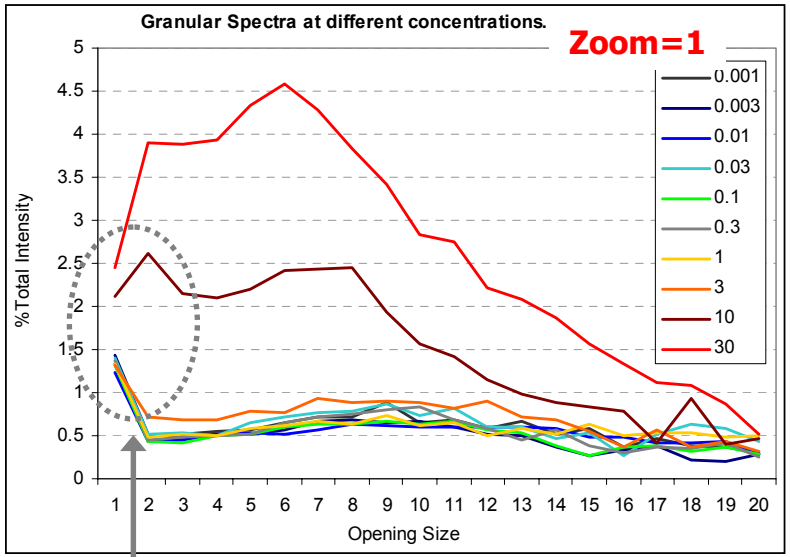

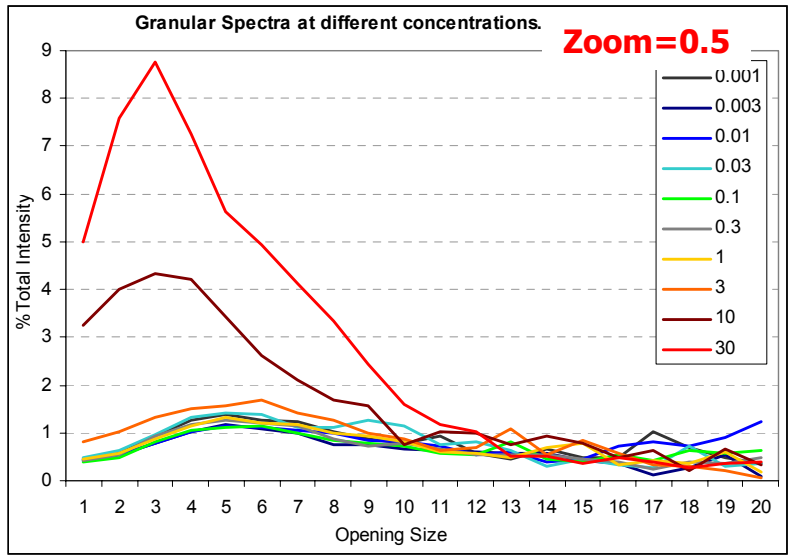

Almost dose-independent granular component suggests some "empty" magnification. Simulation with pixel replication proves it.

Subsampling of 0.25 is chosen for further analysis.

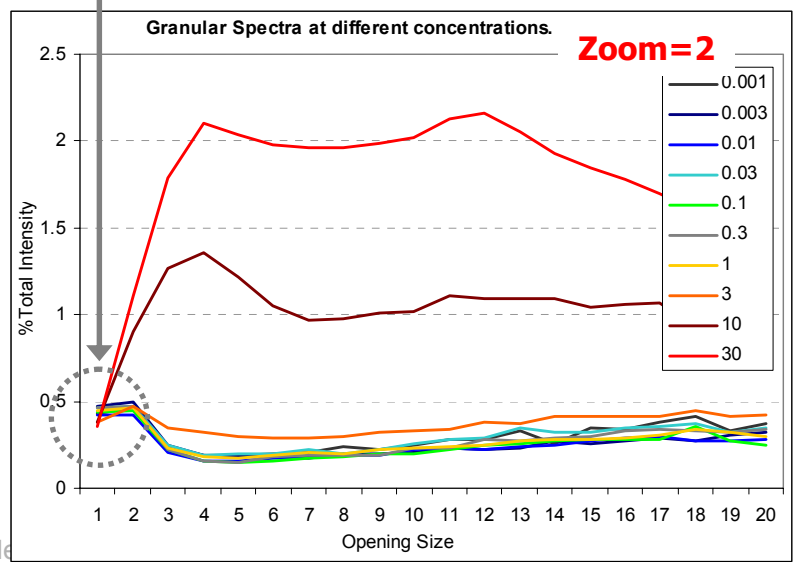

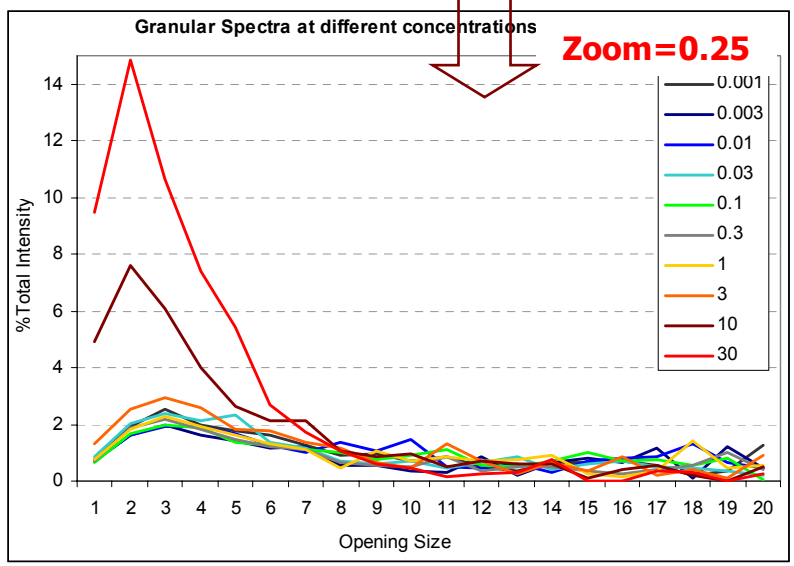

Factors Affecting Assay Quality: Illumination Uniformity (1)

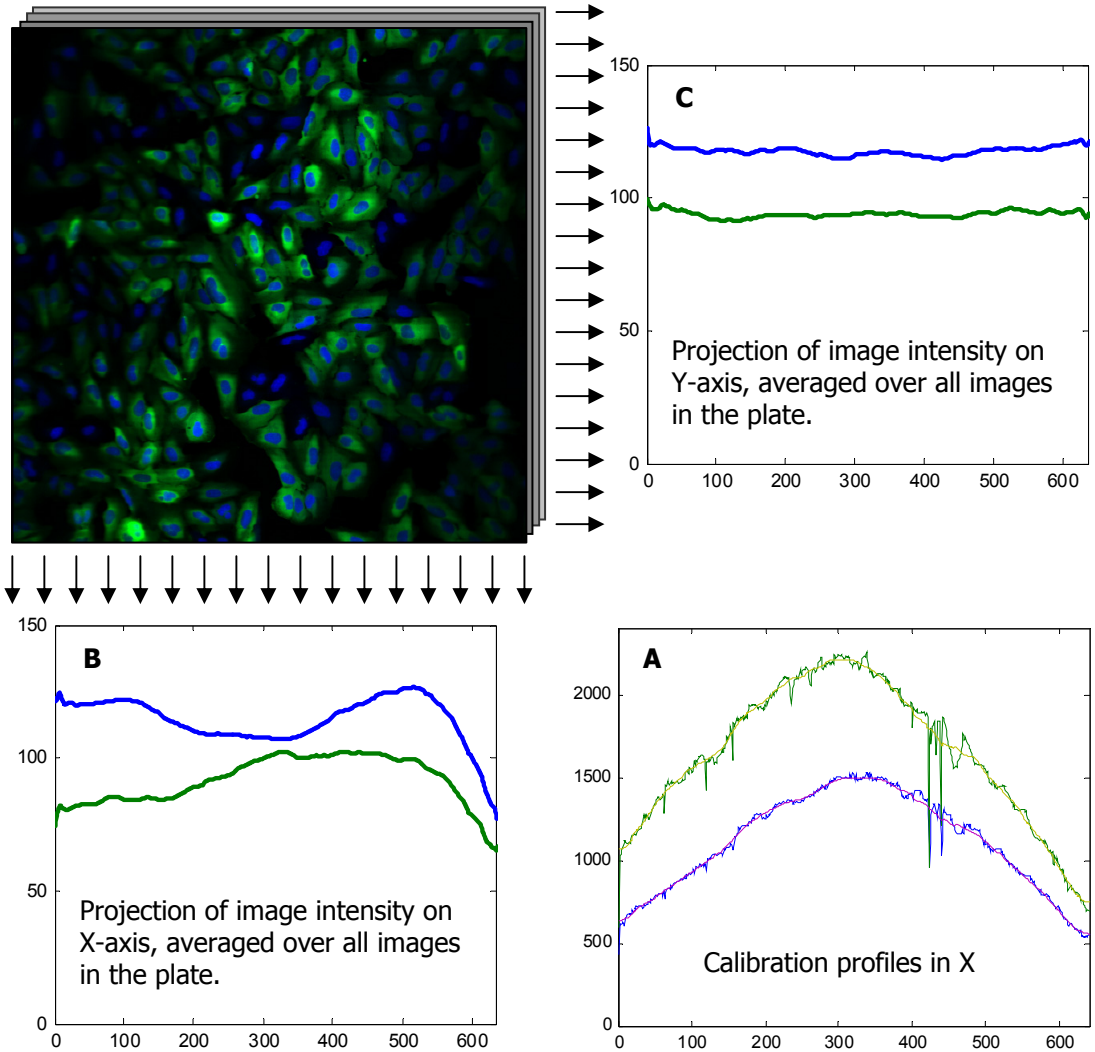

Images acquired on InCell3000 provide a convenient model to study the dependency of cellular measures on non-uniformity of illumination. Y-direction, which corresponds to the stage movement has uniform brightness, but X-direction, which corresponds to the scan of the laser beam has variable brightness. Calibration curves provided with the images are shown in Figure A.

Actual brightness in the two channels averaged over the entire plate to eliminate random errors is shown in figures B (X-projection) and C (Y-projection). The plots show clearly uniform intensity in Y and non-uniform intensity in X.

To assess if the brightness non-uniformity affects the cellular measures produced by the presented family of CNT algorithms, we plotted the measures against X-coordinates of cells and against Y-coordinates of cells. Two of the measures are shown below. The plots show that there is no dependency on either X or Y position of cells. Other measures, which are not shown, exhibit similar behavior.

This allows us to conclude that variation in brightness alone does not affect cellular measures if the algorithm is specifically designed to compensate for it.

Factors Affecting Assay Quality: Illumination Uniformity (2)

Slope1

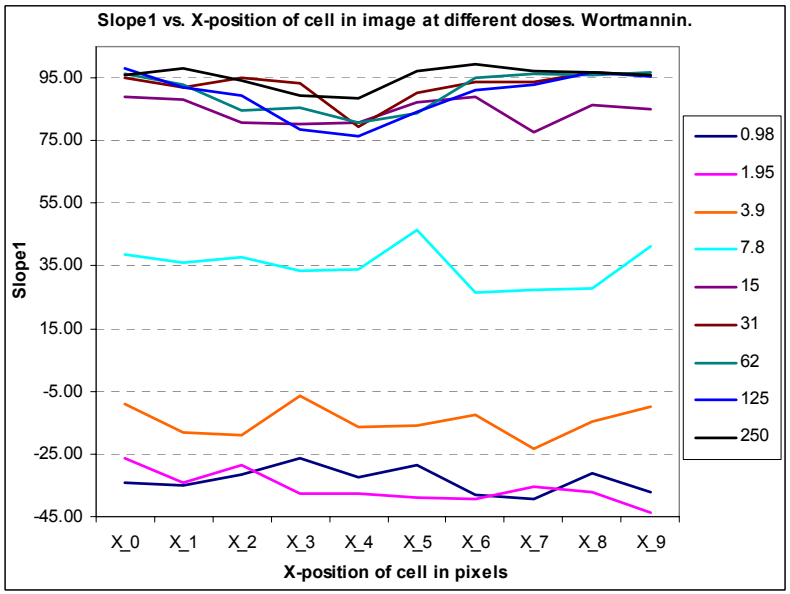

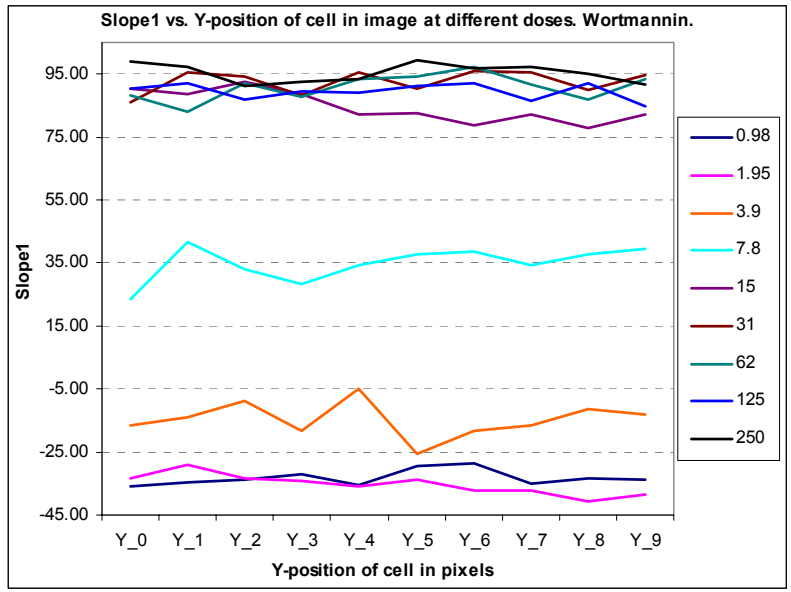

N2R_TW

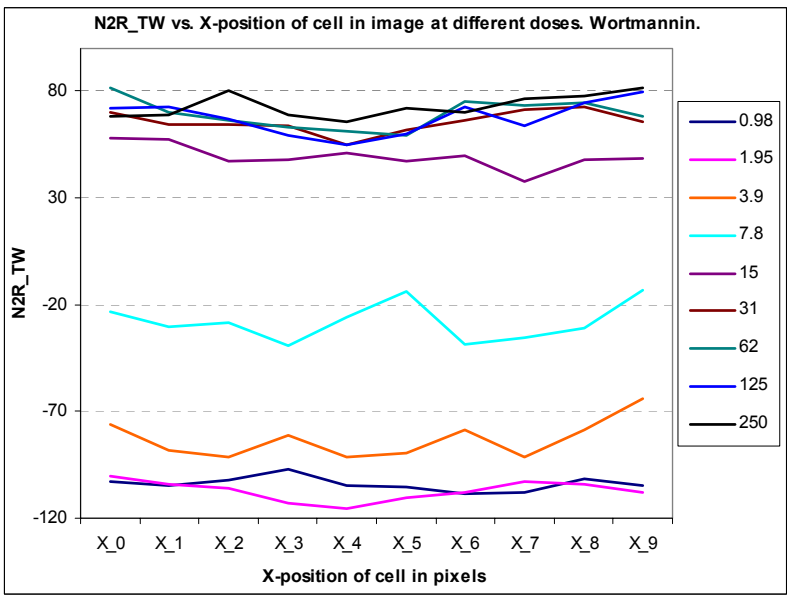

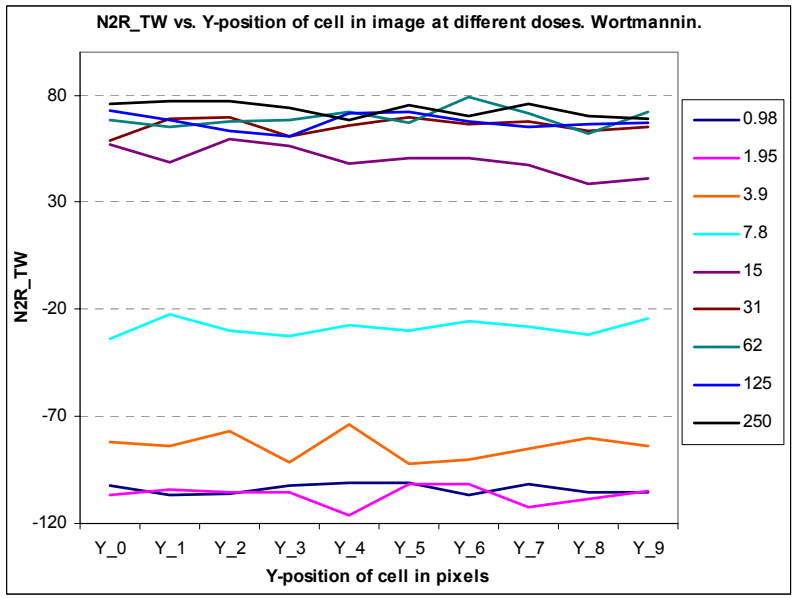

X-position **Y-position**

Factors Affecting Assay Quality: Pixel Shift Between Channels

Images at 10X

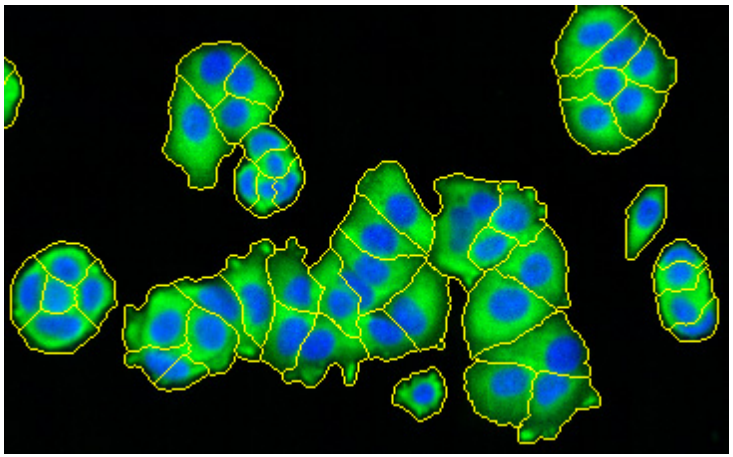

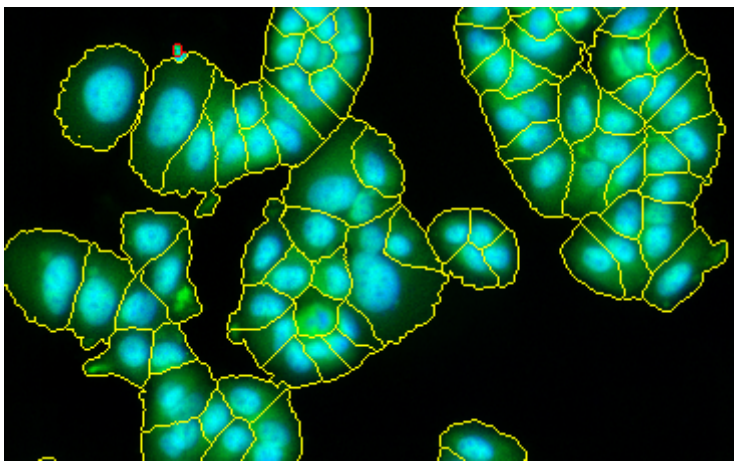

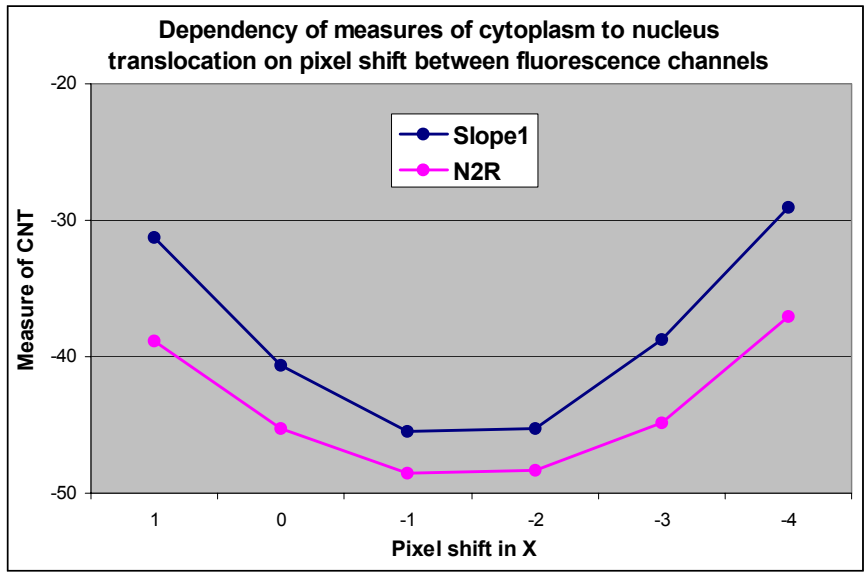

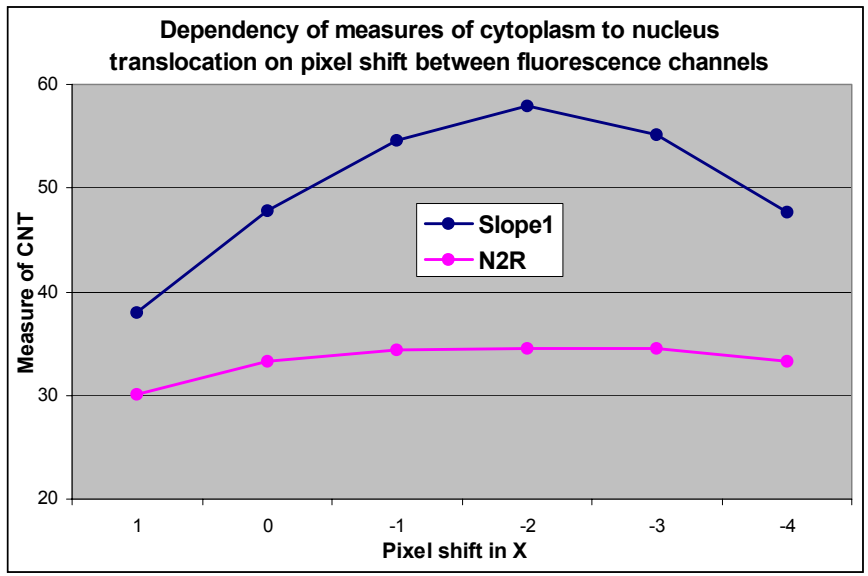

- CNT measures show strong dependency on pixel shift
- On negative cells Slope1 and N2R behave similarly relative to pixel shift
- On positive cells Slope1 is more dependent on pixel shift than N2R

Factors Affecting Assay Quality: Accuracy of Focusing

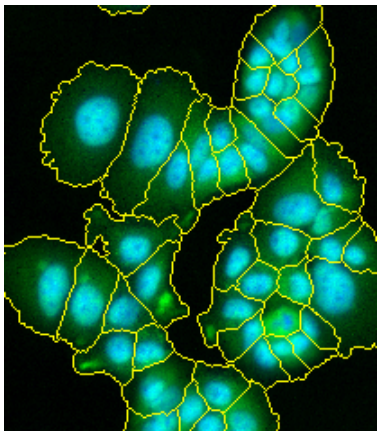

Positive

Images at 10X

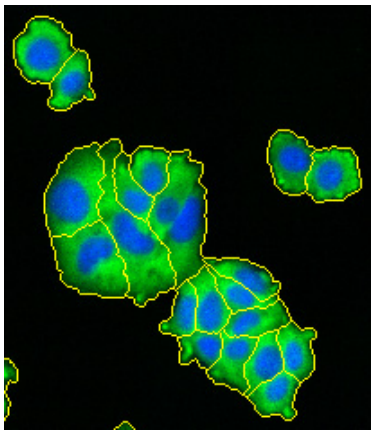

Negative

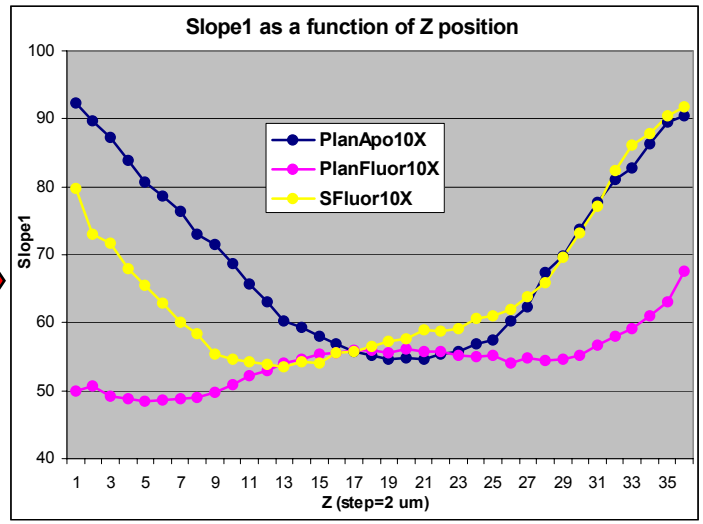

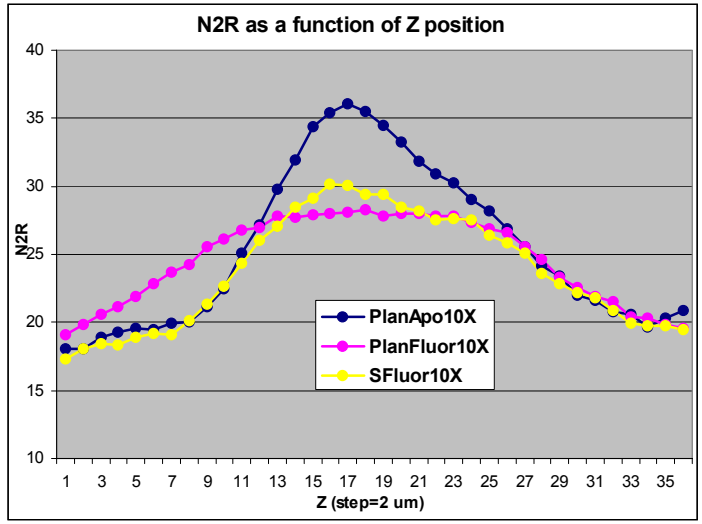

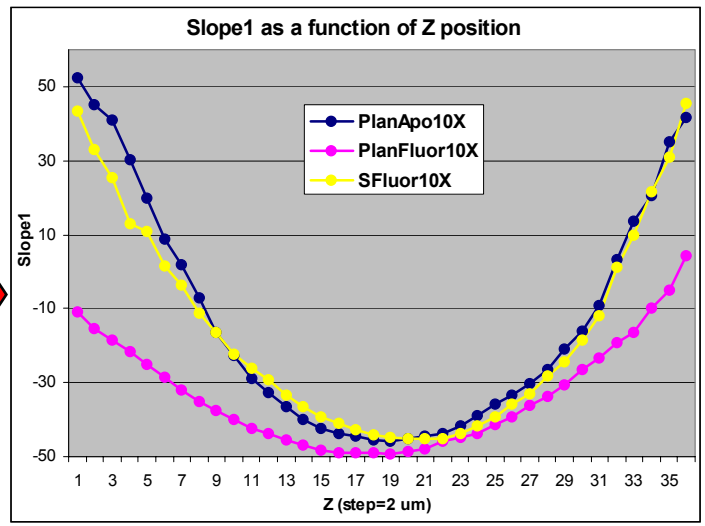

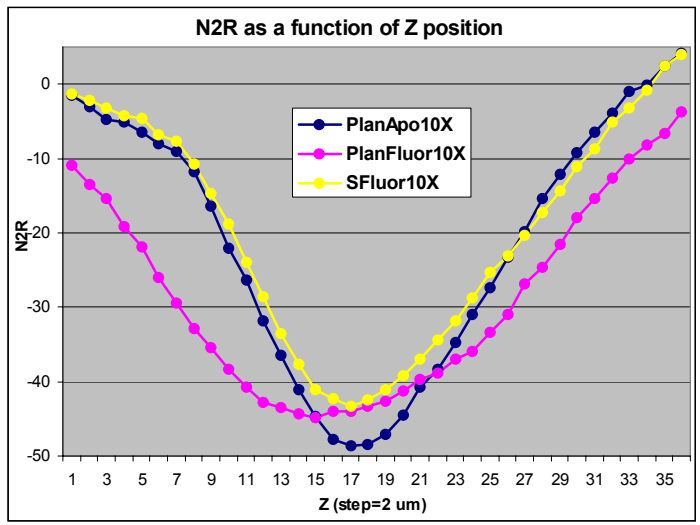

- CNT measures are almost identical within 10-15 µm from the best focus position in 10X (less for PlanApo with N2R_AM).
- Objectives with lower NA are more tolerant to focusing inaccuracy.
- Slope1 and N2R_AM show similar dependency on Z-position on negative cells and opposite dependency on positive cells.
- For Slope1 dynamic range of the assay does not depend on objective NA; for N2R_AM higher NA gives the greatest dynamic range of the assay.
- The importance of this dependency is not only in setting focusing requirements, but also in establishing the need for flat field.

Factors Affecting Assay Quality: Depth of Field in a Non-confocal System (1)

It is convenient to study dependency of assay quality on the depth of field by comparing objectives with the same magnification but different numerical aperture. Difference in image brightness can be equalized by adjusting integration times. The Vitra plate was scanned two times: with a PlanFluor 10X 0.3NA objective and with a SFluor 10X 0.5NA objective (Nikon). The images were processed with the same parameters: Nuclear erosion=1, Gap=2, Ring=4. PlanFluor gives better results for all measures. Measures based on total amount of fluorescence (as opposed to average) suffer the most.

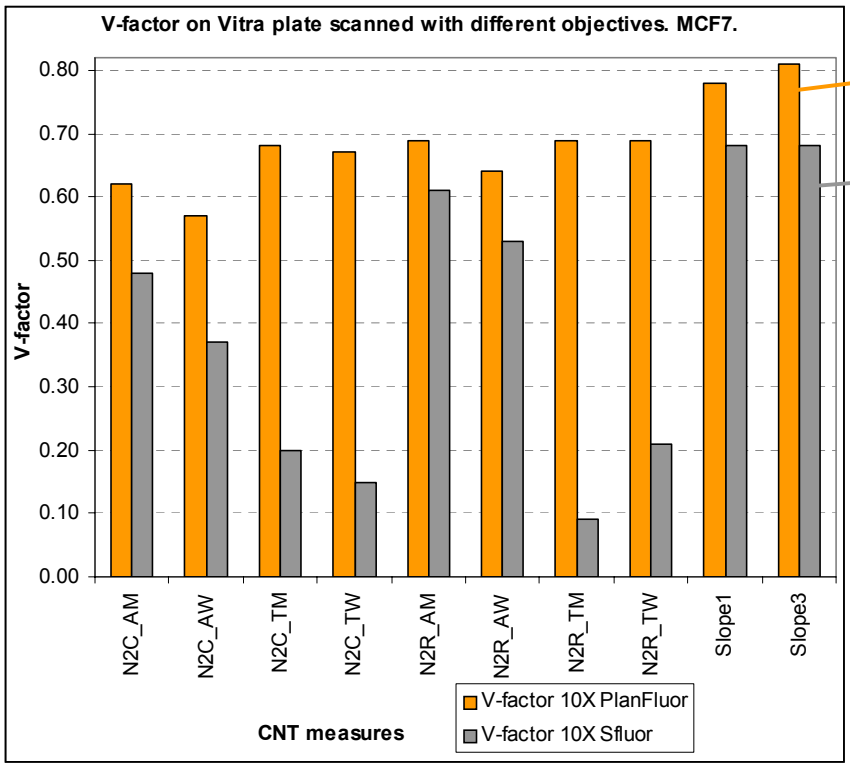

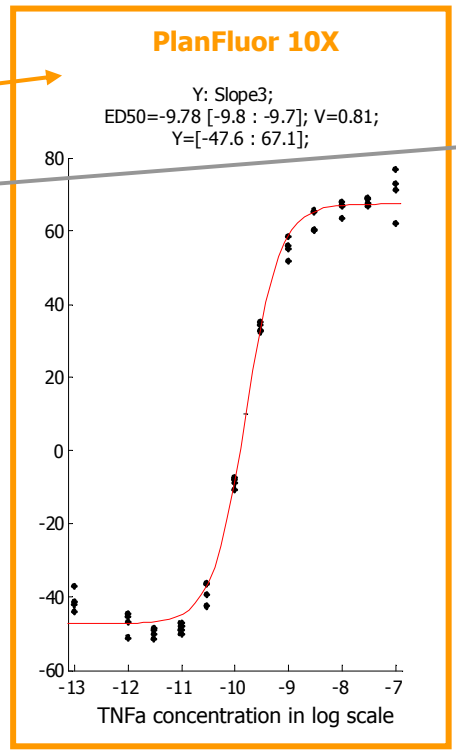

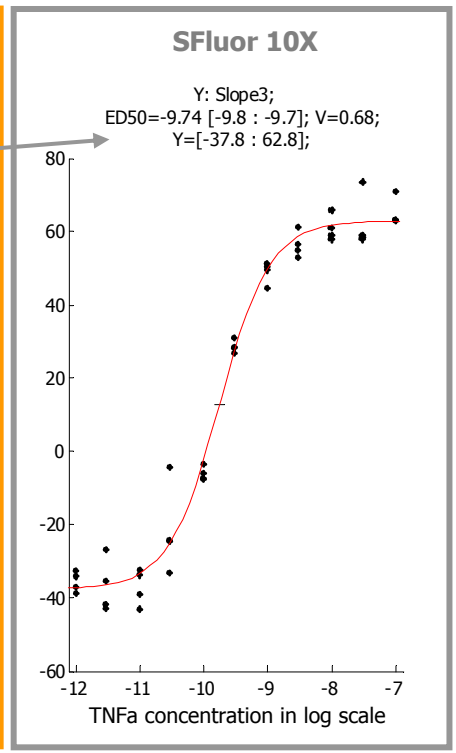

SFluor objective shows reduced dynamic range and increased variation among replica wells.

Factors Affecting Assay Quality: Depth of Field in a Non-confocal System (2)

PlanFluor10X, 0.3NA, Depth of field = 8.5 µm

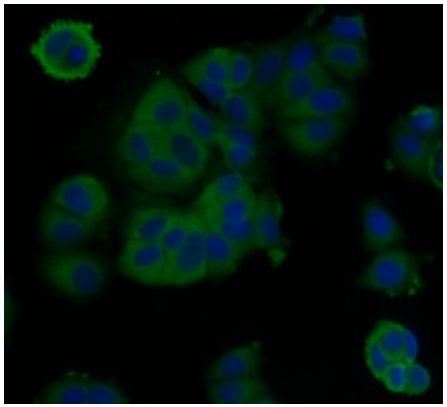

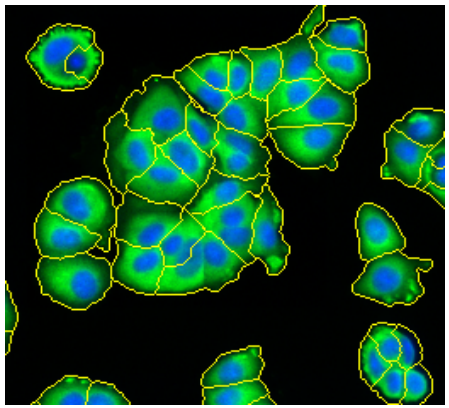

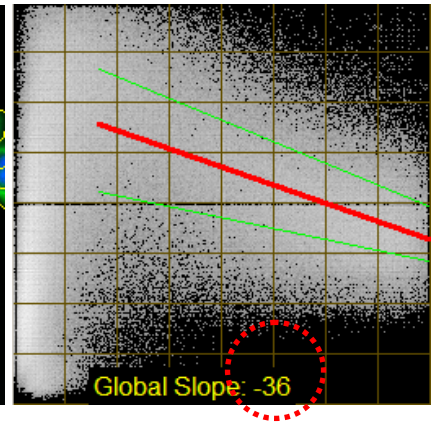

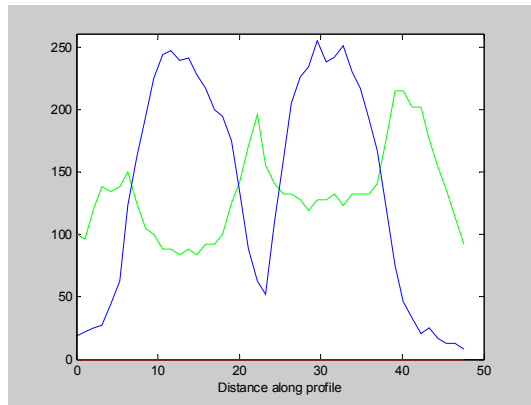

Original | Normalized | 2D distribution | Profiles

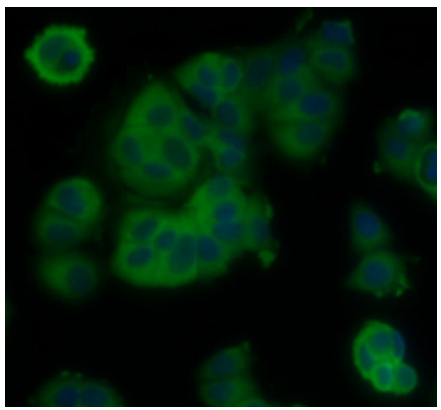

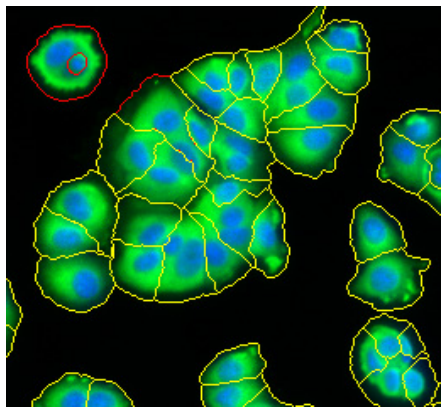

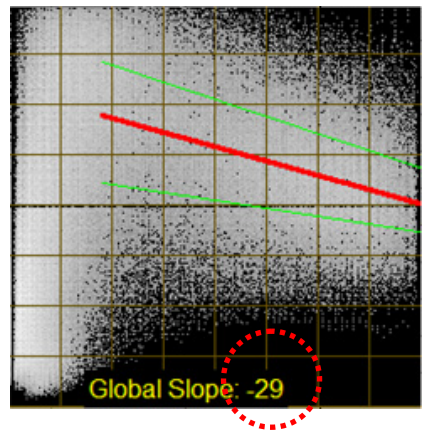

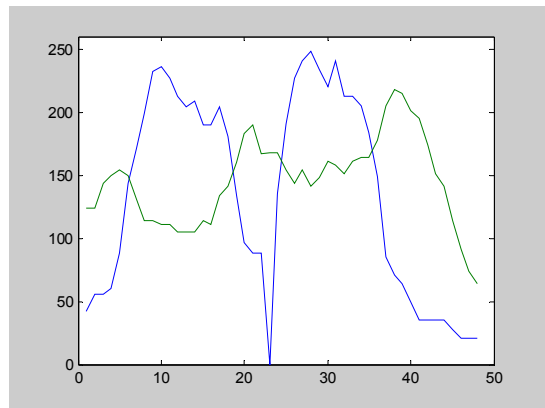

SFluor10X, 0.5NA, Depth of field = 3.6 µm

Our hypothesis is that this result is due to the relative thickness of cells and the depth of field of the two objectives. The depth of field of 0.3NA PlanFluor 10X is about 8.5 µm, and the depth of field of 0.5NA SFluor 10X is about 3.6 µm. The thickness of attached cells is probably between these two values. If the cell is thicker than the depth of field of the objective it appears fuzzy. This makes negative cells look less negative and reduces the dynamic range of the measurements. This also makes focusing more difficult and can increase variability due to inaccurate focusing.

Factors Affecting Assay Quality: Widefield vs. Confocal (1)

Comparison of widefield and confocal systems was performed on cytoplasm to nucleus translocation assay; Vitra plate; MCF7 cells; zero and saturation concentration of TNFα.

Images of the same field were acquired on Nikon TE2000 with Retiga EX camera and with Nikon Confocal Attachment - both with 0.3NA 10X PlanFluor objective.

With the confocal system negative cells look more negative and give more negative numbers …

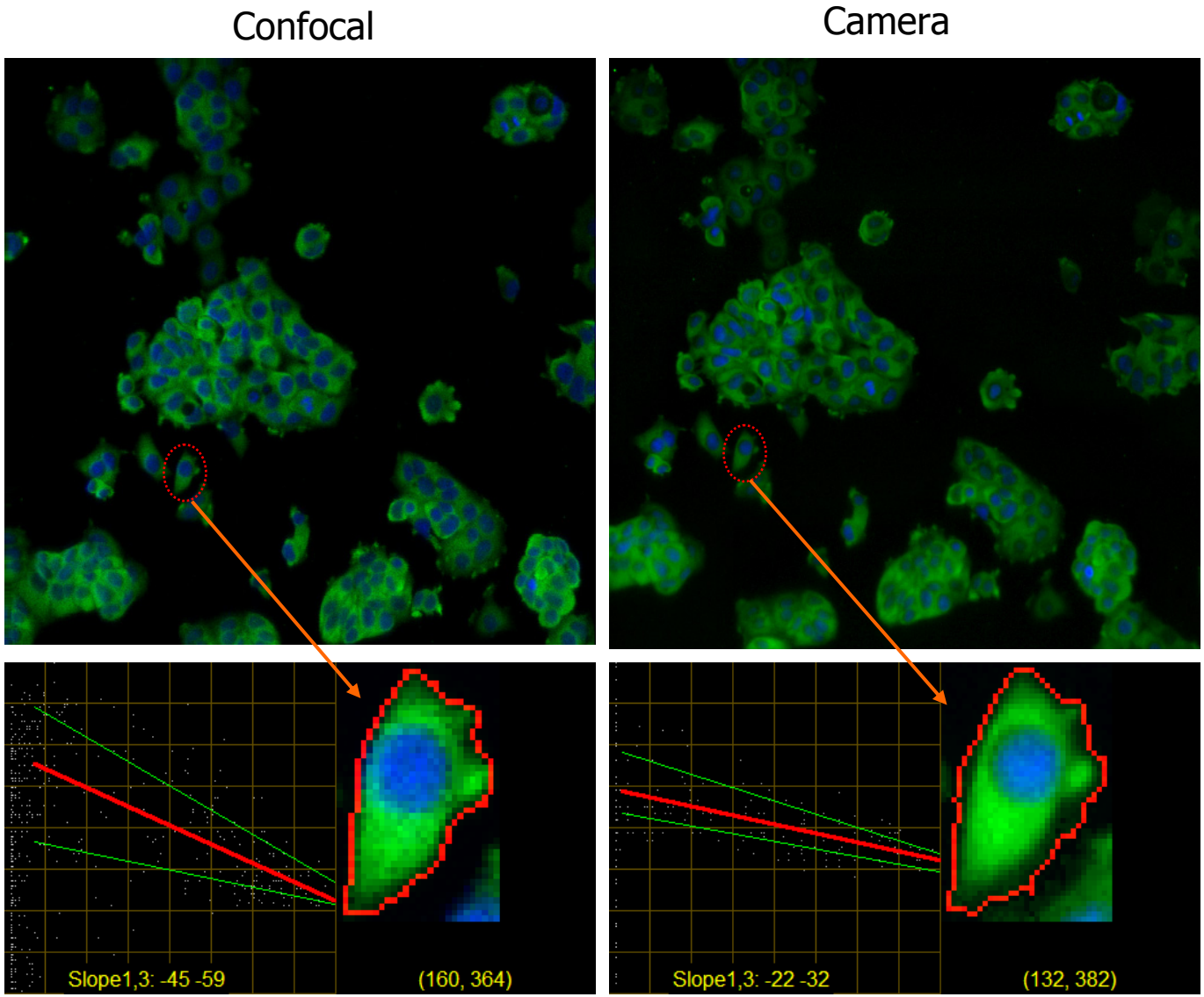

Slope1 = -45, Slope3 = -59

Slope1 = -22, Slope3 = -32

Factors Affecting Assay Quality: Widefield vs. Confocal (2)

Confocal

Camera

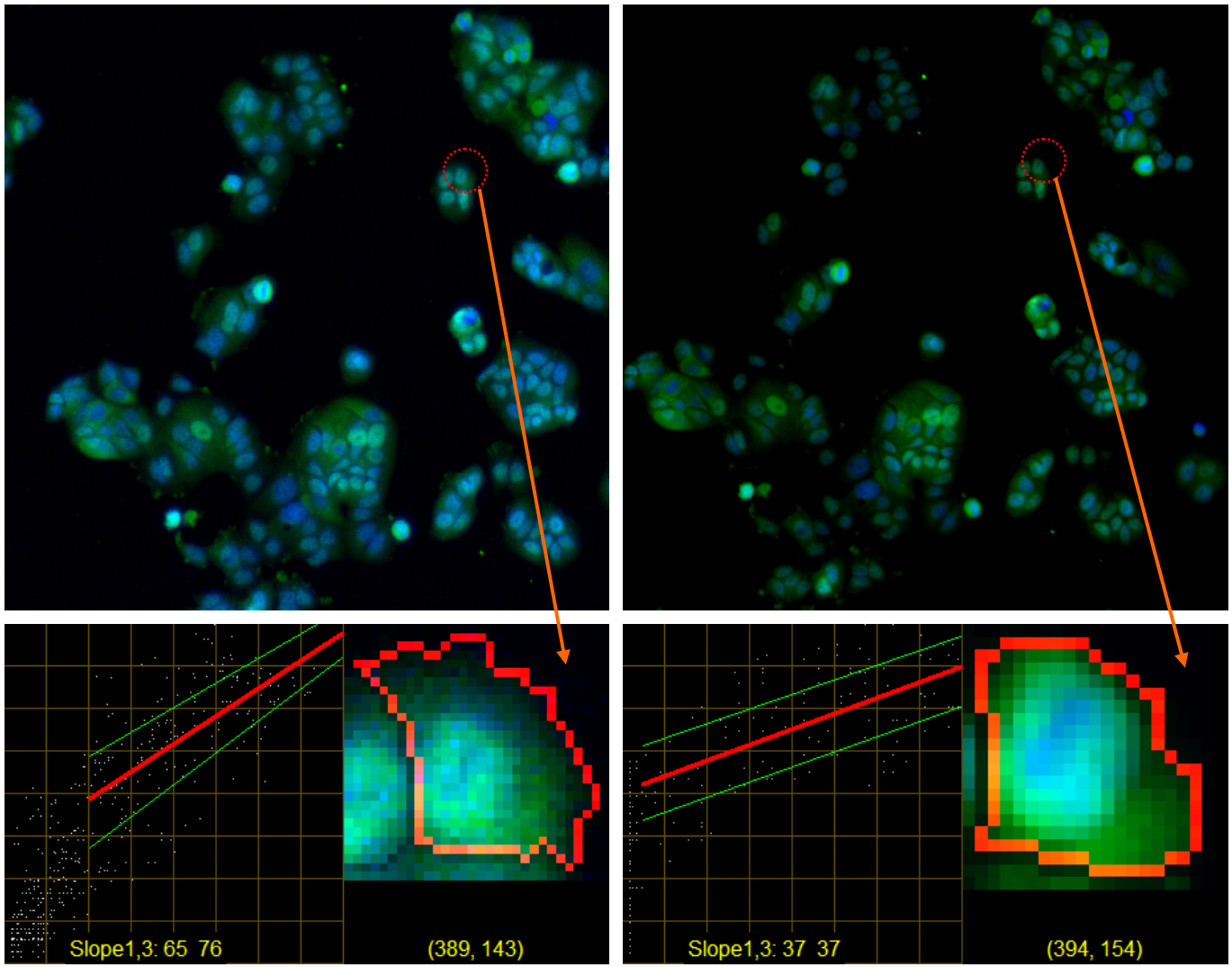

… and positive cells look more positive and give more positive numbers.

Slope1 = 65, Slope3 = 76

Slope1 = 37, Slope3 = 37

Widefield vs. Confocal - Results

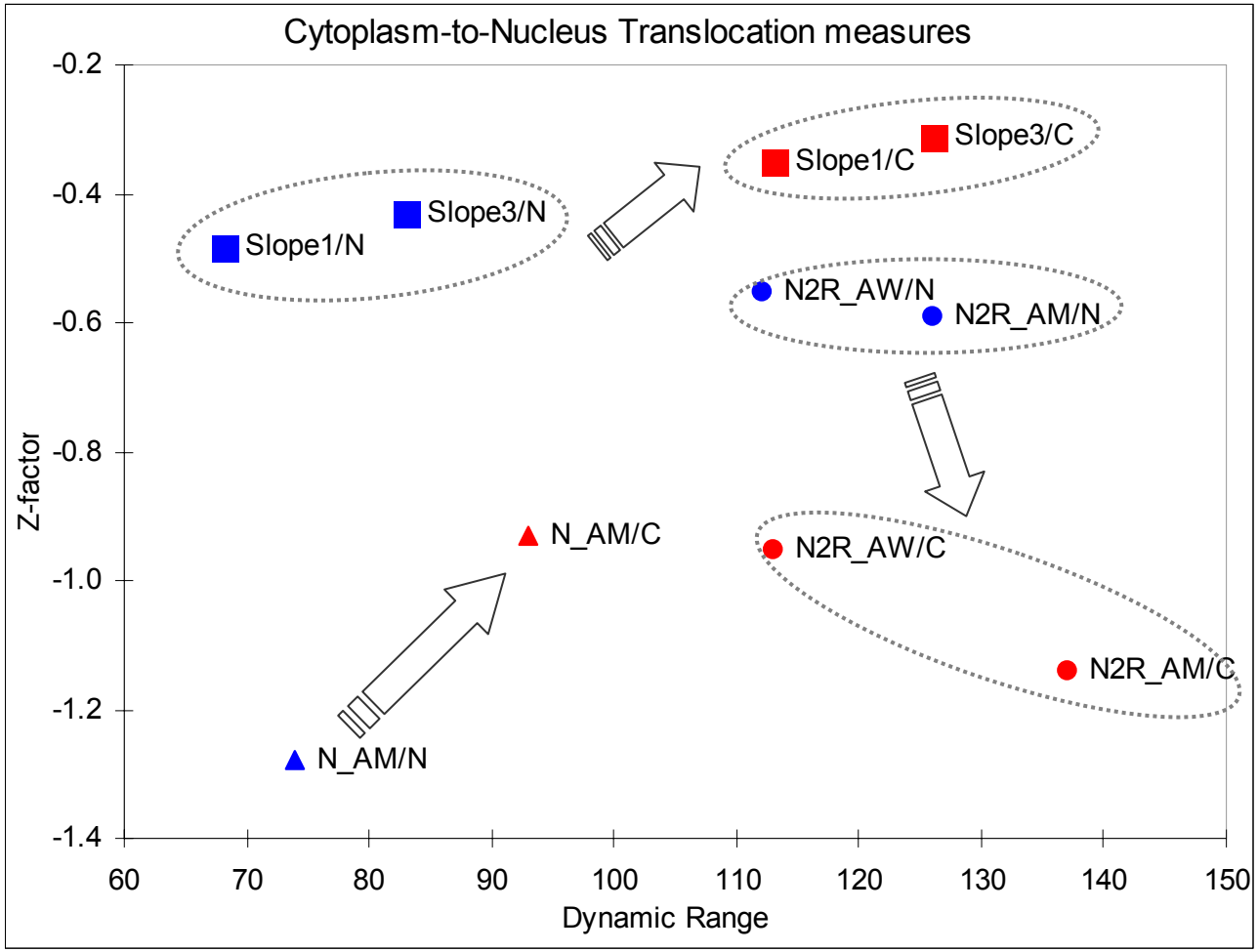

1. Slope measures are better than other measures regardless of imaging mode (confocal or widefield)
2. For slope measures confocal is better than widefield.
3. For nucleus-to-ring measures widefield is better than confocal.
4. Images should have only in-focus information – either by keeping the whole object in focus by large depth of field, or by cutting the out-of-focus light with a confocal system

Red – Confocal (/C)

Blue – Non-confocal (/N)

– Slope measures

– Ring measures

– Nuclear measure

Quality was measured by Z-factor applied not as usual to populations of replicas, but to populations of cells in positive and negative states. This gives numerically very low Z values, but provides a direct comparison of different measures.

Factors Affecting Assay Quality: Surface Coating (1)

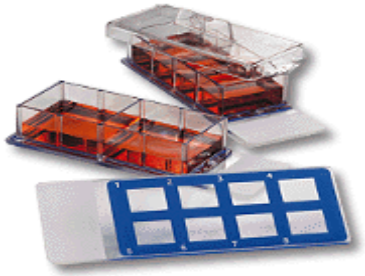

Surface options: Collagen I, CultureSlide, Fibronectin, Poly-D-Lysine

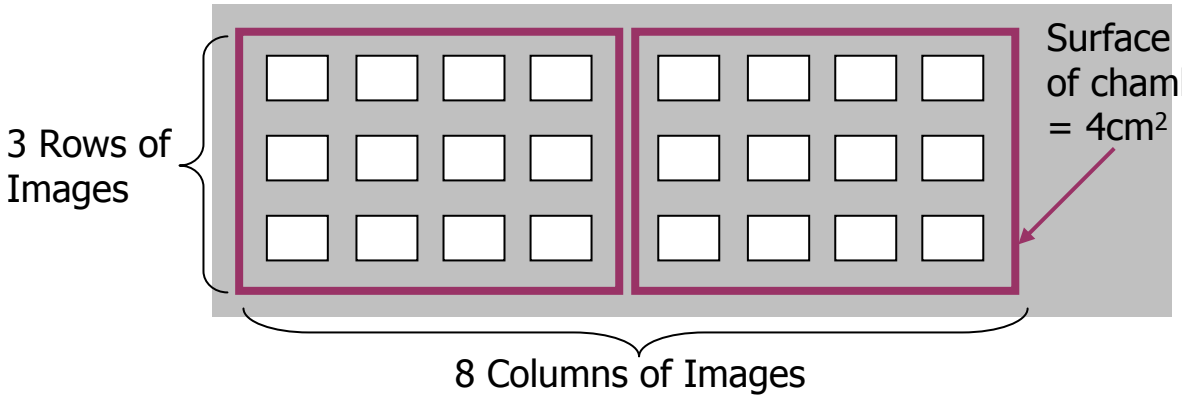

The study was performed on untreated MCF7 cells grown in chamber slides (BD Biosciences). Chamber slides were chosen because they provide a choice of surface treatments on a flat surface, eliminating possible effects of non-flat bottom of microplates on cytoplasm to nucleus translocation measures.

Images were acquired on the CellCard reader (Vitra Bioscience) with Nikon 0.2NA 4X PlanApochromat objective and Retiga EX camera (resolution 1360*1024 pixels). Pixel size in image plane = 1.62µm; frame size = 2.20mm*1.66mm. Number of images = 24.

ANOVA

			Slope1			Slope3			N2R_AW			N2R_AM			N_AM		
		DF	Mean square	Fisher's F	Pr > F	Mean square	Fisher's F	Pr > F	Mean square	Fisher's F	Pr > F	Mean square	Fisher's F	Pr > F	Mean square	Fisher's F	Pr > F
Source of variation	Surface treatment	3	3602.0	117.4	< 0.0001	6184.1	115.7	< 0.0001	6028.1	493.0	< 0.0001	14961.4	378.3	< 0.0001	5044.0	276.6	< 0.0001
	Row	2	59.7	1.9	0.149	93.1	1.7	0.182	8.3	0.7	0.511	81.4	2.1	0.134	28.2	1.5	0.219
	Column	7	51.6	1.7	0.124	87.2	1.6	0.138	14.3	1.2	0.330	58.3	1.5	0.188	14.4	0.8	0.596

Analysis of variance was performed for five CNT measures: Slope1, Slope3, N2R_AW, N2R_AM, and N_AM using surface treatment, image row and image column as factors. For all measures surface treatment is a significant factor and image position is not.

Factors Affecting Assay Quality: Surface Coating (2)

The desired result for nontreated cells is to obtain a measure as negative as possible and with as low variation as possible. Each sample consists of 24 values corresponding to the 24 images acquired on the chamber slide.

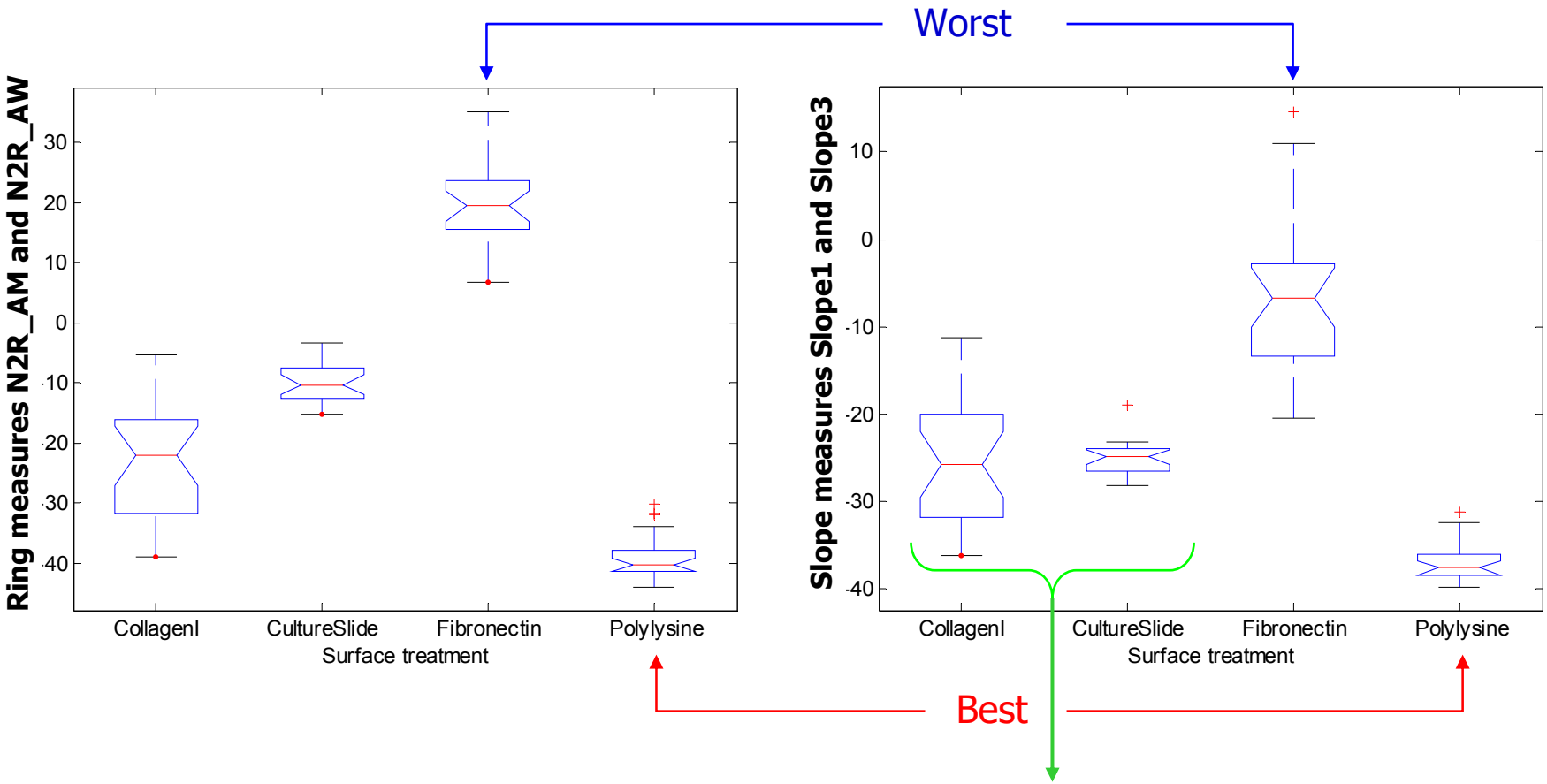

For slope-based measures the untreated CultureSlide gives the same average values as CollagenI, but has much less variation among scan fields.

Factors Affecting Assay Quality: Surface Coating (3)

Greatest amount of signal in the nucleus points to thicker cells

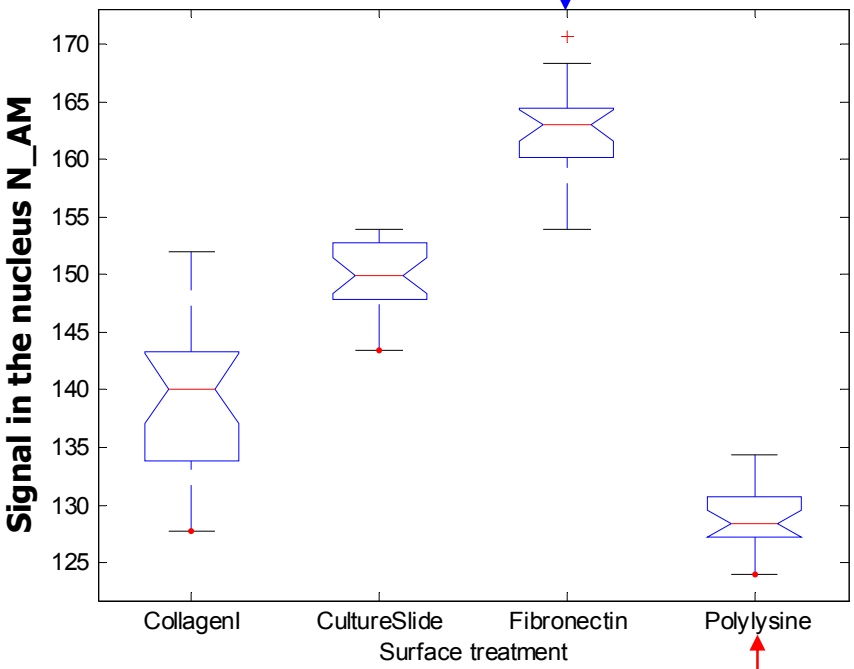

Smallest amount of signal in the nucleus points to flatter cells

Greatest number of cells points to the best attachment

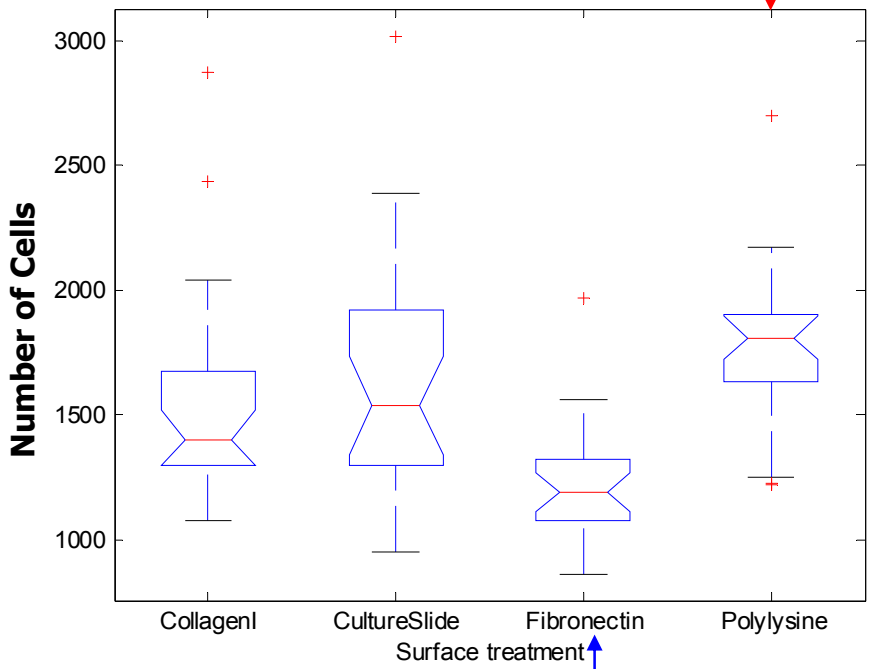

Smallest number of cells points to the worst attachment

Polylysine provides the strongest and the most uniform attachment of MCF7 cells making it the best coating for CNT and cell counting assays for this cell type. Fibronectin provides the weakest attachment and is the least suitable for these assays.

Assay Quality after Statistical Processing: Principal Component Analysis of Slope Distributions (1)

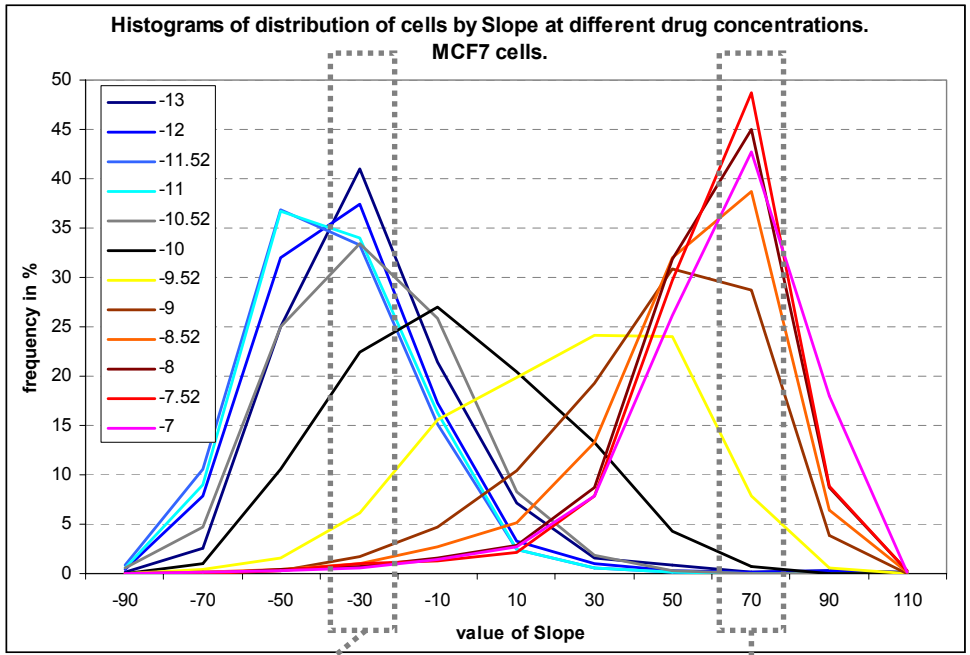

Vitra plate.
MCF7 cells.

Dose curve of frequency of cells in bin "-30", V=0.62

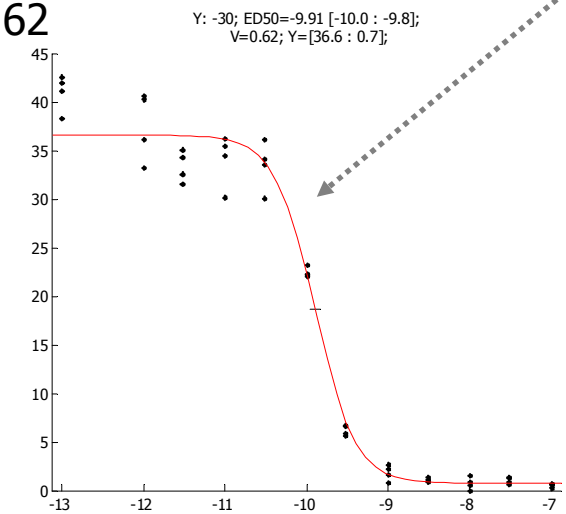

Dose curve of frequency of cells in bin "70", V=0.66

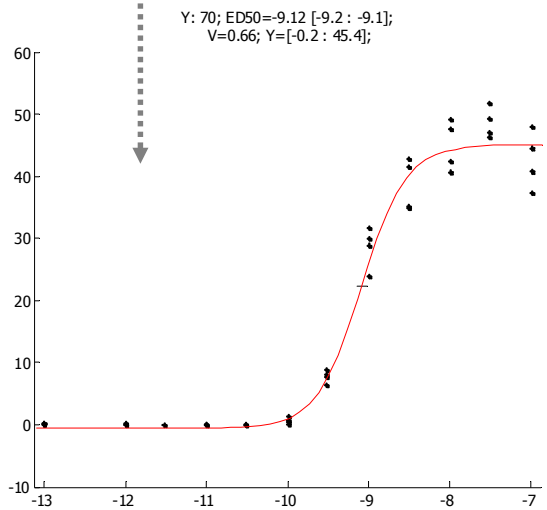

Assay Quality after Statistical Processing: Principal Component Analysis of Slope Distributions (2)

Bins of the histogram – features (columns)

Doses and replicas – observations (rows)

Interpretation from factor loadings:
F1 – negativity, F2 – heterogeneity

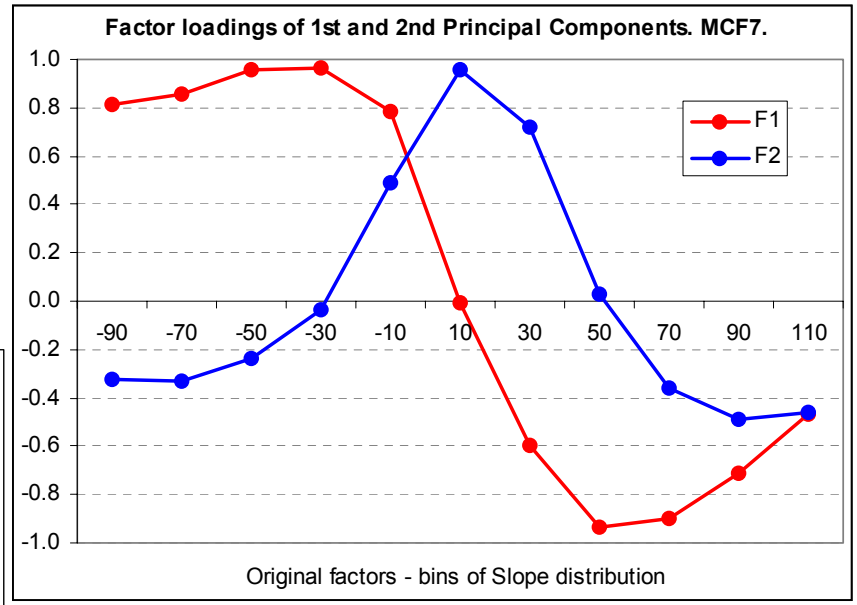

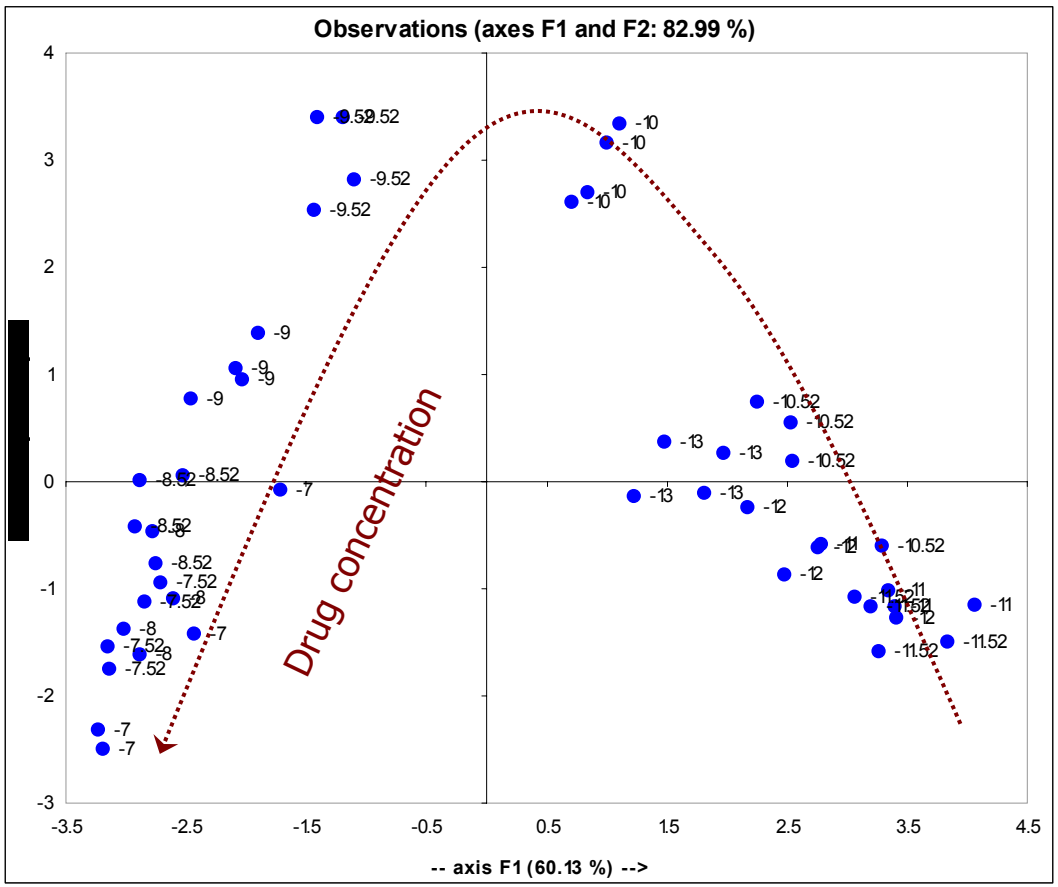

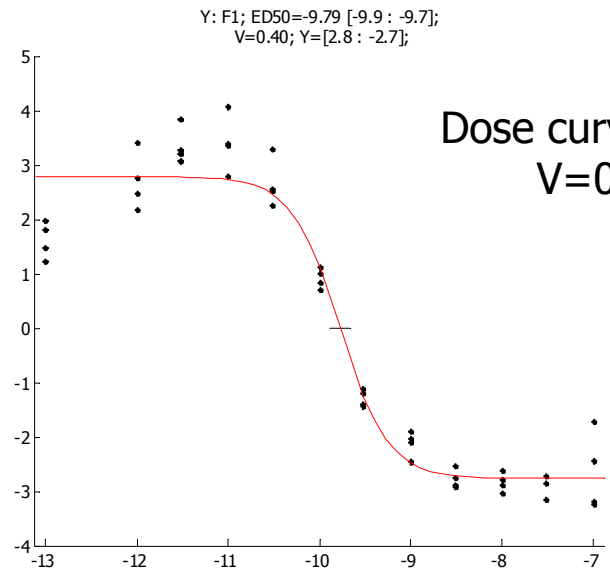

Dose curve of F1, V=0.40

Assay Quality after Statistical Processing: Principal Component Analysis of Granular Spectra (1)

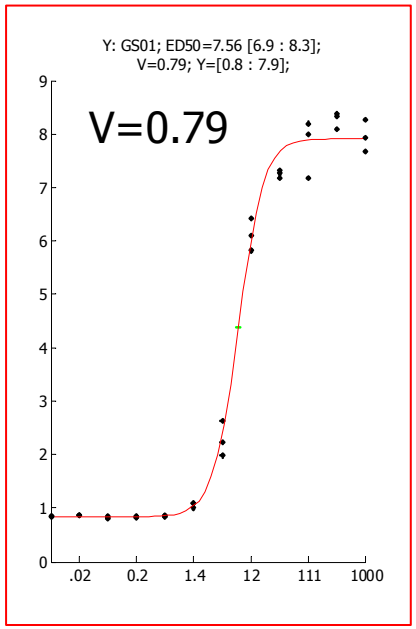

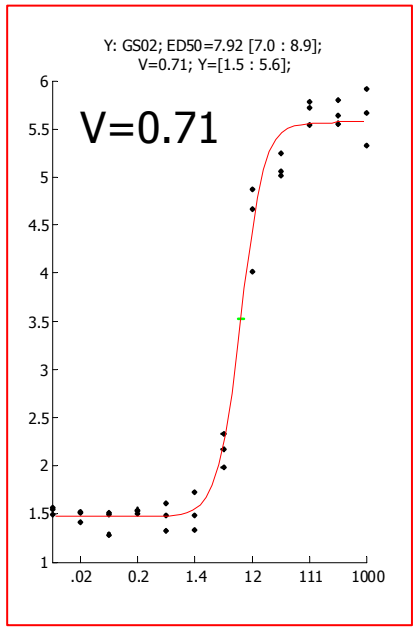

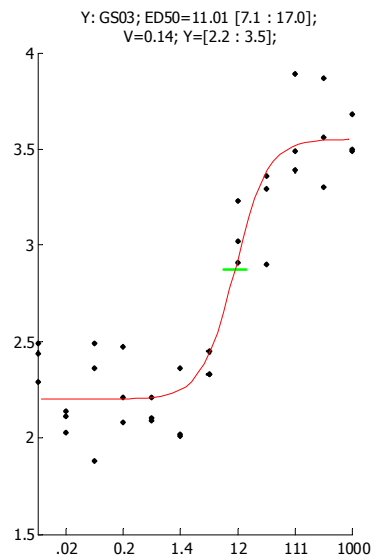

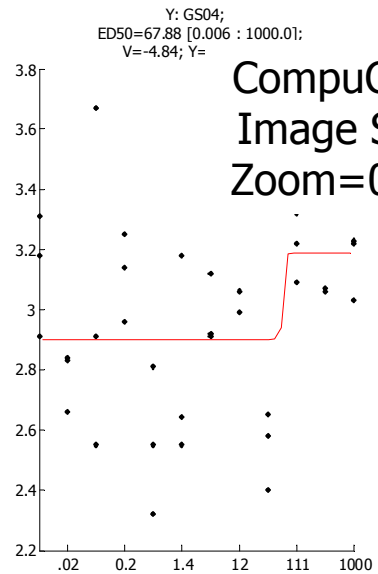

CompuCyte Image Set, Zoom=0.25

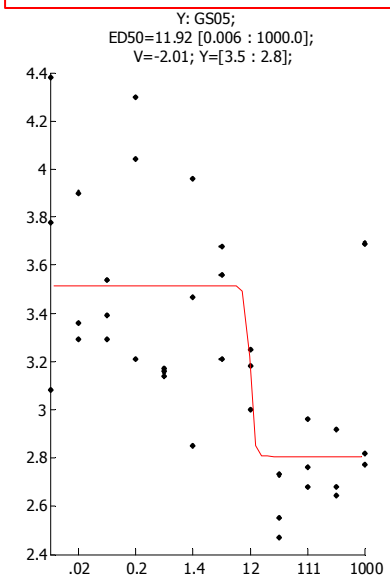

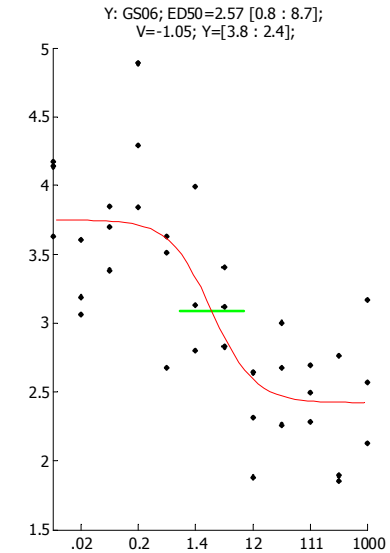

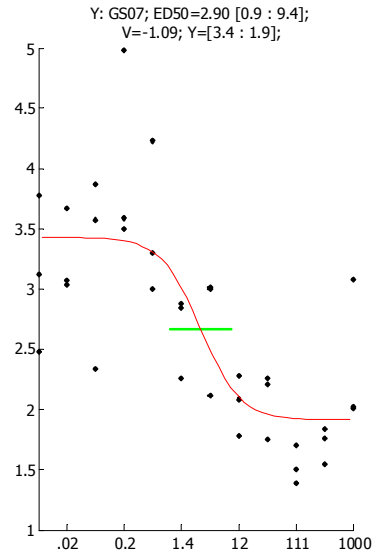

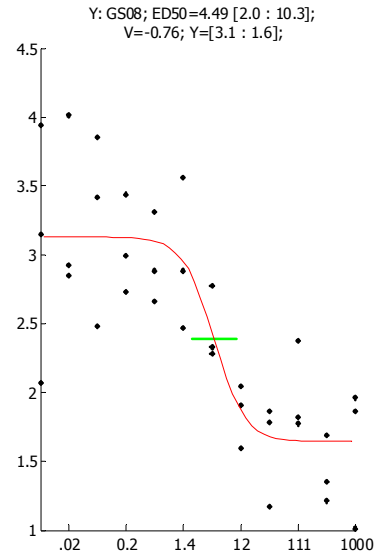

Assay Quality after Statistical Processing: Principal Component Analysis of Granular Spectra (2)

Factor loadings for F1 suggest that it can be interpreted as the difference between the granular and diffuse staining. Interpretational value of F1 is high, but statistical quality is much lower than for GS01 or GS02. The reason is that F1 uses components of granular spectrum that contribute noise but very little dynamic range.

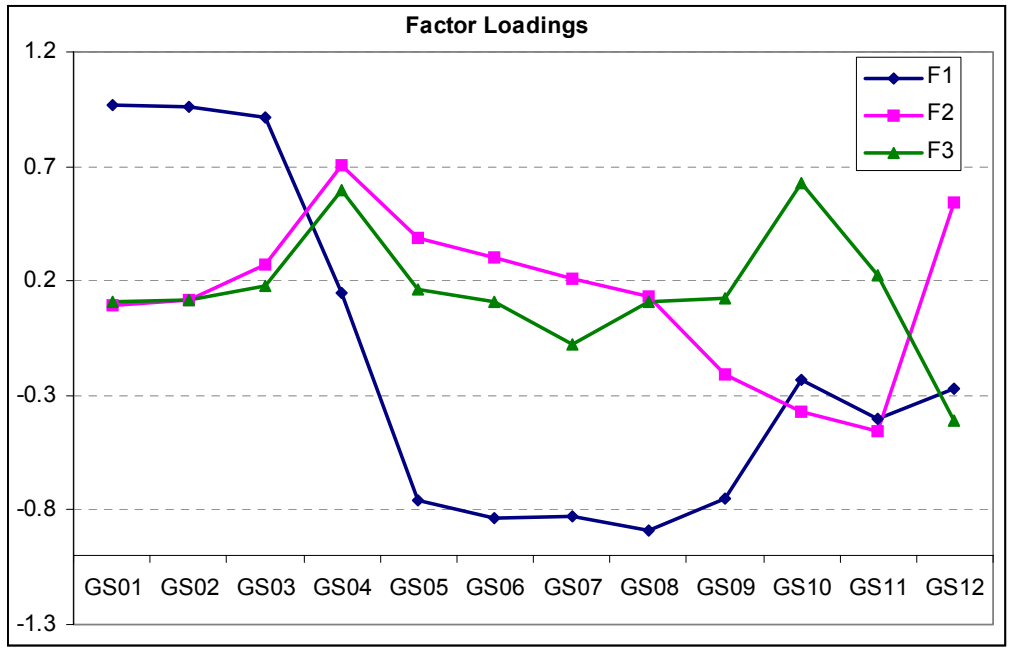

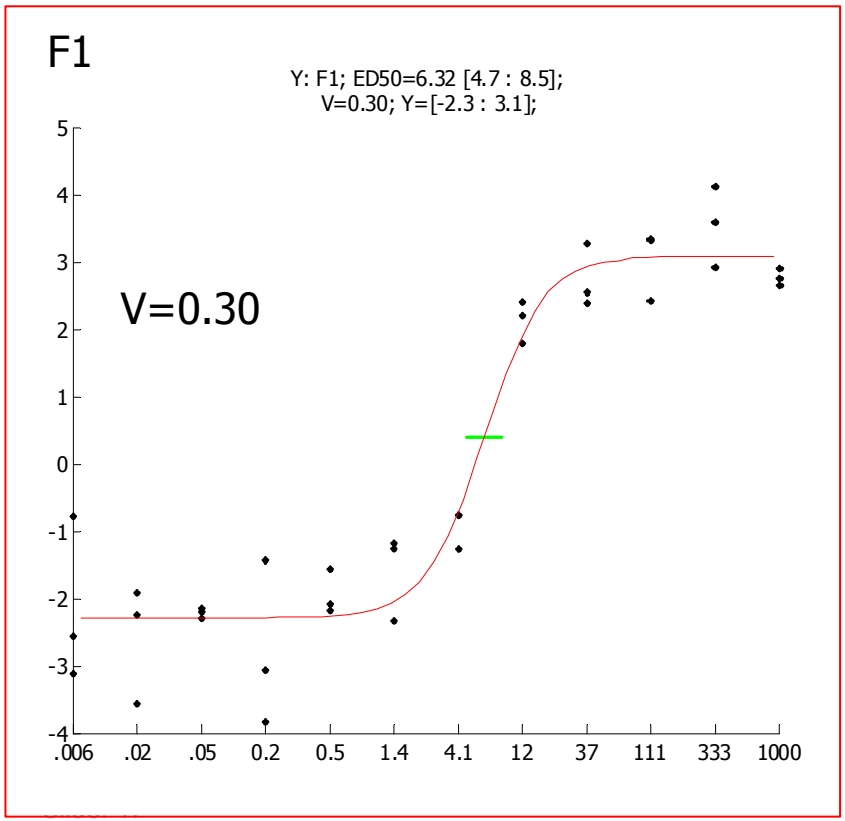

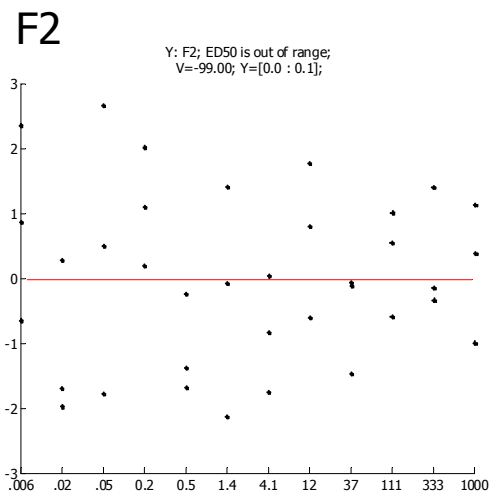

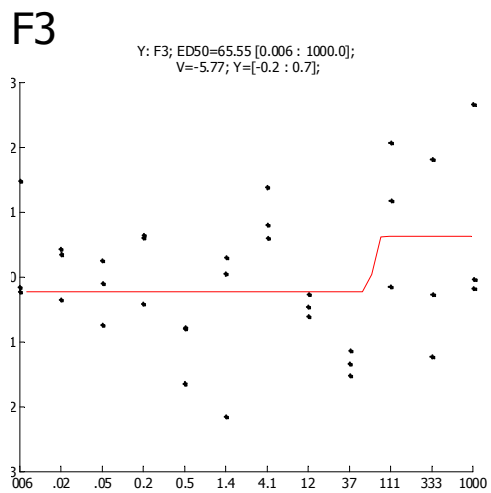

Cell-By-Cell vs. Global Analysis. Cytoplasm to Nucleus Translocation.

Global Slope behaves better than most cell-by-cell measures

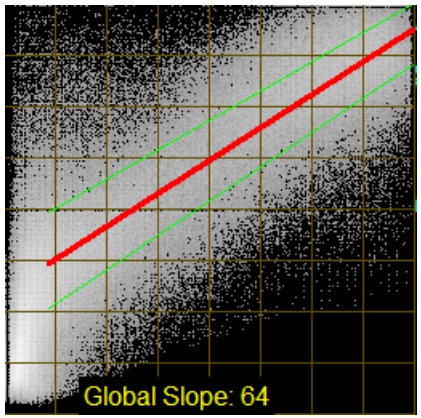

positive

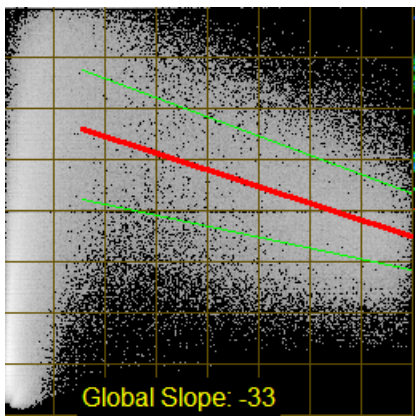

negative

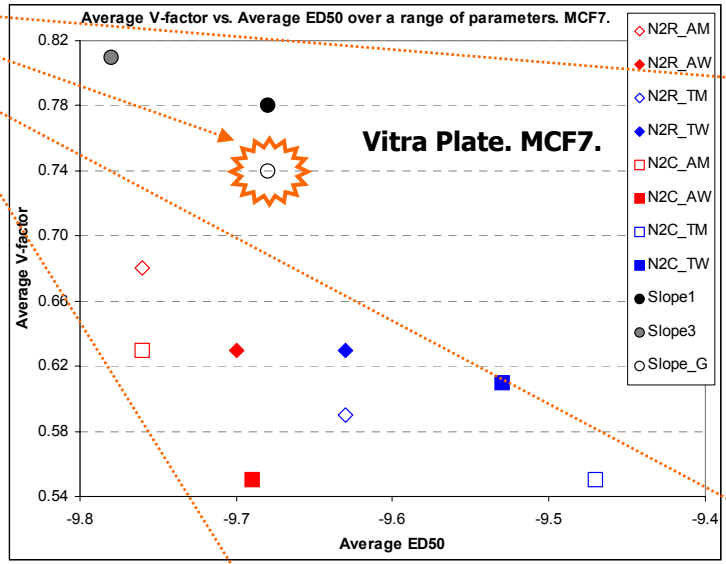

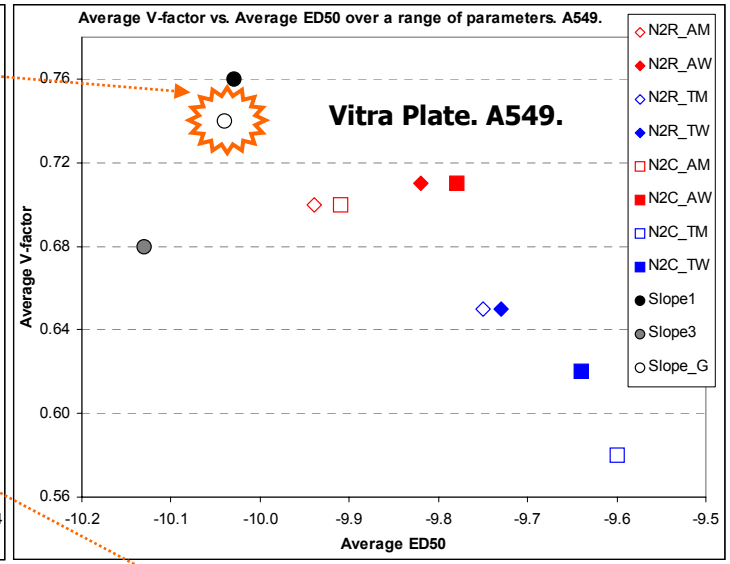

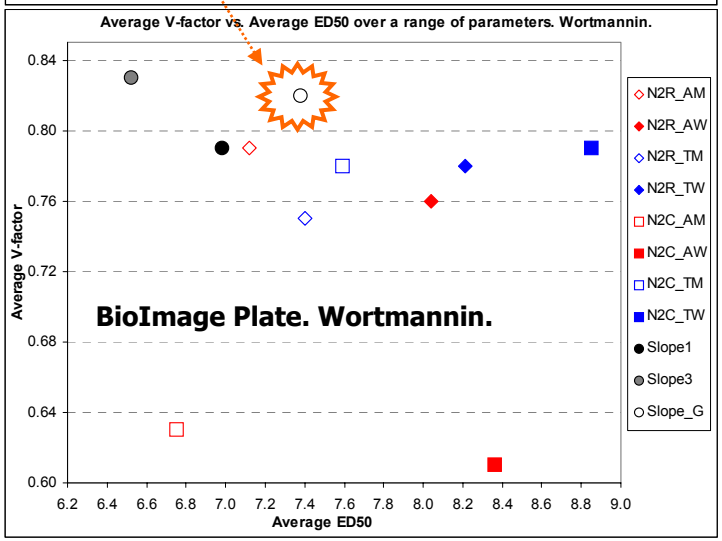

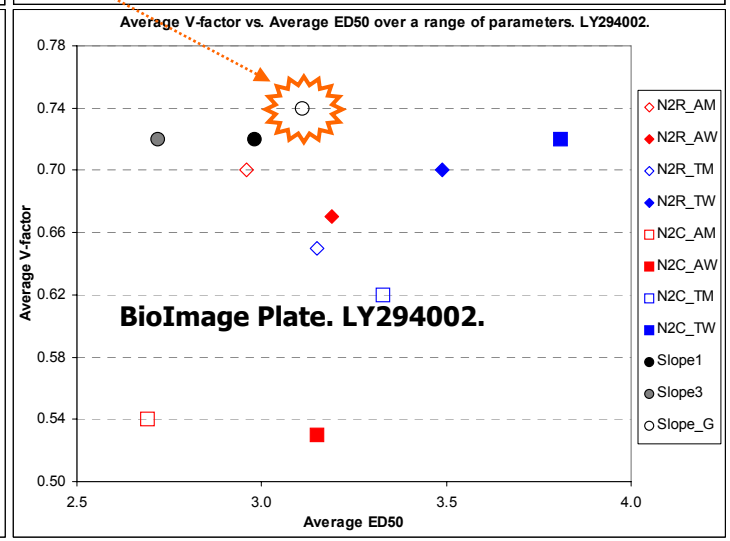

V-factor and ED_{50} averaged over a reasonable parameter range

Cell-By-Cell vs. Global Analysis. Transfluor (1)

CompuCyte Image Set.
Individual Fields.
~65 cells per data point.

Ozawa's Cell-by-Cell Algorithms:

These algorithms require two channels and segmentation into individual cells

K. Ozawa, C. Hudson, K. Wille, S. Karaki, R. Oakley "Development and validation of algorithms for measuring G-protein coupled receptor activation in cells using the LSC-based imaging cytometer platform", Cytometry Part A, Volume 65A, Issue 1, pp.69-76, 2005

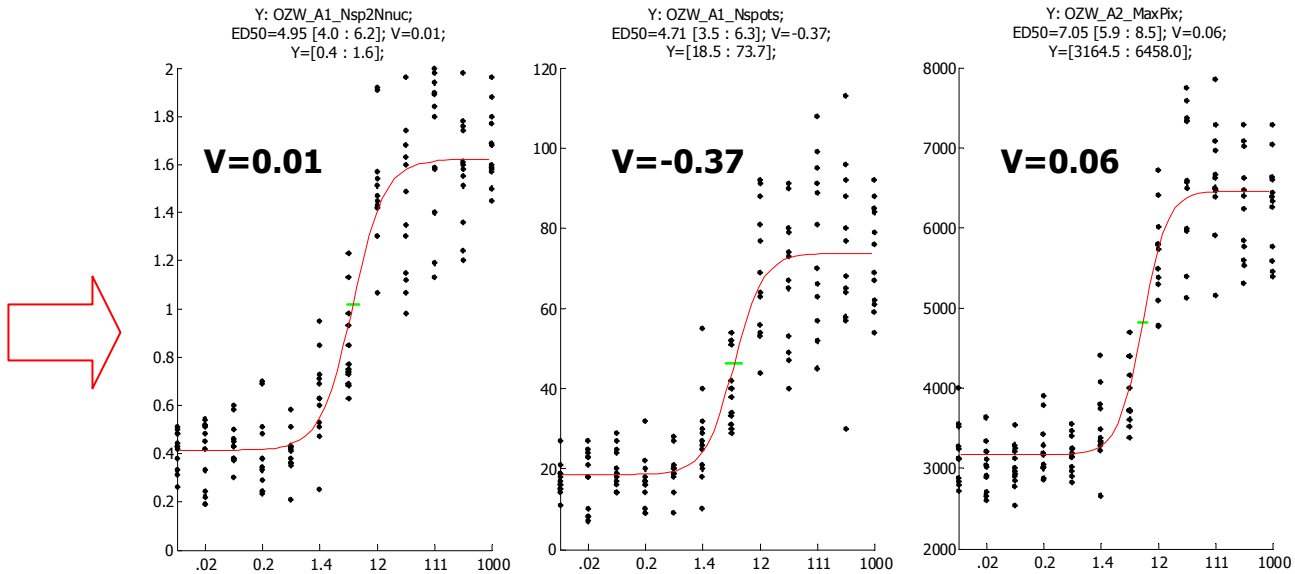

Ozawa's global Algorithm
(personal communication)

Granular Spectrum Algorithm
presented here

These algorithms require one channel and no segmentation into individual cells

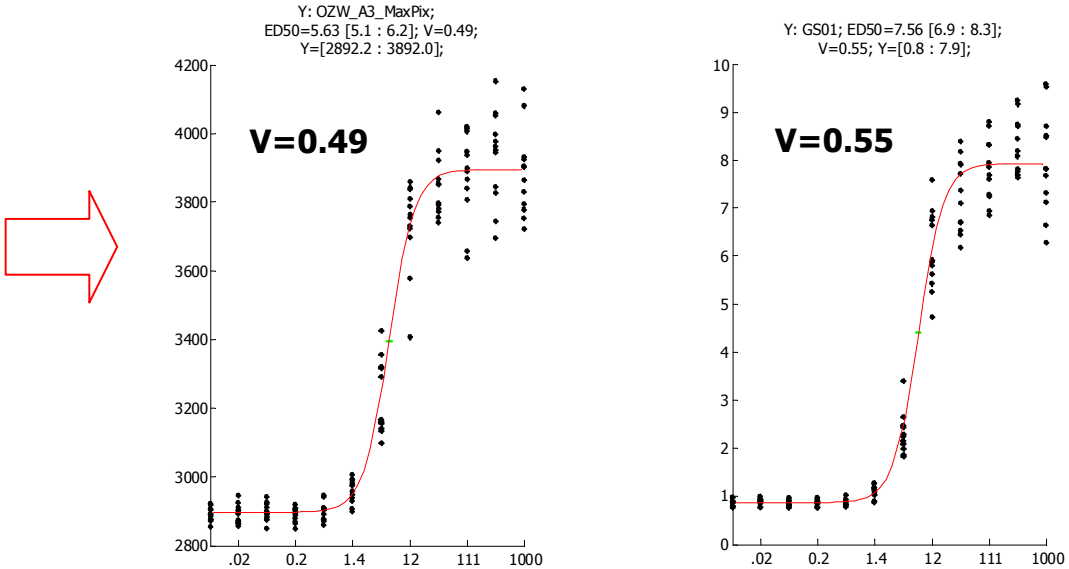

Cell-By-Cell vs. Global Analysis. Transfluor (2)

CompuCyte Image Set.
Pooled Fields.
~260 cells per data point.

Ozawa's Cell-by-Cell Algorithms:

These algorithms require two channels and segmentation into individual cells

K. Ozawa, C. Hudson, K. Wille, S. Karaki, R. Oakley "Development and validation of algorithms for measuring G-protein coupled receptor activation in cells using the LSC-based imaging cytometer platform", Cytometry Part A, Volume 65A, Issue 1, pp.69-76, 2005

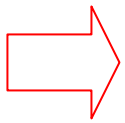

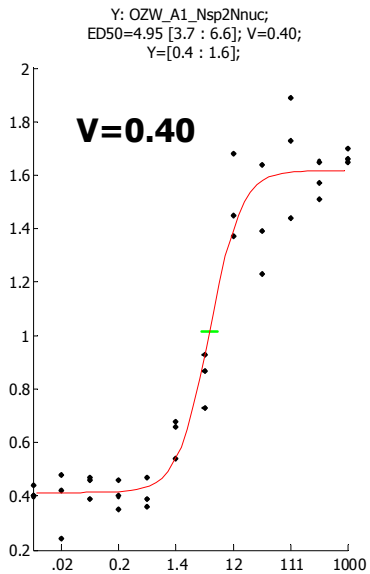

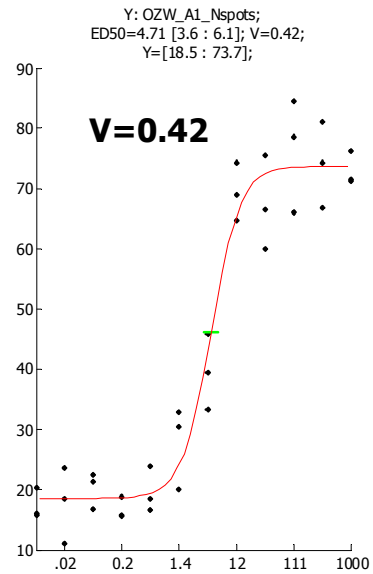

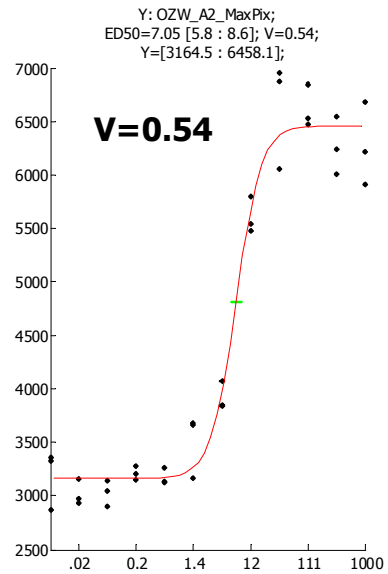

Ozawa's global Algorithm
(personal communication)

Granular Spectrum Algorithm
presented here

These algorithms require one channel and no segmentation into individual cells

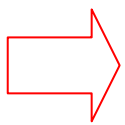

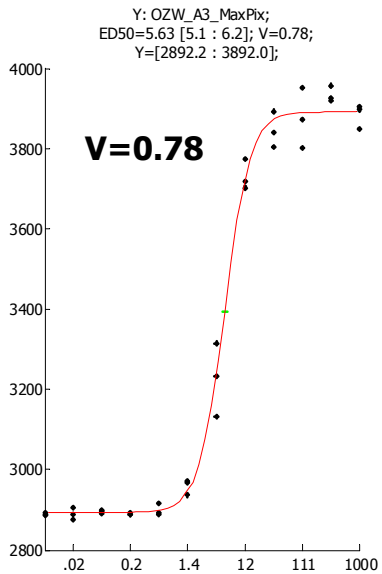

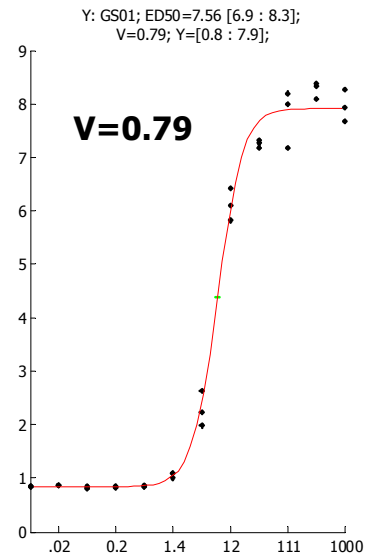

Questions to Answer while Developing an Imaging Assay

(and dependencies between these questions)

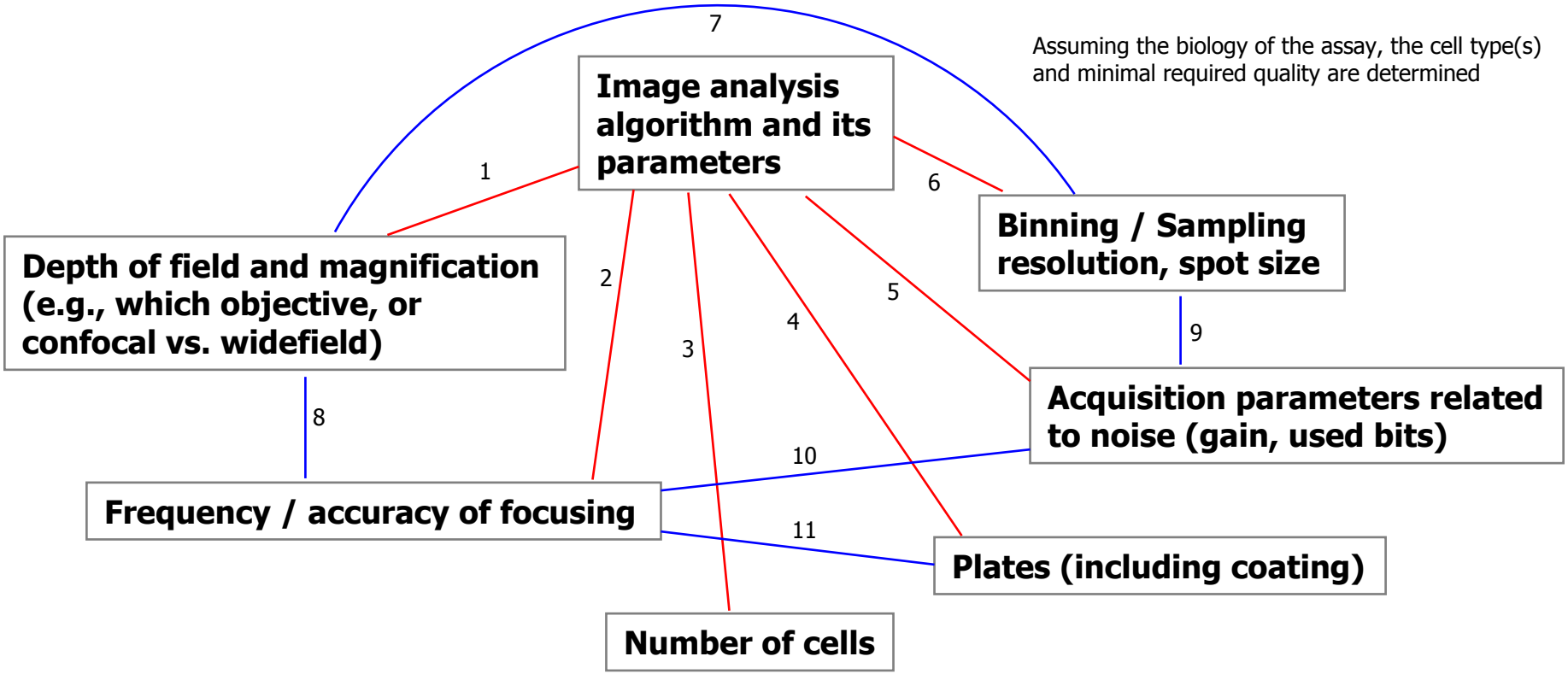

1. Different algorithms may require different resolution (microns/pixel)
2. Different algorithms may have different sensitivity to defocusing
3. Different algorithms reach the same quality at different numbers of cells
4. Different plate surfaces may cause different cell flatness and consistency
5. Different algorithms may have different immunity to noise
6. See 1.
7. Magnification and binning determine pixel resolution
8. The larger the depth of field, the less critical is focusing
9. Binning reduces noise
10. Focusing is more difficult with higher noise (for image-based focusing)
11. Flatter plates have less demand on focusing

Conclusions and Recommendations. Algorithms.

(Mostly based on cytoplasm to nucleus translocation and Transfluor™)

1. There is a systematic shift between ED_{50} of different measures. If the goal is comparing drugs or cell types, then the same measure should be used for the whole experiment. This points to the need for a uniformly best measure across experimental conditions.

2. Different measures have maximum quality at different parameter values, which depend on drug and cell type. For a realistic comparison, the quality of different measures must be averaged over a reasonable parameter range. Therefore, measures which do not strongly depend on parameters have a big advantage.

3. Conceptually similar measures implemented by different vendors can show significant difference in quality.

4. The fact that a measure is calculated on a cell-by-cell basis is not a guarantee that it is a good measure. Global measures may have higher quality.

5. Segmentation into cellular compartments or even into separate cells may not be required for high quality measures.

Conclusions and Recommendations. Hardware Factors of Assay Quality.

More important

Less important

Based on this presentation and other sources

Optical flatness of field	critical and cannot be easily compensated for algorithmically
Flatness of substrate	
Accuracy of focusing	
Channel alignment	
Depth of field	must be chosen appropriately for the thickness of analyzed objects
Illumination non-uniformity	does not play an important role if the algorithms can compensate for it
Detector Noise	below a certain limit does not play an important role

Caveat: Relative importance depends on the assay and on the algorithm, e.g. for highly specular assays (Transfluor) the dependency on focusing-related issues is much higher than for measuring DNA content.

Conclusions and Recommendations. Experiment Design.

1. Objectives in a wide-field system should be chosen based on their depth of field and cell thickness.

2. Focusing accuracy of the system must be evaluated and focusing strategy established to provide for small error (e.g., <10μm in 10X).

3. Required number of cells can be established by analyzing a fraction of images and selecting a number above which quality does not significantly improve with cell number.

4. Statistical processing may reveal valuable knowledge but may also reduce statistical assay quality.

References

1. J.-H. Zhang, T.D.Y. Chung, K.R. Oldenburg "A simple statistical parameter for use in evaluation and validation of high throughput screening assays", J. Biomol. Screening 4: pp. 67-73, 1999

2. I. Ravkin "Quality Measures for Imaging-based Cellular Assays" SBS 2004 conference poster #P12024

3. I. Ravkin, V. Temov, A.D. Nelson, M.A. Zarowitz, M. Hoopes, Y. Verhovsky, G. Ascue, S. Goldbard, O. Beske, B. Bhagwat, H. Marciniak "Multiplexed high-throughput image cytometry using encoded carriers", Proc. SPIE Vol. 5322, pp. 52-63, 2004 (Imaging, Manipulation, and Analysis of Biomolecules, Cells, and Tissues II; Dan V. Nicolau, Joerg Enderlein, Robert C. Leif, Daniel L. Farkas; Eds.)

4. US Patent 6,671,624 "Machine readable storage media for detecting distribution of macromolecules between nucleus and cytoplasm in cells".

5. Ilya Ravkin, Vladimir Temov, "Image analysis without segmentation - A new method to measure cytoplasm to nucleus translocation", poster, High Content Analysis Conference, San Francisco 2005 .

6. US Patent application 20050186554A1 "Image analysis and assay system"

7. I. Ravkin, V. Temov "Comparison of several classes of algorithms for cytoplasm to nucleus translocation" SBS 2005 Conference poster #P02025

References for granularity analysis on Transfluor™ images

1. J. Serra, *Image Analysis and Mathematical Morphology,* Vol. 1. Academic Press, London, 1989

2. Maragos, P. "Pattern spectrum and multiscale shape representation", IEEE Transactions on Pattern Analysis and Machine Intelligence, 11, N 7, pp. 701-716, 1989

3. L. Vincent "Granulometries and Opening Trees", Fundamenta Informaticae, 41, No. 1-2, pp. 57-90, IOS Press, 2000.

4. L. Vincent "Morphological Area Opening and Closing for Grayscale Images", Proc. NATO Shape in Picture Workshop, Driebergen, The Netherlands, pp. 197-208, 1992.

5. I. Ravkin, V. Temov "Bit representation techniques and image processing", Applied Informatics, v.14, pp. 41-90, Finances and Statistics, Moskow, 1988 (in Russian)

6. K. Ozawa, C. Hudson, K. Wille, S. Karaki, R. Oakley "Development and validation of algorithms for measuring G-protein coupled receptor activation in cells using the LSC-based imaging cytometer platform", Cytometry Part A, Volume 65A, Issue 1, pp.69-76, 2005